Numerical investigation of AB2 metal hydride systems for hydrogen storage.

Numerical Investigation of AB_2 Metal Hydride Systems for Hydrogen Storage

By

MOLEFE NTSWANA

214354683

Research for degree

Masters in Engineering: Chemical (Structured & Research)

in the

Department of Chemical, Metallurgical, and Materials

Engineering

FACULTY OF ENGINEERING AND THE BUILT ENVIRONMENT

Tshwane University of Technology

Supervisor: Dr. ML Moropeng

Co-Supervisor: Dr. D Makhwedza-Ramutshatsha

2023

Declaration

I hereby declare that the dissertation submitted for the degree **MASTER OF ENGINEERING IN CHEMICAL ENGINEERING** at the **Tshwane University of Technology** is my own original work and has not previously been submitted to any other institution of higher education. I further declare that all sources cited or quoted are indicated and acknowledged through a comprehensive list of references.

Ntswana Molefe

Dedication

I would like to dedicate this body of work to all my families, Ntswana, Sesane, Msiza and Rantlhoatlhoa.

I say without you I wouldn’t be where I am at in this life.

Thank you.

Acknowledgment

I would like to express my sincere gratitude and appreciation to: My supervisor, Dr Moropeng-Mavhungu M.L, for her positive attitude and guidance. And not forgetting Dr D Makhwedza-Ramutshatsha

Abstract

The are many challenges that are to be overcome to establish the substantial ground to develop an effective solution for on board hydrogen storage in the field of metals, hydrogen, and storage system. In this study, numerical investigation i.e. modelling and simulation of hydrogen storage in AB_2 type metal hydride packed inside the reactor was performed. The study focused on the development of coupled energy and mass models describing heat and mass transfer taking place between gas and solid metal hydride during absorption and desorption processes inside the reactor. The developed models were solved with the aid of the COMSOL 5.2 Multiphysics simulation tool. The simulation results demonstrated the importance of mutual dependence between temperature propagation in the body of metal hydride, the absorbed concentration of hydrogen, and the gas pressure of absorption/desorption of hydrogen gas in the metal hydride. The results clearly demonstrated that temperature plays a pivotal role in influencing the sorption process. The absorption, process was observed to be favoured by a range of temperatures from low to high, with concentration increasing as the temperature rises. This trend was also observed in the behaviour of pressure and velocity. Conversely, when pressure is increased from a lower level to a higher level, the opposite effect is observed. Furthermore, it was discovered that the ideal operation conditions for temperature and pressure were 303.15 K and 10 atm. The observation of desorption suggests that the process is endothermic, but it does not necessitate excessively high temperatures. With 293.15 K being a favourable operating temperature, and 3 atm for pressure. The pressure discharge in desorption in vice versa to that of absorption. In summary, it can be concluded that high temperatures are conducive for absorption but are less favourable for desorption processes. Desorption in general is favoured by condition close to ambient conditions. And it was recommended that disruptive metals should be discovered for hydrogen sorption in order for hydrogen economy to be established at a lower cost.

Keywords: Hydrogen, Metal hydride reactor, Absorption/desorption, Heat and mass transfer, Simulation and COMSOL

Contents

Abstract 4

LIST OF FIGURES 8

LIST OF TABLE 11

Nomenclature 12

GLOSSARY 15

Chapter 1 1

1. Introduction 1

1.1. Background 1

1.2. Problem statement 2

1.3. Justification of the project 3

1.4. Aim 3

1.5. Objectives 4

1.6. Hypothesis 4

1.7. Significance of study 5

Chapter 2 6

2. Literature Review 6

2.1. Hydrogen 6

2.1.1. Thermo-physical properties 7

2.1.2. Availability 8

2.1.3. Uses 9

2.2. Hydrogen storage 10

2.2.1. Compressed Hydrogen Gas (CGH2) 11

2.2.2. Liquid Hydrogen (LH2) 12

2.2.2. Solid Storage Hydrogen (SSH_2) 13

2.3. Metal hydride 14

2.3.1. AB alloy 15

2.3.2. AB_5 alloy 16

2.4.1. Pressure-composition-isotherm (PCI) 17

2.4. Metal hydride review 19

Chapter 3 24

3. Model 24
3.1. Process description 24
3.2. Chemical Reaction Equation 24
3.3. Mass Balance 25
3.4. Energy balance 25
3.5. Effective Thermal Conductivity (ETC) Model 27
3.6. Mass source term 28
3.7. Initial and boundary conditions 28
3.7.1. Initial conditions 28
3.7.2. Boundary conditions 29
3.8. Geometry 29
Chapter 4 31
4. Research Methodology 31
4.1. Materials 31
4.2. Procedure 32
4.3. Methodology 33
4.4. Simulation 33
4.4.1. Physics 33
4.5. Data Collection 34
4.6. Data Analysis 34
Chapter 5 35
5. Results and Discussions 35
5.1. Absorption 35
5.1.1. Effects of temperature 35
5.2. Effect of pressure 39
5.3. Operational parameters 41
5.3.1. Temperature 41
5.3.2. Pressure 43
5.4. Desorption 44
5.4.1. Effect of temperature 44
5.4.2. The effect of pressure 49
5.5. Desorption operation parameters 51

5.5.1. Temperature 51
5.5.2. Pressure 53
5.6. Model development 55
5.6.1. PCT 55
5.6.2. Temperature profiling 56
5.6.3. Concentration profiling 57
5.6.4. Pressure and Velocity Profiling 59
5.7. Effective thermal conductivity influence 60
5.8. Validation of results 61
Chapter 6 63
Conclusion and recommendations 63
Reference 65
Appendixes 71

LIST OF FIGURES

Figure 2.1.1: hydrogen phase diagram.

Figure 2.1.2.1: Steam reforming PFD.

Figure 2.1.3.1: Energy content of fuels.

Figure 2.2.2.1: Linde cycle.

Figure 2.2: Storage methods.

Figure 2.2.1.1: Components of a pressurized hydrogen storage tank.

Figure 2.4.1: Pressure – Composition- Temperature diagram.

Figure 2.4.2: P-C-T curve for MH_x compressor.

Figure 3.8.1: Asymmetric geometry of MH reactor.

Figure 3.8.2: Three-dimensional geometry of MH.

Figure 5.1.1: The effect of temperature on the concentration.

Figure 5.1.1.a: The effect of temperature on the concentration.

Figure 5.1.2: Metal-to-hydrogen ratio.

Figure 5.1.3: Pressure evolution with temperature.

Figure 5.1.4: Velocity profile of MH bed at various temperatures.

Figure 5.2.1: Influence of pressure on temperature.

Figure 5.2.2: Impact of pressure on concentration**.**

Figure 5.2.3: Pressure-induced velocity profile.

Figure 5.3.1.1: Temperature profile at different gas temperatures.

Figure 5.3.1.2: Equilibrium pressure rate.

Figure 5.3.2.1: Supplied pressure.

Figure 5.3.2.2: Pressure effect on equilibrium.

Figure 5.4.1.1: Effect of temperature on dehydrogenation.

Figure 5.4.1.1.a: Effect of temperature on dehydrogenation.

Figure 5.4.1.2: Effect of temperature on pressure.

5.4.1.2.a: Effect of temperature on pressure.

Figure 5.4.1.3: Effect of temperature velocity.

Figure 5.4.2.1: The effect of pressure on temperature.

Figure 5.4.2.2: Pressure effect on concentration.

Figure 5.4.2.3: Pressure-velocity profile.

Figure 5.5.1.1: Heating temperature.

Figure 5.5.1.2: Desorption equilibrium pressure rate.

Figure 5.5.2.1: Reactor-hydrogen pressure.

Figure 5.5.1.3: Equilibrium-gas pressure rate.

Figure 5.5.2.2: Equilibrium pressure rate at different operating pressure.

Figure 5.6.1: PCT model.

Figure 5.6.2.1: Absorption temperature profile.

Figure 5.6.2.2: Desorption temperature profile.

Figure 5.6.3.1: Absorption concentration profile.

Figure 5.6.3.2: Desorption concentration profile.

Figure 5.6.4.1: Desorption pressure profile.

Figure 5.6.4.2: Desorption velocity profile.

Figure 5.7.1: Temperature profile using various ETC.

Figure 5.8.1: Simulation validation.

LIST OF TABLE

Table 4.1.1: Properties of $Ti_{0.98}Zr_{0.02}V_{0.43}Fe_{0.09}Cr_{0.05}Mn_{1.5}$

Table 4.1.2: Properties of hydrogen

Table 2.3.1: Qualitative analysis of main criteria of solid hydrogen storage families

Nomenclature

A — Area (m^2)

Ca — Adsorption rate constant (s^−1)

Cd — Desorption rate constant (s^−1)

cp — Pressure specific heat capacity (Jkg^−1K^−1)

cv — Volume specific heat capacity (Jkg^−1K^−1)

E — Energy(J)

Ea — Adsorption activation energy (Jmol^−1)

Ed — Desorption activation energy (Jmol^−1)

g — Gravity(ms^−2)

h — Convection heat transfer coefficient (Wm^−2K^−1)

(H/M) —Hydrogen to metal ratio (-)

K — Permeability(m^2)

k — Specific thermal conductivity (Wm^−1K^−1)

Keq — Equilibrium constant (-)

m — Mass(kg)

$\dot{m}$ — Mass flowrate (kgs^−1)

M — Molecular weight (gmol^−1)

n — Number of mols (mol)

p — Pressure (Pa)

$\dot{Q}$— Heat flux (W)

q˙i — Conductive heat flux (Wm^−2)

Ru — Universal gas constant (Jmol^−1K^−1)

Rg — Specific gas constant (Jkg^−1K^−1)

Re — Reynolds number (-)

Sm — Mass source/sinkterm (kgm^−3s^−1)

ST — Energy source/sink term (Wm^−3)

t — Time (s)

T — Temperature (K)

~u — Velocity field (ms^−1)

V — Volume (m^3)

˙V— Volumetric flow (m^3s^−1)

W — Work (W)

Greeks

∆h — Enthalpy(J)

ΔH — Formation enthalpy (Jmol−1)

ΔS — Entropy (Jmol^−1K^−1)

ε — Porosity (-)

θ — Desorbed hydrogen fraction (-)

μ — Dynamic viscosity (kgm^−1s^−1)

ρ — Density (kgm^−3)

Subscripts

0 —Initial

emp — Empty

eq — Equilibrium

MH — Metal hydride

sat — Saturation

Superscripts

eff — Effective

g — Gas

m — Metal

ref — Reference

GLOSSARY

Term	Description
Absorption	Mass transfer where the gas enters the solid or fluid
	In the context of this study is used interchangeably with charging to indicate the metal hydride forming reaction and the subsequent storing of hydrogen
Activation energy	The energy required to initiate or activate a reaction
Adsorption	Mass transfer is limited to where the gas physically attaches to the surface of the solid
Chemisorption	Chemical-physical phenomenon where a chemical reaction and sorption occur simultaneously
Computational fluid dynamic	Fluid and thermal simulations are performed with the use of computational power to calculate parameters in a continually changing system
Cycling	The charging and discharging of the system
Desorption	Mass transfer where the gas leaves the solid or fluid. In other words, the inverse of absorption, adsorption, chemisorption and sorption
	In the context of this study is used interchangeably with discharging to indicate the metal hydride decomposition reaction and the subsequent release of stored hydrogen
Energy density	The amount of usable energy in an energy storage method in terms of volume or mass
Enthalpy	A measure equivalent to the total heat in a system
Entropy	A measure of the unavailability of a system’s thermal energy for conversion
Finite element	A method to numerically solve differential equations for systems by dividing the system into a finite number of sections or elements

Fuel cell	A reduction-oxidation cell that coverts the fuel's chemical energy into electrical energy by facilitating the electron exchange of said fuel with an oxidant
Fugacity	An equivalent property of a real gas to allow the applicable use of the ideal gas law by replacing pressure
Gravimetric	Indication that a parameter is in terms of mass
Heat capacity	The amount of energy required per unit mass of a substance to increase its temperature by a single unit
Isotherm	A relationship between two parameters at a constant temperature
Lattice	A repeated three-dimensional arrangement of atoms in a metal or crystalline solid
Porosity	A measure of the space or void in a solid bed or substance
Reaction time constant	A constant to represent the time-based aspect of a reaction or sorption
Sensitivity analysis	A method to determine the influence of input parameters on a system by changing said parameter and then measuring the change in several descriptive parameters of the system
Simulation	To perform an imitation-based experiment by using validated models, often employing the use of computational assistance to solve differential equations
Sorption	Mass transfer which is not limited to the gas staying on the surface of the solid nor is it limited to the gas entering the solid but a combination of both
Thermal conductivity	A measure of the thermal conductance of a solid, alternatively, the inverse of thermal resistance
Thermal Isolation	The heat conduction is so low it is considered to be zero
Thermal resistance	A measure of the resistance a substance gives during the conduction of heat through said substance
Thermo-chemical properties	Thermodynamic and chemical properties encompassing all reactions, thermal and physical characteristics
Volumetric	Indicating that a parameter is in terms of volume

Chapter 1

1. Introduction

1.1. Background

Metal hydride (MH) technology application has become the centre of alternative energy storage, separation, and purification systems which allow heat-driven hydrogen non-mechanical compression components, heat operations (refrigeration, heat upgrade, heat transformation), hydrogen separation and purification with less or no contamination, and many other gaseous hydrogen processes (Mat M.D. and Kaplanb Y., 2001; Colbe J.B et al., 2019). When it comes to the combination of one or more described hydrogen processes in a merged mechanism, the MH technology has the ability to adapt and provide reversal on-board hydrogen storage at ambient conditions (Madridis SS., 2016). The MH bed is considered an intermetallic compound that is made of two metallic components, A and B. The A component is from a stable hydride, where else B forms an unstable hydride, and they are grouped according to their stoichiometry, such as AB, AB2, AB5, and others. AB2 and AB5 are the most promising, as they have passed the prototype phase (Ragheb M., 2011). For this study, AB2 metal hydride will be used.

In the past, extensive experimental and modelling & simulation work has been performed to make the hydrogen economy viable. (Mayer 1987), performed a one-dimension (in a radial direction) simulation and experimental work to validate the results. The found from experimental data suggested that the temperature profile did not only vary in the radial direction (r-direction), but also in the length direction (z-direction). Lucas and Richards (1984) also developed the same model but did not include the transient heat of conduction which is the major driving force of heat and mass transfer.

And when validating the model with the experimental data there was a huge disagreement between both data (Mat M.D. and Kaplanb Y., 2001 & Maceiras R et al., 2015). In several papers, Jemni and Ben Nasrallah (1997) followed or examined a two-dimensional model using two mathematical equations for fluid and solid. However, with all that they discover that the fluid and solid are at local thermal equilibrium with each other.

Currently, researchers are doing more modelling and simulation and their work with the existing experimental work of which they have been validated over the years. Moropeng L.M., et al (2019) performed a simulation on a thermodynamic Pressure composition temperature (PCT) diagram using the numerical technique to validate the model by Lacher. And the results agreed with the literature meaning the purpose of the numerical technique was achieved. Wang C., et al., (2011), works were composed into three (3) parts. Firstly, ETC was predicted by using the adopted Sung and Deng's (1990) model, then experiments were done to measure ETC value then finally simulations of varied ECT are done and validated with experimental work data. In the study, it was clear that the varied model was good in the hydriding/dehyding process than using constant ETC value. In this study, the model adopted by Wang C (2011) et al will be used in the design of an MH bed for hydrogen storage.

In this study the focus will follow the recommendation by Wang et al., to further investigate the varied ETC model as ETC affects the heat and mass transfer of MH bed. By using the ETC model an appropriate design of MH reactors from small to large scale which will transcend the underlying problem, with a good understanding of different parameters' influence on the heat and mass transfer performance is useful and in need. To establish all that, a suitable mathematical model of heat and mass transfer processes in the MH bed must be developed and modelled through a computer, followed by verification of the model based on experimental data and refined if needed. The modelling task is complicated by the presence of the source term in the heat conductivity equation whose contribution strongly depends on several parameters, including properties of MH material, operating pressure/temperature conditions, and process time (Mat M.D. and Kaplanb Y., 2001; Wang C et al., 2011 & Maceiras R et al., 2015).

1.2. Problem statement

Hydriding and dehydriding are complex processes because they occur simultaneously with heat and mass transfer during chemical reactions the MH bed. The situation then becomes more complex because of gas motion in the porous medium and change in physical properties (Mat M.D. and Kaplanb Y., 2001). And low effective thermal conductivity (ETC) of powdered MH beds is the main obstacle hindering the upscaling of the MH hydrogen storage units and MH elements for related applications (e.g., hydrogen compressors) where high dynamic performances are

required. Moreover, the ETC value is strongly dependent both on the design and technological characteristics of the MH beds and on the operation conditions (Wang C et al., 2011).

Current work on MH bed modeling and simulation work has been focused on heat and mass transfer at constant ETC. Ragheb M (2011) performed a 2-dimensional simulation with a model without varied ETC equation and discovered the properties of the AB_2 MH bed he used were good behaving especially when it comes to discharging. And in the experimental study of Wang C et al, (2011), AB_5 compound La_5Ni was used to determine heat and mass transfer at constant and varied ETC. It was found that heat and mass transfer improved with a varied than with constant ETC and also good design of MH bed hydrogen storage reactor can be achieved with the use of varied ETC at transient conditions (Maceiras R et al., 2015 & Wang C et al., 2011).Thus, in this study $Ti_{0.98}Zr_{0.02}V_{0.43}Fe_{0.09}Cr_{0.05}Mn_{1\ 5}$, AB_2 material will be used as the MH bed to improve the hydriding/dehydriding time, capacity, and operating/ design parameters.

1.3. Justification of the project

Looking into the driving factors of developing countries and developed countries you would find that energy is one of the huge factors. The current economic driver is fossil fuels which are non-renewable resources and take hundreds of years to be formed. Due to their harmful effect on the environment and mankind, and having low reserves there is a need for an alternative source of energy to take over from fossil fuels. Hydrogen has been labelled as a candidate, the problem arises when it comes to a safe and economical storage of hydrogen. In this instance modelling and simulation will be used to design a proper storage tank and determine the safe operating conditions for the tank with the aid of a simulation tool/package

1.4. Aim

In this project, the 1D, and 2D hydrogen absorption/desorption processes will be modelled based on the developed kinetics equations, hydrogen transport equations, and heat transfer equations in metal hydride reactors. The mathematical algorithms will be solved with the aid of COMSOL software to predict values of temperature, hydrogen concentrations, pressure, and velocity distributions inside the MH reactors to better understand heat and mass-determining

factors between MH bed and hydrogen gas. In addition, the performance of the proposed models will be confirmed and validated with the experimental results obtained from the literature.

1.5. Objectives

- To critically examine existing methodologies for modelling heat-and-mass transmission in Metal hydrogen alloy beds and suggest ways to enhance them.
- To develop and verify an advanced model of heat-and-mass transfer in the MH beds and incorporate it into COMSOL software for the estimation and design of MH reactors for hydrogen compression.
- To identify the elements impacting the dynamic performance of MH reactors and validate metal hydride reactor models with the experimental work.

1.6. Hypothesis

- Heat and mass transfer in a metal hydride bed is affected mostly by temperature and the size of the bed. Temperature control according to the type of process (absorption or desorption) and use small size bed to achieve effective cooling.
- Metal hydride formation is considered in a two-dimensional tank.
- The mathematical model can be solved by the commercial software package COMSOL Multiphysics 5.2.
- Metal hydride reactor performance it is affected by ETC, flow rate of the heat transfer fluid and the contact resistance.
- The metal hydride reactor varied ETC model for absorption/desorption was found to be accurate when experimental work was compared to the simulation.

1.7. Significance of study

This study will be conducted to design an on-board hydrogen storage, using Metal hydride reactor, by developing mathematical model and solving it using COMSOL simulation package. The design will be done under unsteady state condition and using varied ETC model to improve the absorption and desorption process, and safe operating condition. The success of the study will lead to a new energy economy driven by a renewable source that can start with water and end with water. And it is environmentally friendly meaning human health will not be a concern when comparing to the present energy source which is also non-renewable and it reserves are running low, the energy demand on the other hand is increasing.

Chapter 2

2. Literature Review

Since the beginning of the industrial revolution in the 18th century, fossil fuels including coal, oil, and natural gas have been the primary source of energy for the technological and transportation network (Crabtree, Dresselhaus et al. 2004). Energy is also a key economic driver, therefore finding a greener supply is essential owing to rising demand brought on by population growth (Meng, Bao et al. 2012). The need for green energy is driven by the fact that fossil fuels are running out and endanger human health, the environment and cannot keep up with the demand (Höök and Tang 2013, Heede and Oreskes 2016). Due to the negative effects of non-renewables (fossil fuels), alternative energy sources, or renewable energy, are required to get rid of the reliance on fossil fuels and offer a sustainable expansion of economies and communities (Madriklridis 2016). Hydrogen, wind, solar, biomass and hydro-energy are examples of renewable energy, and hydrogen energy has gained attention, also expected to be the future of energy (Panwar, Kaushik et al. 2011). The attention hydrogen caught was due to its thermodynamic property, as an energy carrier years after it was discovered in 1671 by Robert Boyles (Stwertka 1996). The purpose of this project was to study hydrogen energy and methods suitable for storage through modelling and simulation.

2.1. Hydrogen

Of all the elements in the cosmos, hydrogen is the most prevalent (Cleveland 2014). Original hydrogen atoms or other elements that were produced from hydrogen atoms were used to create the heavier elements (Zuttel 2004). Years passed before hydrogen was acknowledged as an element by scientists (Madriklridis 2016). Robert Boyle is known to have created hydrogen gas as early as 1671 when working with iron and acids, according to written sources (Stwertka 1996). Henry Cavendish identified hydrogen as a separate element for the first time in 1766. Composed of a single proton and a single electron, the first chemical element on the periodic table, exist as

a diatomic molecule, colourless and odourless under normal conditions (Stwertka 1996, Cleveland 2014).

2.1.1. Thermo-physical properties

There are three isotopes of hydrogen, with ^{1}H making up the majority and known as protium is the name for hydrogen's common isotope (Stwertka 1996). The discovery of the stable isotope deuterium (D), having an atomic weight of 2, was reported by Urey in 1932 (Zuttel 2004). About 0.015 percent of natural hydrogen contains deuterium. Tritium (^{3}H), an unstable isotope with an atomic weight of 3, was found two years later (Linde 2005). Under normal condition hydrogen exists as a gas, with the lowest boiling point after helium, forms liquid below 20 K and solidify 14 K and atmospheric pressure. The hydrogen phase diagram, shown in Figure 2.1.1 below, provides information on the pressure and temperature ranges that are ideal for heating or cooling hydrogen The hydrogen phase diagram, shown in Figure 2.1.1 below, provides information on the pressure and temperature ranges that are ideal for heating or cooling hydrogen (Zuttel 2004, Charitos and Makridis 2021).

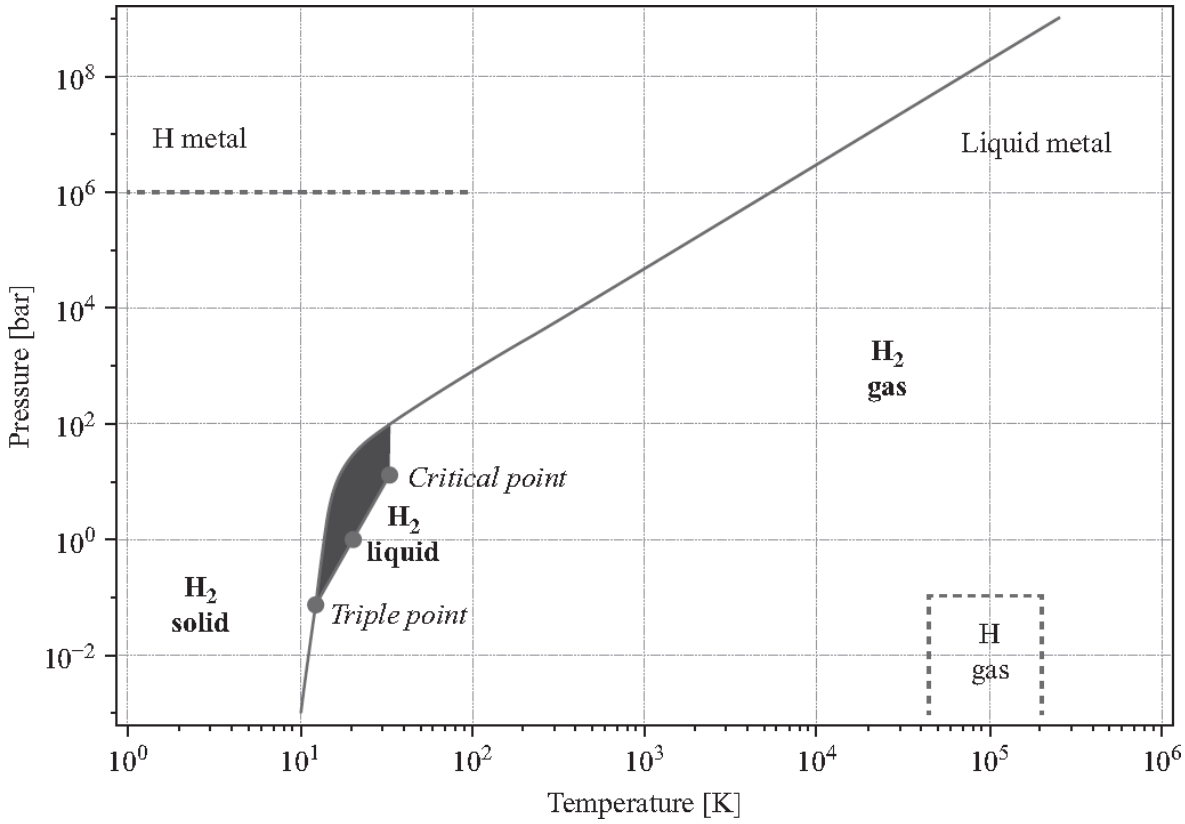

Figure 2.1.1: hydrogen phase diagram (Tzimas, Filiou et al. 2003, Zuttel 2004)

2.1.2. Availability

Natural gas, oil, coal, and electrolysis are the four primary processes used to produce hydrogen in the commercial sector; they account for 48 percent, 30 percent, 18 percent, and 4 percent, respectively, of global hydrogen production (Press, Santhanam et al. 2008). The main source of industrial hydrogen is fossil fuels (Häussinger, Lohmüller et al. 2011). For the manufacture of hydrogen, carbon dioxide may be extracted from natural gas with a 70–85% efficiency and from other hydrocarbons with variable degrees of efficiency (Charitos and Makridis 2021, Raghav, Anand et al. 2021). Particularly, the steam reformation of methane or natural gas typically results in the production of bulk hydrogen (Press, Santhanam et al. 2008).

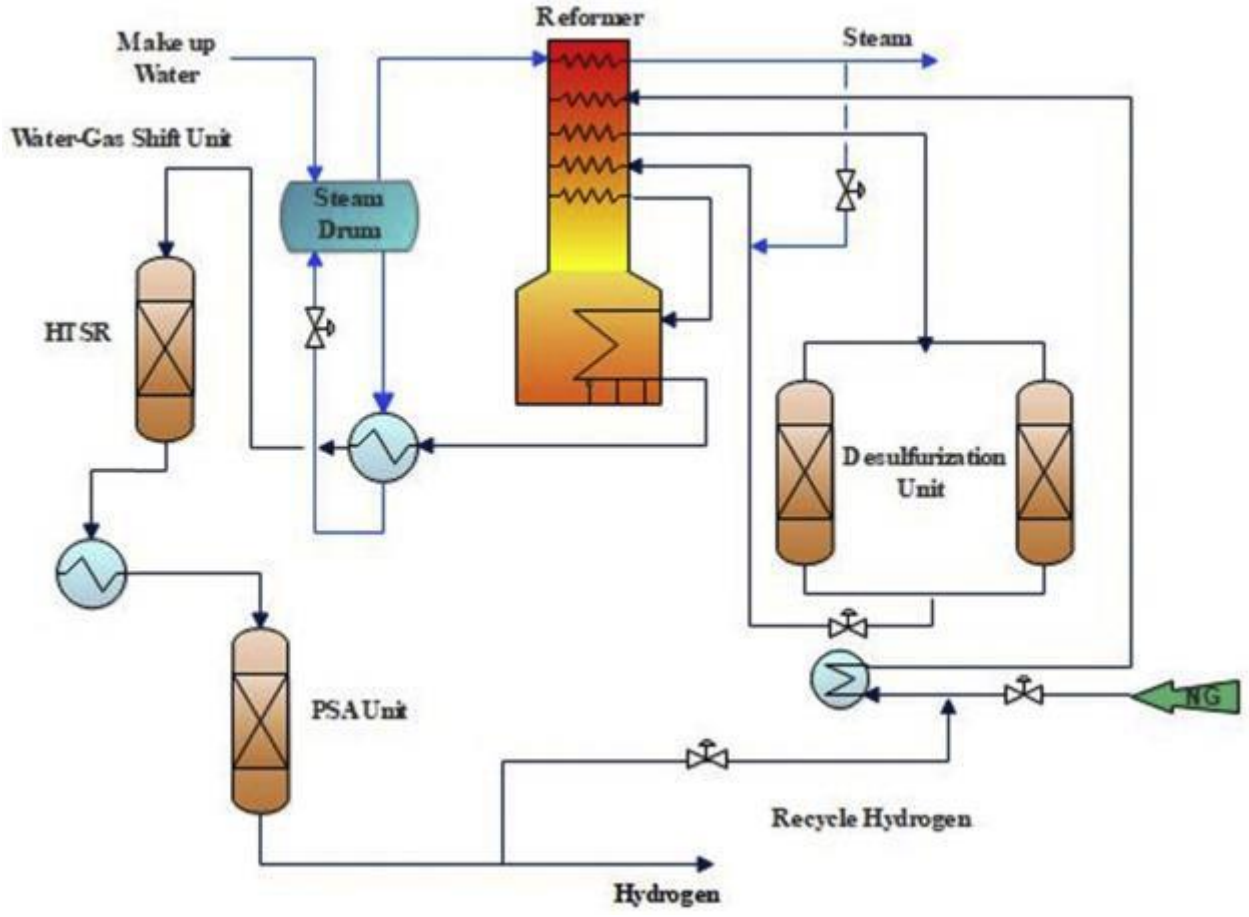

Figure 2.1.2.1: Steam reforming PFD (Taji, Farsi et al. 2018)

Natural gas is used in the hydrogen manufacturing process during the steam reforming process. This process is presently the most cost-effective way to get industrial hydrogen. The procedure involves heating the gas to around 700-1100 °C in the presence of steam and a nickel catalyst. Because this is an endothermic process, it breaks apart the methane molecules and produces carbon monoxide (CO) and hydrogen (H2). After that, the carbon monoxide gas is transported by steam over iron oxide or other oxides. Then it travels through a water gas shift process, which produces more H2 (Zuttel 2004, Press, Santhanam et al. 2008, Taji, Farsi et al. 2018, Raghav, Anand et al. 2021). Figure 2.1.2.1 in the previous page, shows a process flow diagram of steam reforming process. The equation of steam reforming reaction and water gas shift reaction are presented by equation 2.1.2.1 and 2.1.2.2. The production of hydrogen does not take precedence in this investigation.

Steam-methane reforming reaction

$$CH_4 + H_2O \text{ (+ heat)} \rightarrow CO + 3H_2 \qquad \text{eq.2.1.2.1}$$

Water-gas shift reaction

$$CO + H_2O \rightarrow CO_2 + H_2 \text{ (+ small amount of heat)} \qquad \text{eq.2.1.2.2}$$

2.1.3. Uses

Hydrogen is a very significant chemical with a vast range of applications and uses. It is now employed in a variety of sectors, including chemical and refining, metallurgical, glass, and electronics (Ramachandran and Menon 1998). The primary application of hydrogen is as a reactant. In chemical production, fertilizer, Ammonia is the backbone of the fertilizer business and is created by the interaction of nitrogen and hydrogen. Ammonia uses over half of all hydrogen generated in the globe. The reaction occurs at high pressures and involves the reaction of H and N to form ammonia (Amhamed, Shuibul Qarnain et al. 2022). Hydrogen is utilized in the reduction step of the Sherritt Gordon Process to produce nickel. In this stage, nickel in solution as sulfate is transformed and precipitated as elemental nickel, leaving ammonium sulfate (Stopić and Friedrich 2020). Since H_2 burns more efficiently than gasoline and is the cleanest burning fuel, there is considerable interest in using it as a fuel in cars (Ramachandran and Menon 1998, Zuttel 2004). Refer to figure 2.1.3.1 to compare the energy given off by hydrogen rather than using it only as a reactant. Hydrogen utilization in the energy sector is challenged by safety, storage, and efficient combustion of hydrogen; so, hydrogen storage, safety, and combustion efficiency are prioritized in this study.

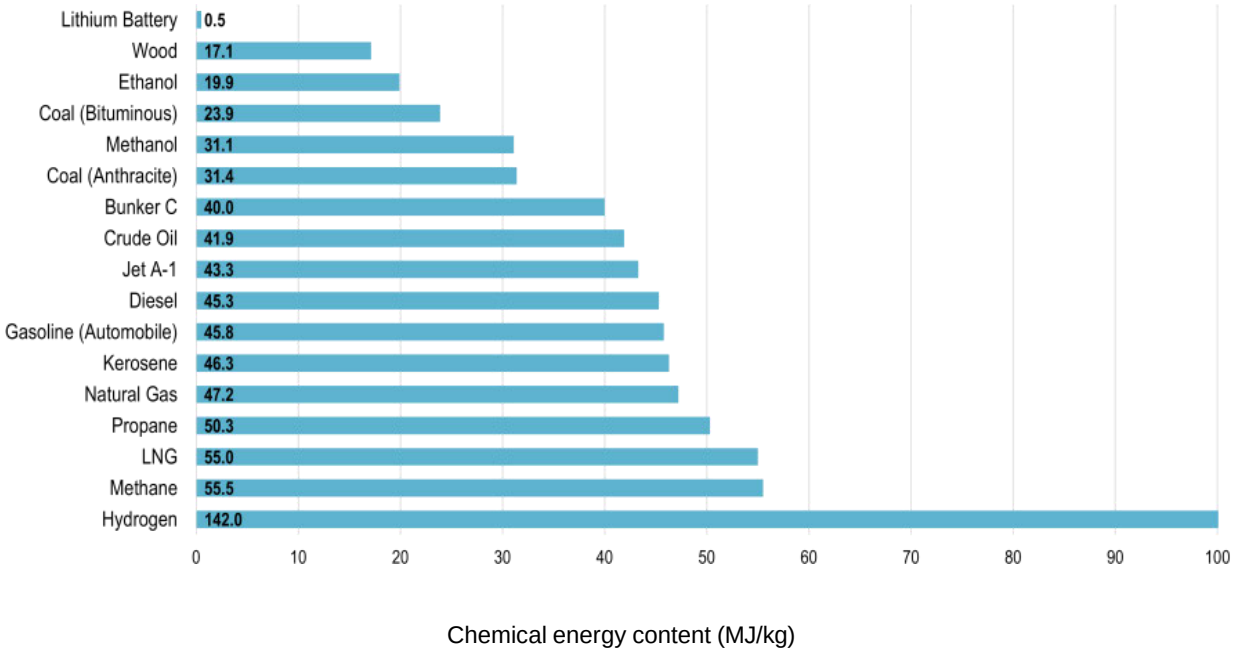

Figure 2.1.3.1: Energy content of fuels (Rodrigue 2020)

2.2. Hydrogen storage

Hydrogen may be stored in three (3) fundamental ways: compressed, liquid, and solid (given acronyms CGH_2, LH_2 and SSH_2) (Durbin and Malardier-Jugroot 2013). The first two, as said, may be used by manipulating hydrogen's physical state in gaseous or liquid form using pressure and temperature, however solid storage hydrogen is not mechanical and is classified into following groups: Physisorption in porous materials, Absorbed on interstitial sites in a host metal, Complex compounds, and Metals and complexes with water (Zuttel 2004). The substance under consideration was SSH2, which undergoes hydrogen sorption onto and into the material, implying that the other material undergoes absorption/desorption and other adsorption/desorption (Xiao and Yuan 2009, Visaria, Mudawar et al. 2010). In this work, a review of storage types was performed, and SSH2 was focused on as a storage type due to its hydrogen sorption characteristics and use of none moving components.

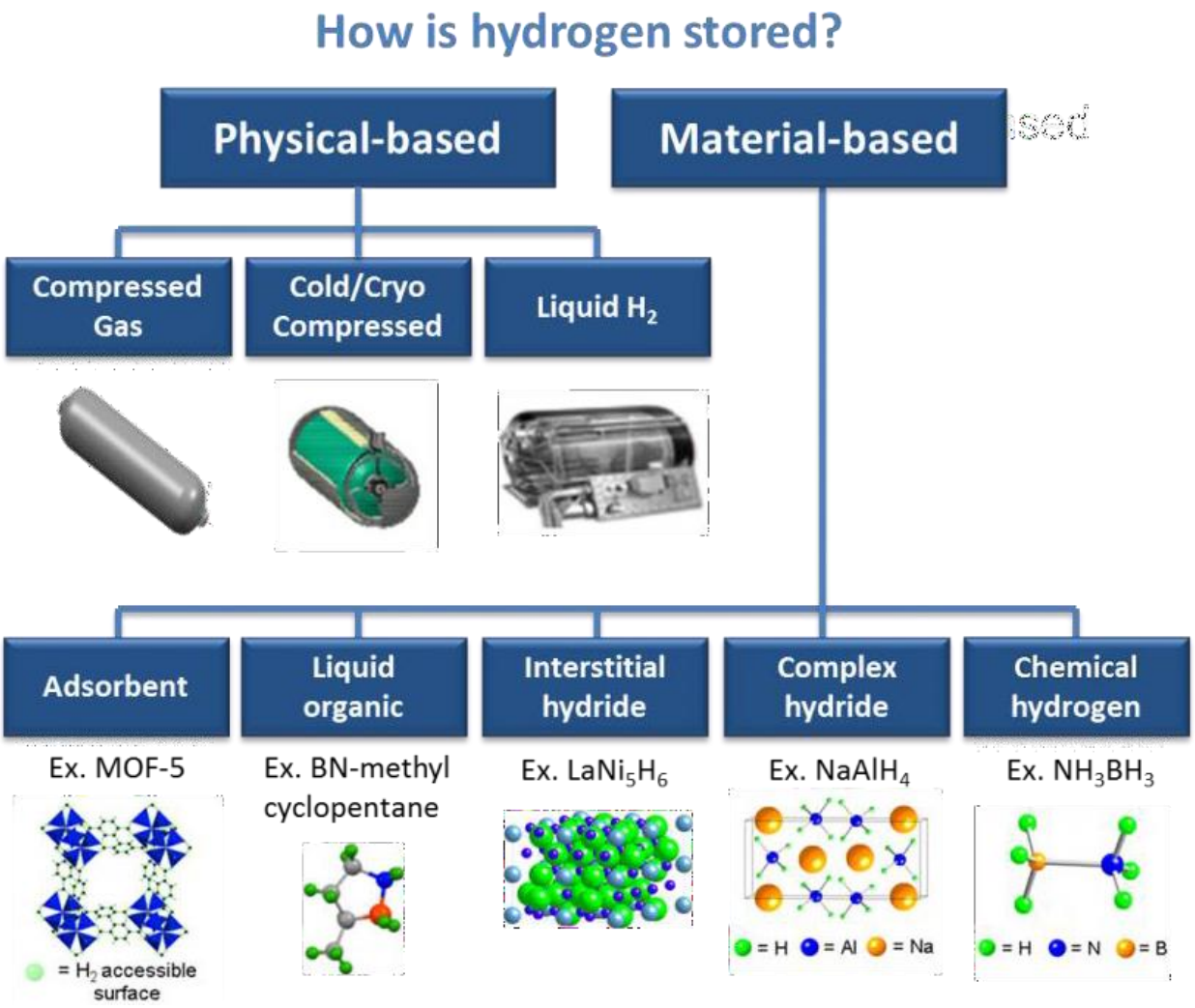

Figure 2.2: Storage methods (Zuttel 2004)

2.2.1. Compressed Hydrogen Gas (CGH2)

Compressed hydrogen is a type of storage in which hydrogen gas is held under pressure to enhance storage density (Madriklridis 2016). Based on type IV carbon-composite technology, compressed hydrogen in hydrogen tanks at 350 bar and 700 bar is utilized for hydrogen tank systems in cars. This approach has been developed by car manufacturers such as Honda and Nissan (von Helmolt and Eberle 2007, Eberle, Müller et al. 2012). New lightweight composite cylinders capable of withstanding pressures of up to 800 bar have been developed, allowing hydrogen to achieve a volumetric density of 36 kg/m3, nearly half as much as in its liquid form at normal boiling point (Cho, Kim et al. 2021). Although compressed hydrogen is normally kept at near-ambient temperatures, cold (sub-ambient but more than 150 K) and cryogenic (150 K and below) compressed hydrogen storage are being researched due to the higher hydrogen densities

that may be reached at lower temperatures (von Helmolt and Eberle 2014, Baroutaji, Wilberforce et al. 2019). Despite research looking towards lower temperature compression, safety is still a major worry, which is why it was not chosen for this study.

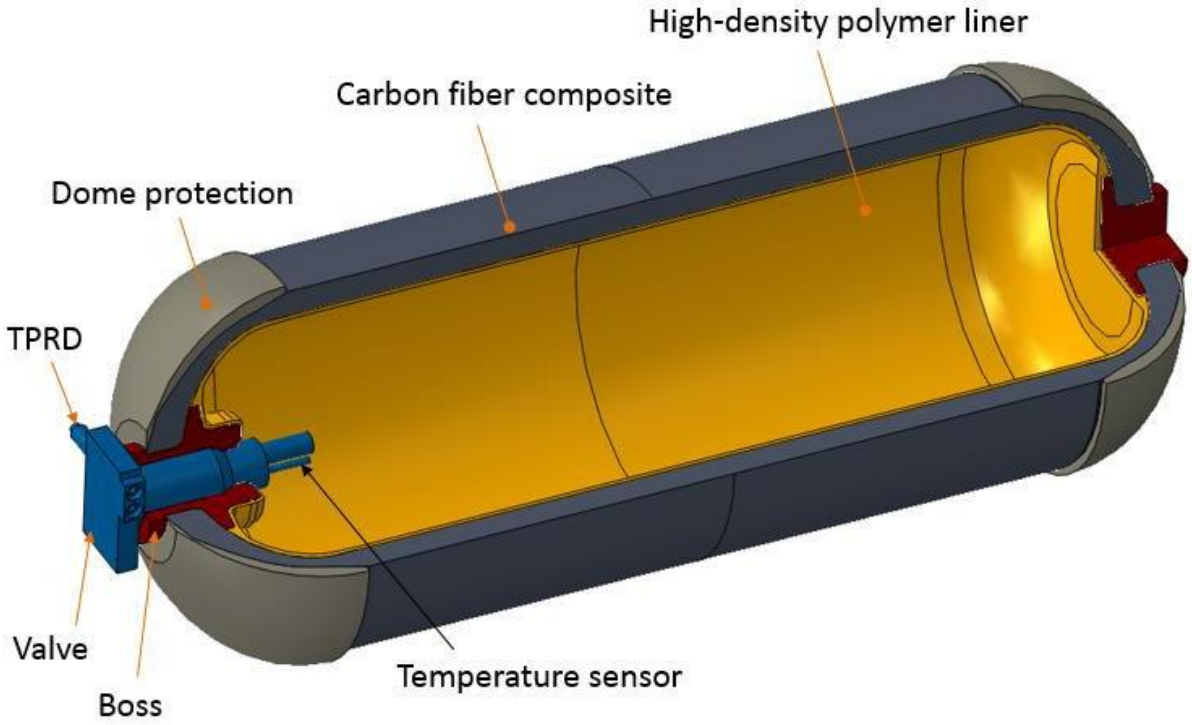

TPRD = Thermally Activated Pressure Relief Device

Credit: Process Modeling Group, Nuclear Engineering Division. Argonne National Laboratory (ANL)

Figure 2.2.1.1: Components of a pressurized hydrogen storage tank (Rivard, Trudeau et al. 2019).

2.2.2. Liquid Hydrogen (LH2)

Hydrogen is liquefied by cooling it to - 253 °C, similar to how liquefied natural gas (LNG) is held at - 162 °C. A theoretical efficiency loss of just 12.79 percent, or 4.26 kWh/kg out of 33.3 kWh/kg, is possible (Sadaghiani and Mehrpooya 2017). Depending on the quantity of mass to be liquefied, the number of chilling steps might rise, incorporating refrigeration in the mix, increasing the amount of energy consumed (Sadaghiani and Mehrpooya 2017, Rivard, Trudeau et al. 2019). Liquid hydrogen is kept in cryogenic tanks at - 253 °C at atmospheric pressure (Crabtree,

Dresselhaus et al. 2004, von Helmolt and Eberle 2014). The liquefaction cycle of hydrogen is known as Linde cycle developed by William Hampson and Carl von Linde during late 1800s (Züttel 2003). The figure below represents a typical Linde cycle process.

The Linde cycle is based exclusively on the Joule-Thomson phenomenon, which has the benefit of eliminating the requirement for moving parts on the cold side of the cooling apparatus (de Waele 2017). Liquid hydrogen was not a good option for our research since it requires a lot of energy.

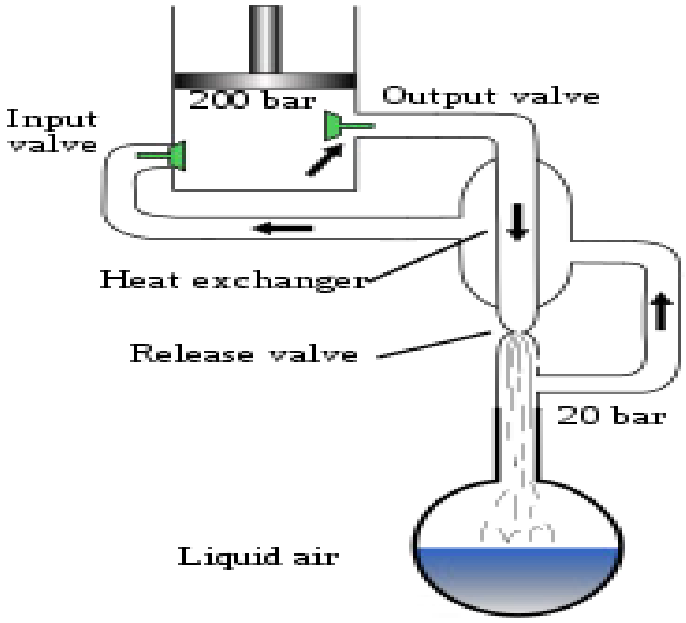

Figure 2.2.2.1: Linde cycle (de Waele 2017)

2.2.2. Solid Storage Hydrogen (SSH_2)

Traditional hydrogen storage facilities are complex, and liquid hydrogen necessitates the installation of a refrigeration unit to maintain a cryogenic state, increasing weight and energy expenses, as well as a 40% loss in energy content (Madriklridis 2016). In the solid state storage there are various types of potential hydrogen storage materials from metal hydride (Absorbed on interstitial sites in a host metal), MOF (physisorption in porous materials) to light elements hydride such as boron, aluminium and nitrogen hydrides (complex compounds) to name a few (Zuttel 2004, Jianjun and Wenqing 2012, Møller, Sheppard et al. 2017).

The storage is by absorption of chemical compounds or by adsorption onto the material. Every technical solution has benefits and disadvantages, and the choice of a technology is determined by the nature of the problem in such a manner that the downsides have a minimal influence on the entire application (Zuttel 2004, Madriklridis 2016). In this study, MH storage material was studied into detail because hydrogen energy is at the forefront of the global economy.

2.3. Metal hydride

Metal hydrides are composed of metal that are hydride forming (A) and poor hydrating (B) and primarily the alloys existed as four ratios AB_5, AB_2, AB and A_2B but with time AB_3, A_2B_7, A_6B_{23}, A_2B_{17}, A_3B were discovered (Madridis SS., 2016; Ragheb M., 2011 & Rayner-Canham G and Overton T., 2009). Their density ability to weigh less than that of the original metal because of the change it undergoes to form metallic crystal lattice and the component brittleness but has less electrical conductivity. When it comes to absorption/desorption it offers great thermodynamic properties to work with (Madridis SS., 2016). And it comes as the favorites when compared to other storage due to the fast hydriding / dehydriding reaction rate, capacity and immune to toxic matters (Yartys V.A., et al 2019 & Hagstrom M.T., 2000). They can be prepared by heating up the metal with hydrogen under certain pressure (Madriklridis 2016). The qualitative analysis of SSH2 is shown in Table 2.2.3.1.1, and the results indicate that the method of storage chosen and material for absorption is suitable. The equation below represents the chemical interaction between the alloy and hydrogen:

$$M + \frac{X}{2}H_2 \leftrightarrow MH_X + Q \qquad \text{eq. 2.3.1}$$

Table 2.3.1: Qualitative analysis of main criteria of solid hydrogen storage families (Yartys, Lototskyy et al. 2019)

Compound families	Gravimetric capacity	Volumetric capacity	Minimum and maximum delivery temperature	Absorption / desorption rates	Toxicity, abundancy
Metallic hydrides (AB_2, AB_5..)	🔴	🟢 🟡	🟢	🟢	🔴 🟡
Magnesium hydride and alloys	🟢 🟡	🟡	🔴 🟡	🟡	🟢
Complex hydrides (alanates, borohydrides)	🟢	🟡 🟢	🟡 🔴	🟡	🔴 🟡
Chemical hydrides (amides, aminoboranes..)	🟢	🟡	🟡 🔴	🔴 🟡	🔴 🟡
Adsorbent materials (nanocarbon, MOFS)	🟢 🟡	🟡	🔴	🟡	🟢 🟡

Color code: Red = deficient; Yellow = Fair; Green = Good

The equilibrium pressure, which is the pressure of absorption in a condition of dynamic equilibrium, shows the response direction (Lototskyy 2016). If the hydrogen gas pressure exceeds the equilibrium pressure, the reaction continues to the right to generate a metal hydride and if pressure falls below the equilibrium pressure, hydrogen is released, and the metal reverts to a gaseous form. The Van't Hoff expression is used to describe the equilibrium pressure equation below (Koultoukis, I Gkanas et al. 2014). The expression is in its simplest form, and the equation has been modified by researchers throughout the years (Lototskyy 2016). With all mentioned reason, AB_2 alloy was studied further and used as an ideal material.

$$\ln P_{eq} = \frac{\Delta H_f}{RT} - \frac{\Delta S}{R} \qquad \text{eq. 2.2.3.1.2}$$

2.3.1. AB alloy

In the midst of hydrogen storage material, AB has a high absorption capacity (1.8-1.9 wt percent), good kinetics for sorption and desorption of hydrogen following activation, adequate equilibrium

pressures (5-10 bar), and a reasonable cost among hydrogen storage materials (Reilly and Wiswall 1974). However, TiFe has the significant drawback of being difficult to activate at room temperature (Reilly and Wiswall 1974). However, despite the benefits, its drawbacks must be overcome before this combination may be used in a practical application. As previously stated, insertion of replacing elements is a popular way for modifying a hydride's hydrogen sorption capabilities (Thompson, Reilly et al. 1979). V, Mn, and/or other transition metals are commonly added to partially substitute Fe in this combination. For instance, when a trace of Mn is swapped for Fe in the TiFe parent compound (Reilly and Wiswall 1974, Thompson, Reilly et al. 1989, Callister and Rethwisch 2018). Unfortunately, the material in issue was not employed in our study for the reasons stated.

2.3.2. AB_5 alloy

The intermetallic group is formed by elements from atomic number 57 – 71 for A and B-elements from Cu, Mn, Co to Si to name a few. The group has a wide range of PCT adaptable to compound ratio substitution, with 25 ℃ plateau pressure varying over the magnitude relying on the composition (Sandrock 1999). With AB_5s, hysteresis develops, but it is minimal, and there is a potential that the plateau will be flat, as with AB_2s, when using a multicomponent alloy (MacDonald and Rowe 2006).

AB_2 alloyAB_2 intermetallic represent a lave phase large group of hydriding material, with A standing for elements with atomic number from 57 – 77 (like Ti and Zr), and B is from 23 – 26 (V – Fe) (MacDonald and Rowe 2006). Laves phases are the most diverse category of intermetallic, with a wide variety of characteristics, their stability is affected by parameters like as geometry, packing density, valence electron concentration, and electronegativity difference, and notably Zr-based alloys, have been identified as promising hydrogen storage materials (Hagström, Klyamkin et al. 2000, Madriklridis 2016). They offer strong hydrogen storage capacity and kinetics, as well as a long cycle life and inexpensive cost, but they are generally too stable at room temperature and are susceptible to gas contaminants (Koultoukis, I Gkanas et al. 2014).

In this study, $Ti_{0\ 98}Zr_{0\ 02}V_{0.43}Fe_{0.09}Cr_{0.05}Mn_{1.5}$ was utilized as an AB2 material, and the material is reported to have acceptable thermodynamic properties since it produces a flat plateau of the PCT, which is still an optimum condition, with pressure from 1- 10 bar and temperature from 0 – 100 ℃ (Hagström, Klyamkin et al. 2000, Koultoukis, I Gkanas et al. 2014). This condition is brought by

partial substitution of element A with Ti and B with Fe, this is done due to the fact that after absorption the AB_2 material becomes too stable and cause the reversible process to take time (Shaltiel 1978, Zhang, Wang et al. 2012). The figure below presents a typical PCT graph of AB_2 intermetallic compound. Because of the foregoing, the study chose this intermetallic.

2.4.1. Pressure-composition-isotherm (PCI)

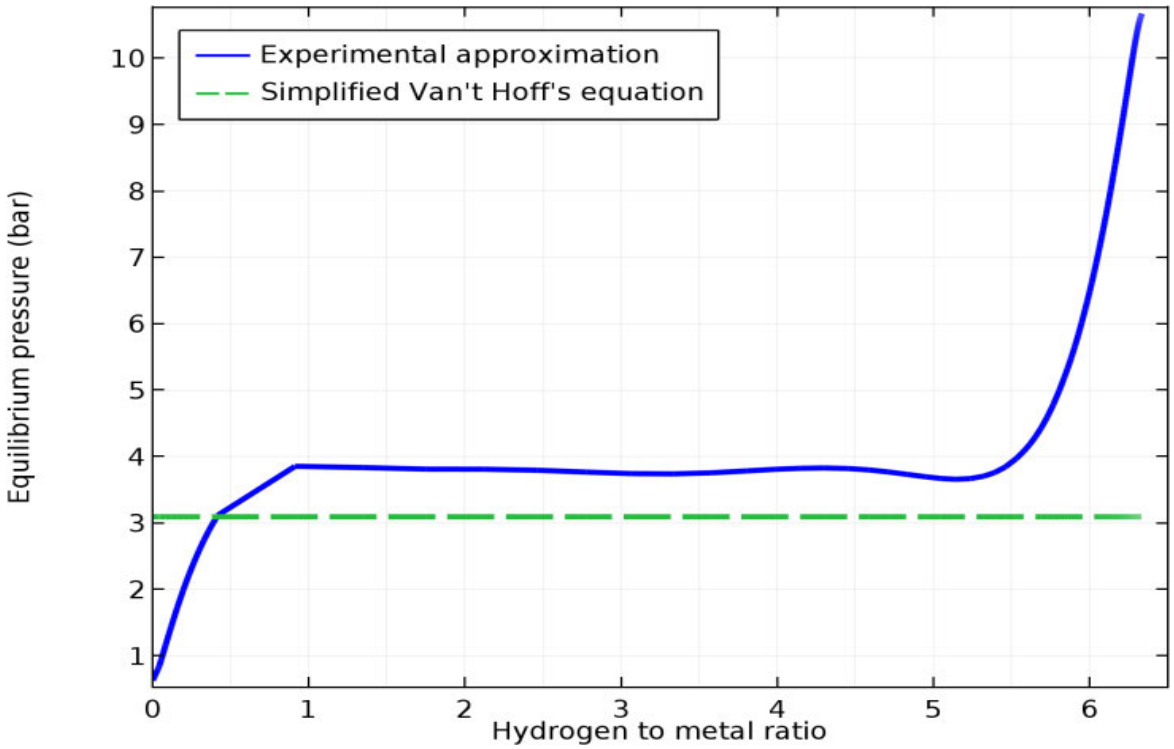

Figure 2.4.1: Pressure – Composition- Temperature diagram (Koultoukis, I Gkanas et al. 2014)

The depicted figure above illustrates the phase equilibria between a gaseous phase and a solid phase, offering insights into the compositional interaction of the gas within the solid material at a constant temperature while manipulating pressure levels (Tserolas, Katagiri et al. 2010). PCI (Pressure-Composition Isotherm) or PCT (Pressure-Composition-Temperature) data can indeed be correlated with various thermodynamic properties of materials, including metal hydrides or other substances in the fields of chemistry and materials science (Gschneidner, Bunzli et al. 2005). By analysing PCI or PCT data, researchers can gain insights into phase transitions, adsorption/desorption behaviour, and thermodynamic properties such as enthalpy and entropy

changes associated with these processes (Zhao and Freeman 2007). This information is critical for the design and optimization of materials and systems, especially in areas like hydrogen storage, gas adsorption, sorption, and energy storage applications. In the study, the PCI was modelled from pressure polynomials experimental data by performing regression or producing an ideal PCI graph and used as a model.

2.4 Metal hydride cycle

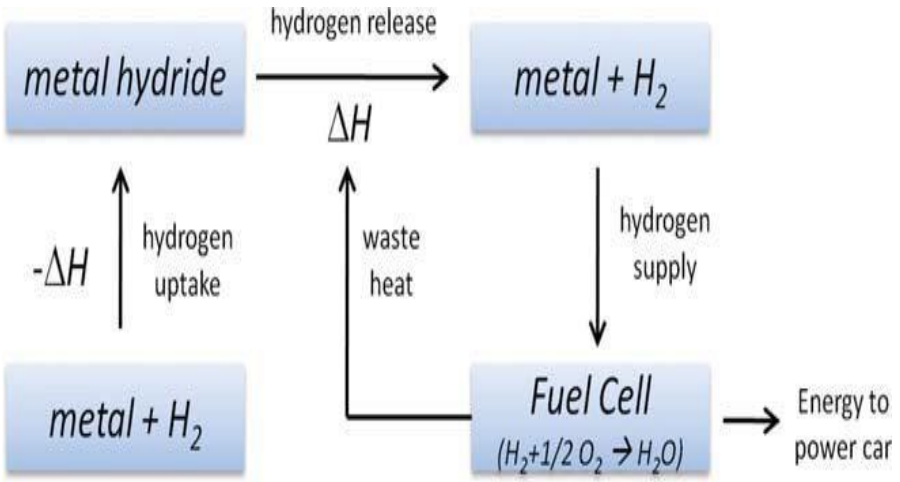

Figure 2.5.1: The principle of metal hydride tank reversible storage of hydrogen (Adelhelm and de Jongh 2011)

The process is thermally driven, operating been two temperatures (low and high) (Lototskyy, Klochko et al. 2012). The operating condition of the metal hydride reactor are shown below in figure 2.4.2 (Popeneciu, Almasan et al. 2009). Metal hydrides offers reversible sorption, which the forward reaction is absorption and said to be exothermic as the temperature increase after hydrogen injection, the reverse reaction (desorption) requires heat to release the stored hydrogen for use (Olaitan and Kolesnikov 2011). The temperature evolution involved in the sorption process, heat removal is also important as it is shown in figure 2.4.1, the cooling system (water jacket) is needed to provide heat removal and addition to the MH bed in the reactor. And has the advantage because of thermal compression reactor is that the energy release from the forward reaction can be used to initiate the reverse reaction (Libowitz G.G. and Brookside 1976, Bouzgarrou, Askri et al. 2016). Hydrogen released is fed into fuel cell to produce energy to be used for stationary and on board applications, depending on demanding of energy it can be used for car as shown as the output on figure 2.4.1.

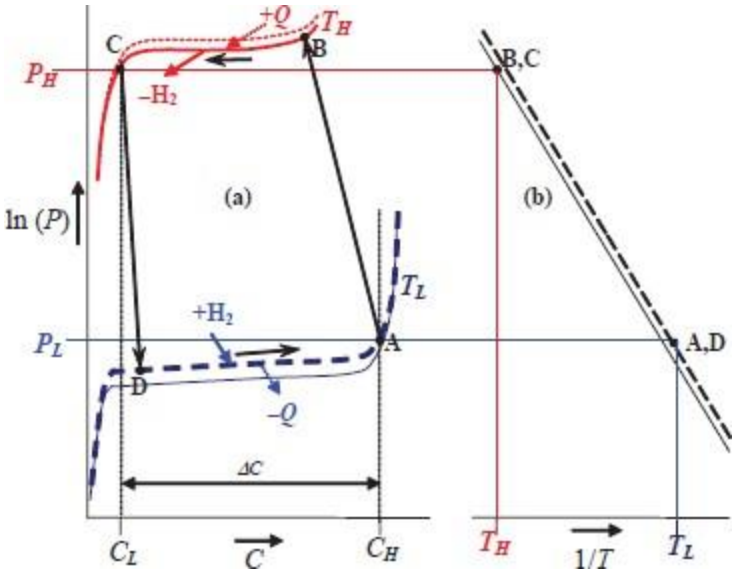

Figure 2.4.2: P-C-T curve for MH_x compressor (Popeneciu, Almasan et al. 2009).

2.4. Metal hydride review

In the late 1980s, Mayer et al. proposed a one-dimensional model for transient heat and mass transfer within the metal hydride bed (Mayer, Groll et al. 1987). The paper presents both experimental and theoretical work which are compared against each other. Thus, the work mainly looks into determining the reaction rate and the pressure-temperature distribution of the metal hydride of the bed. In the findings, it was found that the experimental work suggests the absorption and desorption process is two-dimensional (in r and z-direction), while the simulation work only shows results in the radial (r) direction. Otherwise, a very good agreement in trends between theoretical and experimental data of pressure, temperature, and concentration was discovered (Mayer, Groll et al. 1987, MacDonald 2006).

During the time of Mayer et al., Sun and Deng also provided an extensive body of work on hydrogen storage systems consisting of experiments to simulate and formulate models. In 1988, they studied the attributes of heat and mass of metal hydride beds. The study reflected the effect of hydrogen pressure and hydrogen-metal ratio, physical properties of Metal hydride, and operation parameters using a pragmatic model which comprises effective thermal conductivity in the hydride.

From the obtained results of $TiMn_{1.5,}$ it was seen that the absorption/desorption process occurs in the whole hydride bed, so the intensification of heat transfer is important to shorten the reaction time (Sun and Deng 1988). They continued with their study but in this case, they used a two-dimensional unsteady state model. The main purpose was to anticipate the temperature and hydrogen capacity administering profile of the hydride bed of which a good correlation was found when compared with their experimental data (Sun and deng 1989). All their previous studies paved the way to formulate a theoretical model to predict the effective thermal conductivity of a hydride bed and its fixation on other parameters. The parameters that affect ETC were hydrogen pressure and concentration, reaction temperature, diameter and conductivity of the hydride particle, and void fraction. And it was said that effective thermal conductivity is an important parameter in studying heat transfer enhancement (Sun and Deng 1990). Some of the studies they conducted at the beginning of the 1990s, were repeated work but used the effective thermal conductivity model to better understand its limits by doing experiment and simulation to verify their work. They also employed a new hydride ($MlNi_{4.5}Mn_{0.5}$) and the trends were showing confidence in agreement (Sun and deng 1990).

Jemni A et al. has released a series of paper characterizing the absorption and desorption process and developed analytical mathematical expression. In the 1995 papers, the research was a two-dimensional model based on two sets of mathematical equations accounting for hydrogen gas and metal hydride for absorption and desorption on different papers respectively. The models for the hydriding and dehydriding of hydrogen were the same except for the kinetic expression to differentiate the sorption process (Jemni and Ben Nasrallah 1995, Jemni and Ben Nasrallah 1995). Their study finding undertaken under the assumption to not include the heat transfer by convection found that the thermal equilibrium assumption is not valid throughout the reactor. And the increase in effective thermal conductivity of the bed has a great impact on the performance of the metal hydride reactor. Due to the findings and conclusion drawn in 1995 work, in 1997 research, they came up with new hypotheses on local thermal equilibrium, pressure variance, and the effect of concentration on equilibrium pressure, which is in contrast with their previous work. And all the hypotheses were discovered to be true for a reactor containing $LaNi_5$ (Ben Nasrallah and Jemni 1997). At the end of the 1990s, they conducted an experimental and theoretical study using the very same metal hydride used in the 1997 study. The study was to firstly determine the effective thermal conductivity, then the conductance of the hydride and working fluid (hydrogen), evaluate the pressure-temperature evolution, and derive a mathematical equation for reaction kinetics and equilibrium pressure (Jemni, Ben Nasrallah et al. 1999).

A good agreement between the theoretical and experimental data was found using the derived set of equations. Mat and Kaplan adapted and validated Jemni A et al., model to perform a theoretical study using a different AB_5 metal hydride, the study was validated through experimental studies in literature, and they concluded that the model predicts the same temperature distribution for the formation of the hydride (Jemni, Ben Nasrallah et al. 1999, Mat and Kaplan 2001).

Askri et al., proposed two-dimension transient heat and mass study in a closed process to investigate the effect of parameters such as temperature, hydrogen pressure, dimension of the reactor, alloy-hydrogen ratio, and volume expansion. The study is carried out using the control-volume-based finite element method (CVFEM) in a simulation program. The model was developed in a way to account for every aspect involved in the sorption process from physics, and chemicals to geometry consideration. From the observation taken in the study, it was seen that the volume expansion inside the reactor affects the pressure distribution and hydrogen desorbed.

The other issue that was looked at was the effect of height and radius ratio on the equilibrium state of the process and it was concluded that from a large ratio to a smaller ratio there is a time reduction to reach the equilibrium state (Askri, Jemni et al. 2004). In the other body of work, they used Lattice Boltzmann Method (LBM) to predict a two-domain dynamic heat and mass transfer computationally. The developed algorithm was compared to a well and most developed computational fluid dynamics (CFD), to check if it can be relevant under different operating conditions and validity. The model proved to be effective and versatile and has less CPU time when compared to CVFEM. It was validated by comparing its sorption data with experimental data of which the trends suited or fitted considerably.

The study conducted by Wang et al. constitutes three (3) parts to study the effect of constant and varied effective thermal conductivity (ETC) of metal hydride bed on a hydrogen sorption storage reactor. the first constituent was to use a theoretical Sung and Deng model to prognosticate the ETC of the powder MH bed $LaNi_5$, the second was to experimentally measure the ETC of the same powder, and lastly, experiments along with simulation for the sorption process of hydrogen study was done. From the calculation and experimental data of effective thermal conductivity at different pressure and temperature, a good correspondence was established between the two and the ETC is affected by hydrogen concentration and pressure.

In the findings of the sorption process, the varied ETC showed better comparability than when using the constant model. And from the work and comparison from other researchers' literature, it was deduced that the varied ETC model gives good results, and it can be used to predict other MH's bed ETC (Suda, Kobayashi et al. 1981, Sun and Deng 1990, Wang, Tien et al. 2011).

Recently most of the studies are focused on modification of the metal hydride or on using other numerical methods to solve and providing appropriate PCT conditions of a certain hydriding metal. Moropeng ML., 2019, used the Newton-Raphson method to solve the Lacher concentration of hydrogen equilibrium pressure at a constant temperature model. The Lacher model was developed by Lacher JR, in 1937 under the assumptions that there are an explicit number of pores for hydrogen sorption to take place and absorption is directly proportional to the number of pores (Lacher 1937).

In the study of Moropeng ML, the C++ platform was used to decode the Pressure-Composition isotherms of different AB_5 hydride metals and forecast the correct temperature range aligned with pressure for the hydrogen storage process. And it was unraveled that the sorption process and PCT diagram resulted in a flat pressure plateau at temperatures lower than critical ones for Lacher and Newton-Raphson method, also when corresponded with literature correlation was found between the data set. From the results, it was concluded that numerical techniques are cost-effective and time-efficient when it comes to estimating approximate values for the experimental procedures (Moropeng, Kolesnikov et al. 2019).

Heat and mass transfer is a huge problem faced when it comes to metal hydride storage systems, in the study of Lin X et al., addresses the issue by using pulverization and self-densification models for metal hydride beds. There are using AB_2-type ($Ti_{0.98}Zr_{0.02}V_{0.43}Fe_{0.09}Cr_{0.05}Mn_{1.5}$/ HWT5800) alloy, on the model which is coupled with an existing model to find the radius ratio proportion of the metal hydride to determine the absorption rate and suitable temperature for the process. The process is taken under unsteady state conditions and the effective thermal conductivity is predicted using Zehner-Bauer-Schlunder (ZBS) model. The findings of the study suggest that pulverization causes the thermal diffusivity of the alloy to decrease but increases the reaction constant as well as shortens the absorption rate and through self-densification, the rate of absorption is greater. In closing, it was said that the thermal distribution of the bed from top to bottom has a direct impact on the process along the Z-direction (Lin, Sun et al. 2019).

Thus, in the present study apart from Wang et al., the numerical modelling design of MH reactor adopting varied effective thermal conductivity model for $Ti_{0.98}Zr_{0.02}V_{0.43}Fe_{0.09}Cr_{0.05}Mn_{1.5}$, AB_2 metal

alloy, which is said to have best discharging properties (Maceiras, Alfonsin et al. 2015). In the above studies discussed are focused on heat transfer improvement by altering parameters that affect the effective thermal conductive, height-radius ratio, hydrogen inlet pressure-temperature, or equilibrium properties of the alloy and not on the inside storage tank (or reactor) configuration. And there another limiting factor in the sorption process is that it does not have a model that describes the forward and backward sorption process occurring simultaneously (MacDonald 2006)

Chapter 3

3. Model

3.1. Process description

Hydrogen reacts reversibly with metal/alloys to form metal hydrides and heat; the chemical reaction equation below represents the phenomena. The process of formation of metal hydrides is said to be absorption as stated in the literature and the reverse is desorption, for the reaction to occur a storage system is needed. In this study Wang et al., setup is going to be considered, using AB_2 compound to make design upgrades and establish optimum operating conditions which will be safe and economical for use. All that will be achieved by developing a model describing the reactor and with the aid of COMSOL Multiphysics 5.2 will be able to understand the process inside the storage equipment. With the guidelines are stated below:

Assumption

- The gas phase is ideal, from a thermodynamic point of view.
- The media are in local thermal equilibrium between gas and solid.
- The solid phase is isotropic and has a uniform and constant porosity.
- The reactor is considered in two dimensions.
- Hydrogen is supplied at the inlet to the bed at a known constant pressure.

3.2. Chemical Reaction Equation

Chemical reaction equation representing the exothermic absorption process and endothermic desorption process of hydrogen.

$$M + \frac{X}{2}H_2 \leftrightarrow MH_X + Q \qquad \text{eq. 3.2}$$

Where *M* stands for a metal or alloy, *H* for hydrogen and *Q* for heat released.

3.3. Mass Balance

A continuum equation for both gas and solid mass balance is used to account for absorption / desorption of hydrogen gas (Wanga Y., 2014 & Ha M.Y., 2004)

$$\varepsilon \frac{\partial \rho_g}{\partial t} + \nabla \cdot (\rho_g u) = -\Delta\rho(1-\varepsilon)\frac{\partial x}{\partial t} \quad \text{eq. 3.3.1}$$

$$\Delta\rho(1-\varepsilon)\frac{\partial x}{\partial t} = m \quad \text{eq. 3.3.2}$$

$$\Delta\rho = \rho_{bs} - \rho_b \quad \text{eq. 3.3.3}$$

Where u, $\Delta\rho$ and ρ_{bs} are momentum / velocity of hydrogen gas, change in density and density of MH bed at saturated point. The momentum is expressed by Darcy law, which means the flow is laminar flow and it assumes the following form below:

$$u = -\frac{K}{\mu}\Delta P \quad \text{eq. 3.3.4}$$

K and μ stands for the permeability, dynamic viscosity. The permeability K is calculated by Kozenye-Carman equation as shown below:

$$K = \frac{1}{150}\frac{d_p^2 \varepsilon^3}{(1-\varepsilon)^2} \quad \text{eq. 3.3.5}$$

D_p symbolize particle diameter

3.4. Energy balance

Jemni A et al…, the model considered two-phase reaction solved in the reaction (gas and solid) for storage of MH bed reactor and in conclusion, it was concluded that absorption / desorption of hydrogen in the medium can be considered to be at local thermal equilibrium (LTE) (Mat M.D. and Kaplanb Y., 2001). With the LTE assumption taken, a continuum energy equation was derived and took the form below:

$$\frac{\rho_b c_b}{K_e}\frac{\partial T}{\partial t} = \frac{1}{r}\frac{\partial}{\partial r}\left(r\frac{\partial T}{\partial r}\right) + \frac{\partial^2 T}{\partial z^2} - \frac{\rho_b \gamma_h \Delta H_f}{K_e} \quad \text{eq. 3.4.1}$$

T, r, and *t* denote temperature, radial coordinate, and time, respectively; ρ_b, c_b, and K_e are the density, specific heat, and the heat conductivity of MH bed. And γ_h is the reaction rate and ΔH_f is the heat of formation which is negative for both hydrogen absorption and desorption. Y_h is presented below:

$$\gamma_h = \frac{1000N}{2M}\frac{\partial x}{\partial t} \quad \text{eq. 3.4.2}$$

N, *M*, and *x* symbolise, the, number of metallic atoms, the molecule weight, and the concentration of hydrogen of the MH respectively, which is the ratio of the number of hydrogen atoms to the total number of atoms of the MH. Hydrogen absorption, $\partial x/\partial t$ and γ_h are positive while negative for hydrogen desorption. The equation for $\partial x/\partial t$ is modelled as follows:

$$\frac{\partial x}{\partial t} = \eta\left(\pm\frac{P_b - P_{eq}}{P_{eq}}\right)\frac{x - x_F}{x_I - x_F}\exp\left(\frac{-E}{RT}\right) \quad \text{eq. 3.4.3}$$

η, *E*, and *R* they respectively represent, the rate constant, activation energy, and universal gas constant, respectively. x_I and x_F are the initial and final hydrogen concentrations during the absorption/desorption process; P_b and P_{eq} are the pressure in the reactor and equilibrium pressure. The equation 3.2.2.4, below and figure 2.2 shows the relationship between pressure (P), concentration (C) and temperature (T) characteristics of MH reactor (Moropeng M.L et al., 2020)

$$\ln P_{eq} = \frac{\Delta H_f}{RT} - \frac{\Delta S}{R} \quad \text{eq. 3.4.4}$$

ΔS is the entropy of the hydride formation.

3.5. Effective Thermal Conductivity (ETC) Model

Effective thermal conductivity is one of the factors affecting heat and mass transfer in the metal hydride reactor because it has low conductivity than the parent material of synthesis (Rayner-Canham G and Overton T., 2009 & Maan H.B., et al 2018). Wang et al…, (2011), did some work on both constant and varied ETC by employing the model from Sun and Deng of K_e in MH bed. And the ETC equation (eq. 3.5.1) reckons the following form:

$$K_e = [1 - \frac{4}{\pi}(1 - \varepsilon)](K^* + r\ h\ ) + \frac{\frac{4}{\pi}(1-\varepsilon)(1-\tan\theta)\ \frac{1-\pi}{4}}{\frac{\pi - \tan\theta}{(1-\tan\theta)K^*_g} + \frac{4}{(1-\tan\theta)K^*_g + ((1-\pi)/4)r_p h_{rs}}} + \frac{4}{\pi}(1 - \varepsilon)\tan\theta * K^*$$

where ε, r_p, and θ stands for the void fraction, the radius of the particles, and the contact angle between solid particles, and h_{rs} and h_{rv} the heat transfer coefficients of thermal radiation from solid surface to solid surface and from void to void, respectively. The expressions of h_{rs} and h_{rv} are written as:

$$h_{rs} = \frac{0.2269\omega}{2-\omega}\left(\frac{T}{100}\right)^3 \qquad \text{eq. 3.5.2}$$

$$h_{rv} = \frac{0.2269}{1 + \frac{\varepsilon}{2(1-\varepsilon)^*}\frac{1-\omega}{\omega}}\left(\frac{T}{100}\right)^3 \qquad \text{eq. 3.5.3}$$

In both equations 3.2.1.2/3, *T* and ω, separately, symbolise the temperature and the emissivity of solid surfaces. The thermal conductivities of hydrogen and metal hydride particles in equation 3.2.1.1, K^*_g and K^*_s, represent the effects of hydrogen pressure and hydrogen concentration, respectively.

3.6. Mass source term

Rate of sorption for both sorption processes on the metal hydride is described by Baldissin et al. (2009) as the following:

$$\dot{m} = C_a \exp\left(-\frac{E_a}{RT}\right) \ln\left(\frac{P_g}{P_{eq}}\right) (\rho_{ss} - \rho_s) \quad \text{eq. 3.6.1}$$

$$\dot{m} = C_d \exp\left(-\frac{E_d}{RT}\right) \frac{P_g - P_{eq}}{P_{eq}} (\rho_s - \rho_0) \quad \text{eq. 3.6.2}$$

Where, Cd Ca is the rate constant for absorption and desorption, Ed the activation energy for desorption, ρ^m_{emp} and ρ^m_{sat} the density of the metal hydride powder when it does not or have hydrogen, and peq is the equilibrium pressure for hydrogen desorption

3.7. Initial and boundary conditions

3.7.1. Initial conditions

The metal hydride container is considered to be in thermodynamic equilibrium; thus, the initial conditions are as follows:

$$T = T_0 \, , p = p_0 \, , \rho^m = \rho^m_{ini} \quad \text{eq. 3.7.1}$$

Where ρ^m is the metal hydride density of which in our case is partially saturated with hydrogen with 0.1 content?

3.7.2. Boundary conditions

In terms of boundary conditions, boundary walls are considered to be impermeable, hence no-slip velocity and no-flux conditions are valid. A convection boundary condition is used between the bottle walls and the outer fluid for the energy calculation.

$$k^{eff}\frac{\partial T}{\partial n} = h(T_{ext} - T) \qquad \text{eq. 3.7.2}$$

Where n is the unit normal vector out of the vessel wall and Text is the temperature of the outside fluid. A thin copper coating has been placed to the external limits to mimic the metallic container, in addition to convection with surrounding air. The thickness and thermal conductivity of the conductive material are given in terms of copper embedded in the COMSOL material code.

3.8. Geometry

Figure 3.8.1: Asymmetric geometry of MH reactor

In the above figure 3.8, it is a metal hydride design used for the simulation of hydrogen absorption and desorption. The geometry is 2-dimension asymmetric. The geometry was constructed with two radii of about 15.5 mm and height of about 600 mm. the compartments inside the tank were made with a rectangle of about the width equal the radius and the length equal to 40 mm, the rectangle was then arrayed 8 times, using array function on the COMSOL simulator to make them equal to 9. A three dimension of the tank or reactor is shown in figure 3.8.1, showing an overview of how the tank looks like inside. The material of construction used was copper (solid and polished) and the properties are also found embedded in the software determined at temperature and pressure used to simulate.

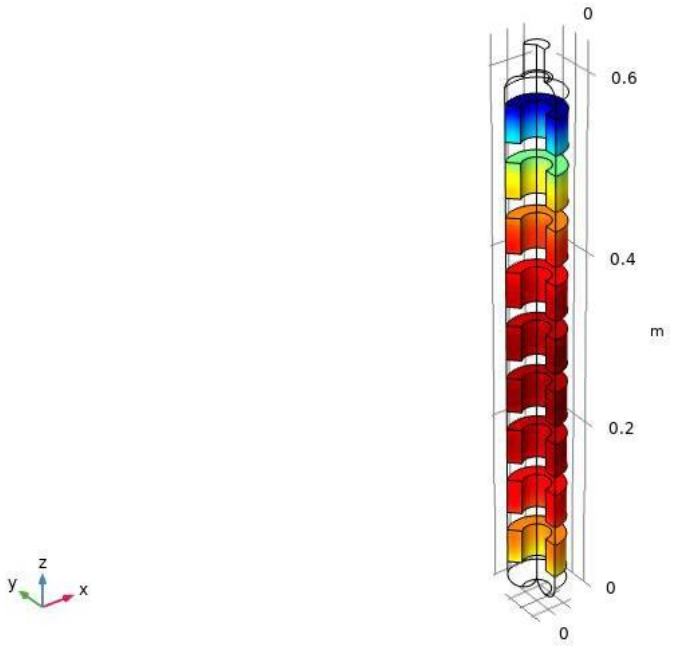

Figure 3.8.2: Three-dimensional geometry of MH

Chapter 4

4. Research Methodology

4.1. Materials

Table 4.1.1: Properties of $Ti_{0.98}Zr_{0.02}V_{0.43}Fe_{0.09}Cr_{0.05}Mn_{1.5}$ (Maceiras R et al., 2015 & MacDonald B.D and Rowe A.M., 2006)

Properties	Values	Units
Crystalline density	5577	Kg/m^3
Empty Density	5500	Kg/m^3
Specific heat	490	J/kg.K
Effective thermal conductivity	1.4	W/mK
Permeability	10^{-8}	m^2
Reaction heat of formation	$-1.359 * 10^7$	J/kg
Porosity	0.43	

The alloy with properties tabled above is assumed to have flat plateaus for absorption and desorption on P-C-T diagram. And it offers great discharge under ambient conditions.

Table 4.1.2: Properties of hydrogen

Properties	Values	Units
Gas molecular weight	$2.02 * 10^{-3}$	kg/mol
Thermal conductivity of the gas	0.127	(W/(m/K))
Universal gas constant	8.314	(J/(mol.K))
Bond energy	436	kJ/mol

Hydrogen is said to be one of the most abundant energy carrier, can be found in water and when combusted with oxygen it produces water.

4.2. Procedure

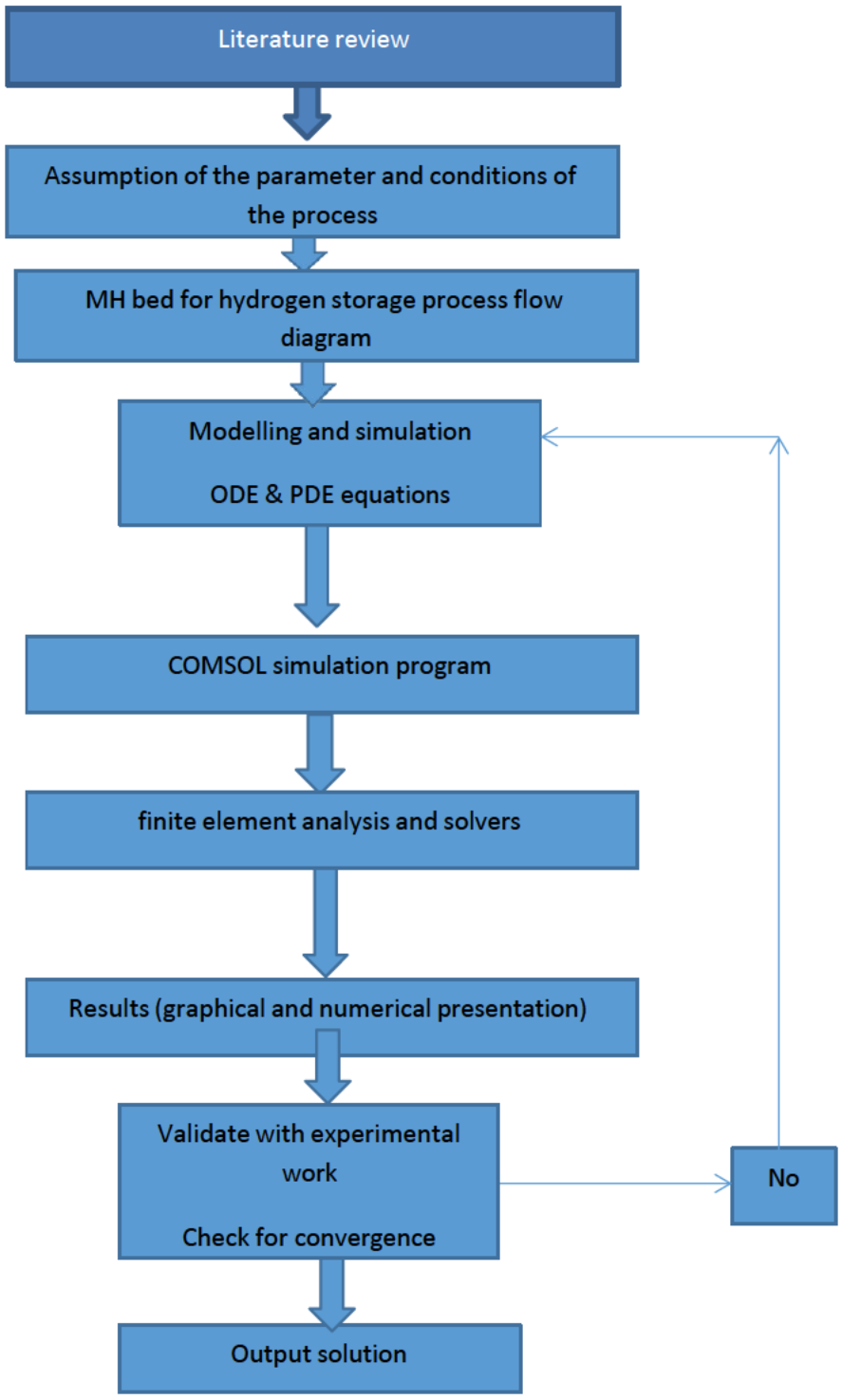

4.3. Methodology

Modelling and simulation rely heavily on literature to develop and compute a suitable mathematical model, which was comprised of partial, ordinary differential and algebraic equations, to better describe the phenomenon of the process involved. In the previous section 3, modelling of hydrogen storage system was modelled, the models include coupled mass and energy balanced models existing inside the metal hydride bed or reactor for solid and gas phase (eq 3.3.1 and 3.4.1 respectively). The equilibrium pressure dependency will be predicted by using the Van't Hoff-equation (eq. 3.4.4), and equation 3.5.1 will be used to estimate the effective thermal conductivity. All these models were taken from various literature concerning hydrogen storage and purification. The models developed will be implemented in a simulation program such COMSOL. COMSOL is a Multiphysics simulation package with mathematics, biology, geographic etc., embedded inside to predict the phenomenon described.

Using section 3 sub-section 3.1, assumptions as the foundation and the mathematical model of hydrogen compression applied into the reactor shown in figure 3.8.1 in section 3.8 containing AB_2 MH bed. The initial parameters such temperature, pressure and concentration of hydrogen were set, and the compression was under laminar flow, following Darcy's principles (eq. 3.3.4), and the discharging condition was set under ambient condition. COMSOL simulation package predicted the profiling on temperature, hydrogen concentration, pressure, and velocity distribution inside the metal hydride reactor. The equilibrium distribution was set as initial values was evaluated to come up with ways to take advantage and come up with ways to overcome the initial conditions. The process was taken under unsteady state and was ran until steady state conditions are established. In doing so, assumptions of the process condition were revisited to bring results closer to reality. In the process, operational conditions and refined design of hydrogen storage reactor were established.

4.4. Simulation

4.4.1. Physics

4.4.1.1. Darcy's law for porous media

Module

- Domains: 1- 10
- Domain, boundary and initial conditions:
  - Fluid properties1: Domains2-3
  - Initial Values: Domains; Po, velocity field = 0
  - Axial symmetry1-10: Boundaries1,2

- Wall1: Boundaries2,32-54; no-slip
- Fluid and Matrix Properties1
- Mass Source1: Domain 2 - 10; mass-source

4.4.1.2. Heat transfer in a porous media

- Domains: 2 - 10
- Variable: Temperature - T[K]
- Domain, boundary and initial conditions:
  - Heat TransferinFluids1:Domains2-3; fluid type: ideal-gas
  - Axial symmetry1: Boundaries: 1,3,5
  - Initial Values1:Domains1-3; T0
  - Heat Flux1: Boundaries: 2,8-10; convective heat flux (htc and T0 or Tf or Text)
  - Heat source: Domain: 2 - 10
  - Inflow: Boundary: 3
  - Heat transfer in porous media1: Domain1; fluid type ideal
  - Thin Layer: Copper [solid, polished]

Both the physics are governed by the equation described in chapter 3. And the domain of undescribed takes the domain of the physics domain.

4.5. Data Collection

For the purpose of this project, data was not collected experimentally; therefore, instead, research was conducted to review past literature in order to obtain pre-existing data to develop our model and use COMSOL computer software to interpret the model.

4.6. Data Analysis

The data obtained in this study was presented in the form of tables and figures (graphs and charts). Then the trends of these plots were analyzed and discussed.

Chapter 5

5. Results and Discussions

In this chapter, experimental data from the literature were used to analyze and evaluate numerical simulation solutions generated using COMSOL software. Using a 2D asymmetrical plane design, a simulation of hydrogen sorption processes in MH pellet beds is performed. The physics model, such as Darcy flow in porous, Heat transfer in a porous media, and coupled differential equations, were used to represent the conservation of Heat and Mass sorption of hydrogen-MH. The assumption developed in chapter 3 is the foundation for the observations obtained on the metal hydride reactor. The temperature, pressure, hydrogen concentration, and velocity dispersion within the metal hydride reactor were the areas of concern as a consequence. On the other hand, the performance of the suggested model was examined, and it was decided what the MH reactor ideal operating states was. A comprehensive overview of the mass and heat transfer processes occurring in the reactor will be the result.

5.1. Absorption

5.1.1. Effects of temperature

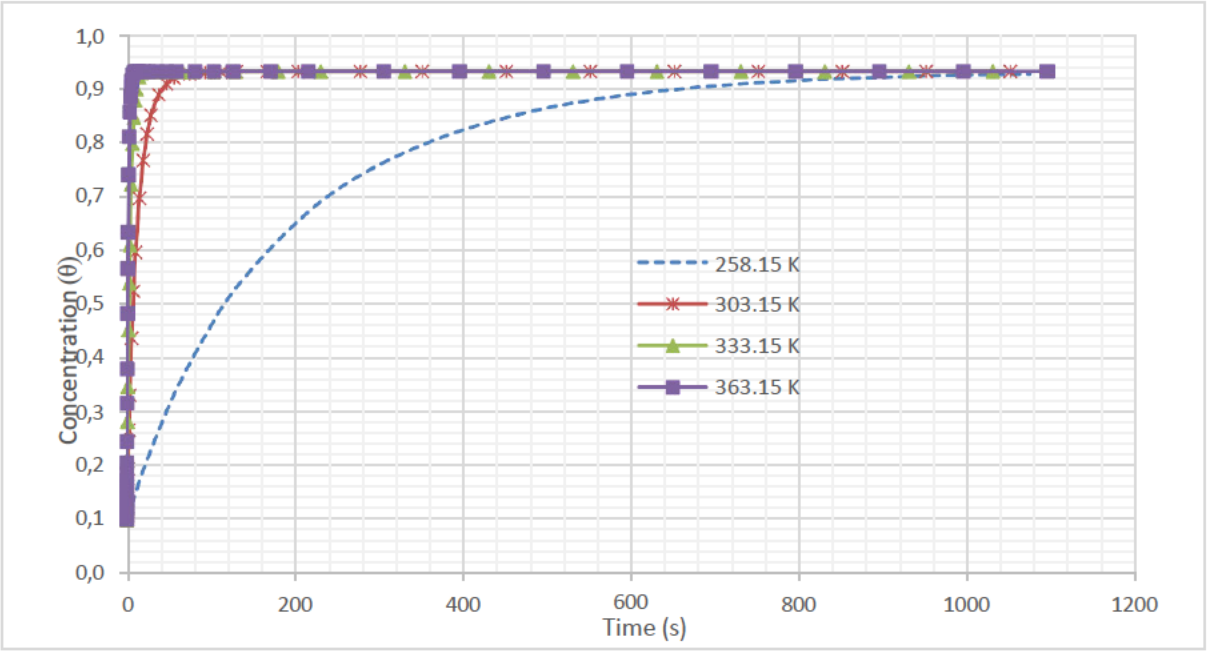

Figure 5.1.1: The effect of temperature on the concentration

Figure 5.1.1 begins at 0.1 because it was initially assumed that the concentration of hydrogen in the reactor tank MH bed was 10% (0.1) by density weight. However, in these cases, after reaching their peak levels and being exposed to cooling, the graph trend does not diminish; instead, it forms a straight flat line parallel to the time axis. The concentration emulates temperature evolution within the reactor but does not drop. Figure 5.1.1. plots the concentration trends at various temperatures while shortening the step duration to 200 seconds. The peak of the variation in hydrogen gas input temperatures occurs at various periods. The curves peak and become stable at the same time that the figure matches Figure 5.1.3 of the metal-to-hydrogen ratio. The similarity of these figures results from the concentration being determined by the metal-to-hydrogen ratio.

The input temperature concentration at 258.15 K achieves a peak of about 0.93 during the absorption of hydrogen at around 1075.78 seconds. A similar peak reached 303.15 K inlet temperature at 75.16 seconds, 333.15 K at 16.44 seconds, and 363.15 K at 8.46 seconds. The temperature development inside the reactor and all of the observations from Figure 4.1.2 point to 303.15 K as the ideal operating temperature at this point. The temperature was chosen because it will be close to the ambient temperature when compared to the other feed temperature, and the reactor operation was considered to operate close to environmental conditions.

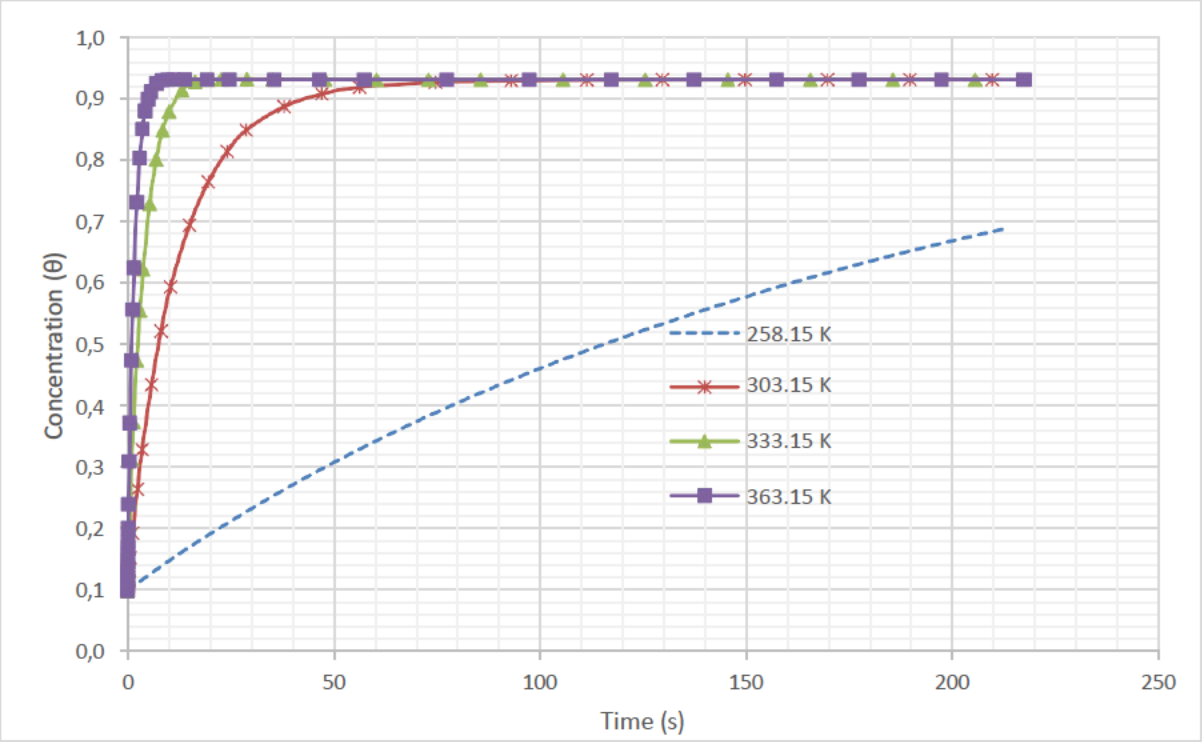

Figure 5.1.1.a: The effect of temperature on the concentration

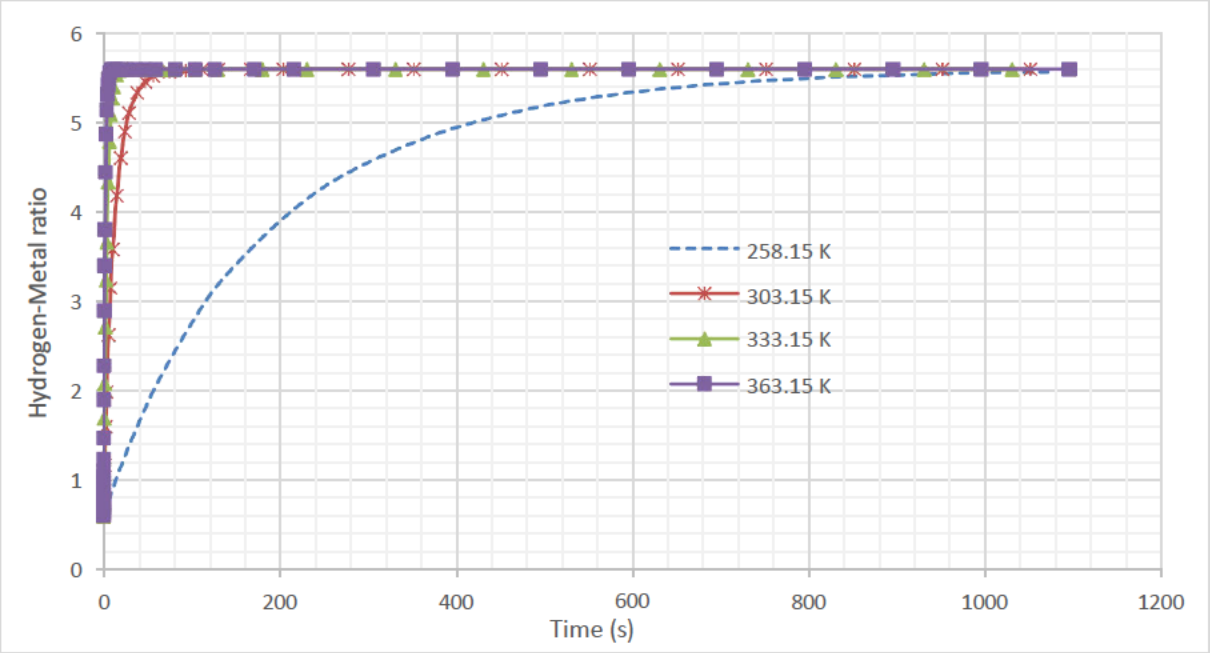

Figure 5.1.2: Metal-to-hydrogen ratio

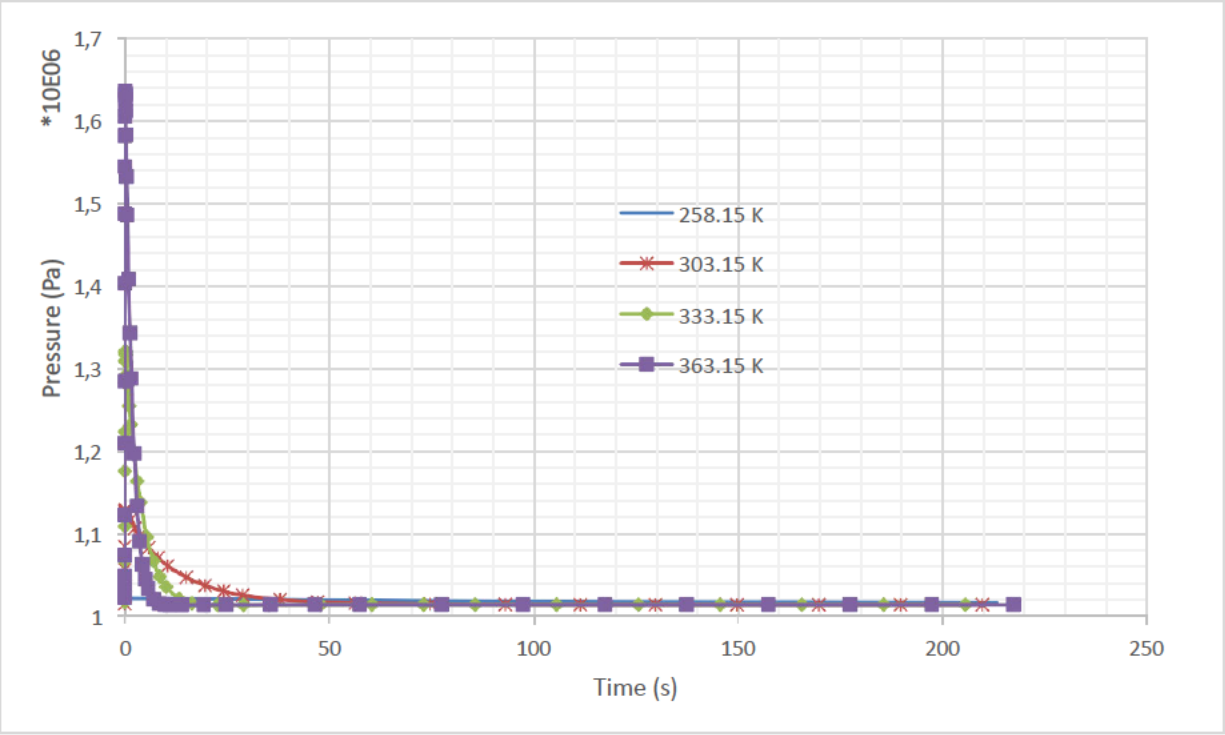

Figure 5.1.3: Pressure evolution with temperature

Figure 5.1.3 illustrates the development of gas pressure within the MH reactor at various incoming gas temperatures and constant pressure. When hydrogen gas is introduced into the reactor initially at a gas pressure of 10 atm, the pressure in the reactor rises to its maximum in a couple of seconds according to the temperatures of the gas and then falls as absorption occurs.

In contrast to when the operating temperature was 333.15 K and 363.15 K, the pressure lowers quickly while the temperature drops gradually. The pressure reduction is rapid at 333.15 K and 363.15 K, reaching starting pressures after between 10 and 15 seconds. The graphs in figure 5.1.3 become indistinguishable when the pressures approach their original values according to their temperature inlet and there is no change in absorption. The pressure rise is less at the lowest temperature compared to the higher temperature, which makes the absorption process take longer. From figure 5.1.3, it may be inferred that temperature affects reactor pressure since pressure rises as temperature rises.

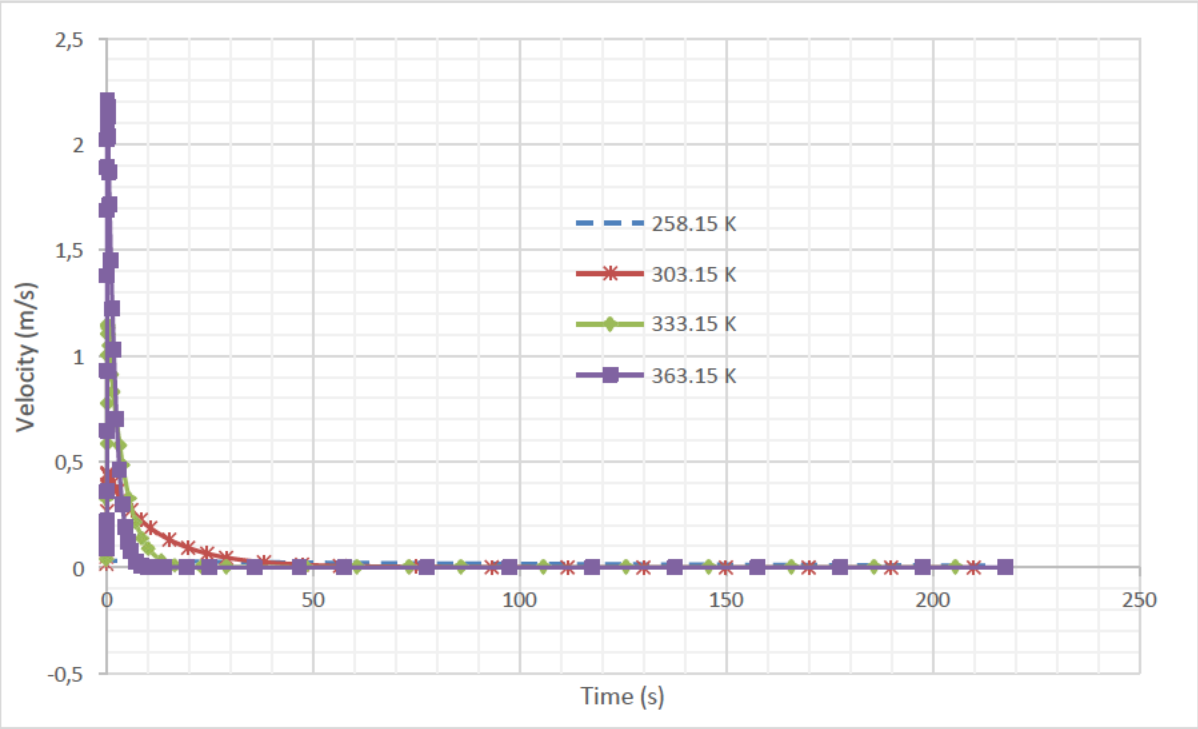

Figure 5.1.4: Velocity profile of MH bed at various temperatures

Using Darsy's equation of porous material, which also agrees with the assumption stated in chapter 3 regarding the kind of flow, laminar flow, the velocity distribution or profile of the hydrogen was computed. The profile of the velocity within the MH reactor is shown in Figure 5.1.5. The pressure gradient within the reactor drives the flow. Similar trends can be seen in Figures 5.1.3 and 5.1.5, with one reaching a steady pressure of 1013250 Pa and the other nearing 0 m/s in less than 200 seconds. Due to the enormous difference in pressure between the metal hydride reactor under ambient conditions and the input gas at 10 atm, the velocities spark off to their peaks in accordance with their temperatures as the hydrogen gas enters at constant pressure, which is 0 m/s. There is no pressure drop within the reactor since the pressure drops dramatically as the reaction proceeds and then stabilizes.

The same holds true for velocity because it is connected with system pressure; in this case, the velocity decreases until the response (absorption) comes to an end. Since velocity depends on

pressure and an increase in temperature is associated with an increase in pressure inside the reactor, the temperature indirectly affects this distribution.

5.2. Effect of pressure

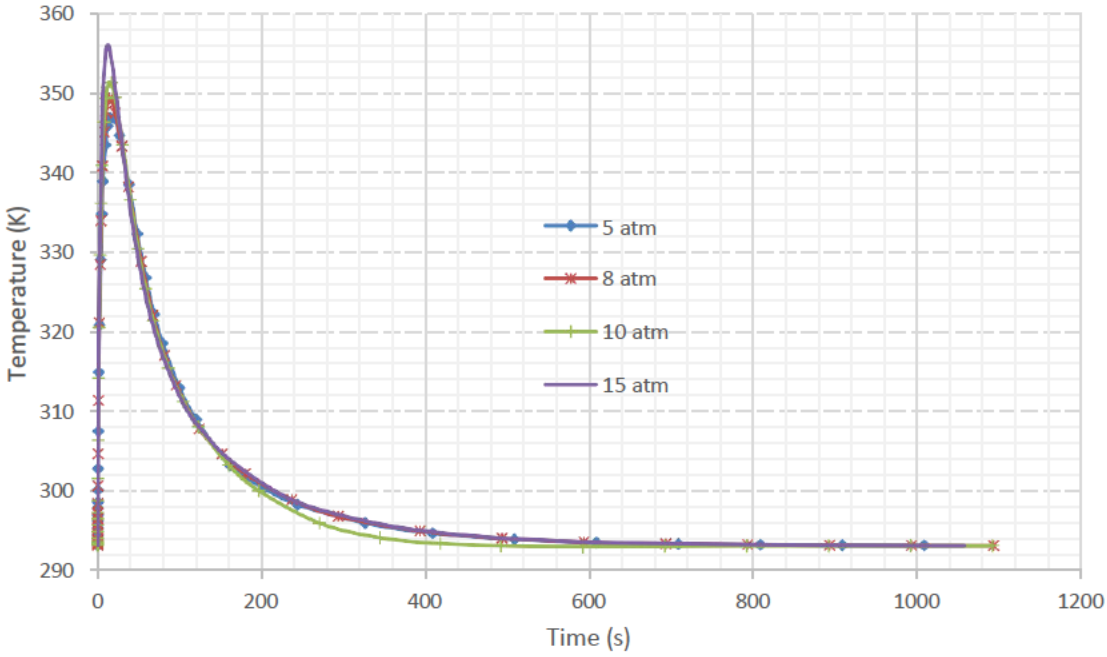

Figure 5.2.1: Influence of pressure on temperature

Figure 5.2.1 shows how pressure affects the temperature within the reactor. Even when the temperature is maintained constant at 303.15 K, pressure increases causing the temperature to rise. The temperature reaches distinct peaks at different pressures, with pressure at 5 atm reaching a high of 346.82 K, 8 atm reaching 349.34 K, 10 atm reaching 351.28 K, and 15 atm reaching 356.06 K, according to the temperature profile. The graph at 10 atm pressure displays strong cooling capabilities after reaching their separate peak, but the graphs at 5 atm, 8 atm, and 15 atm are indistinguishable from one another due to their similar trajectories. These findings from the aforementioned figure imply that the ideal operating state for the MH reactor would be a supply pressure of 10 atm.

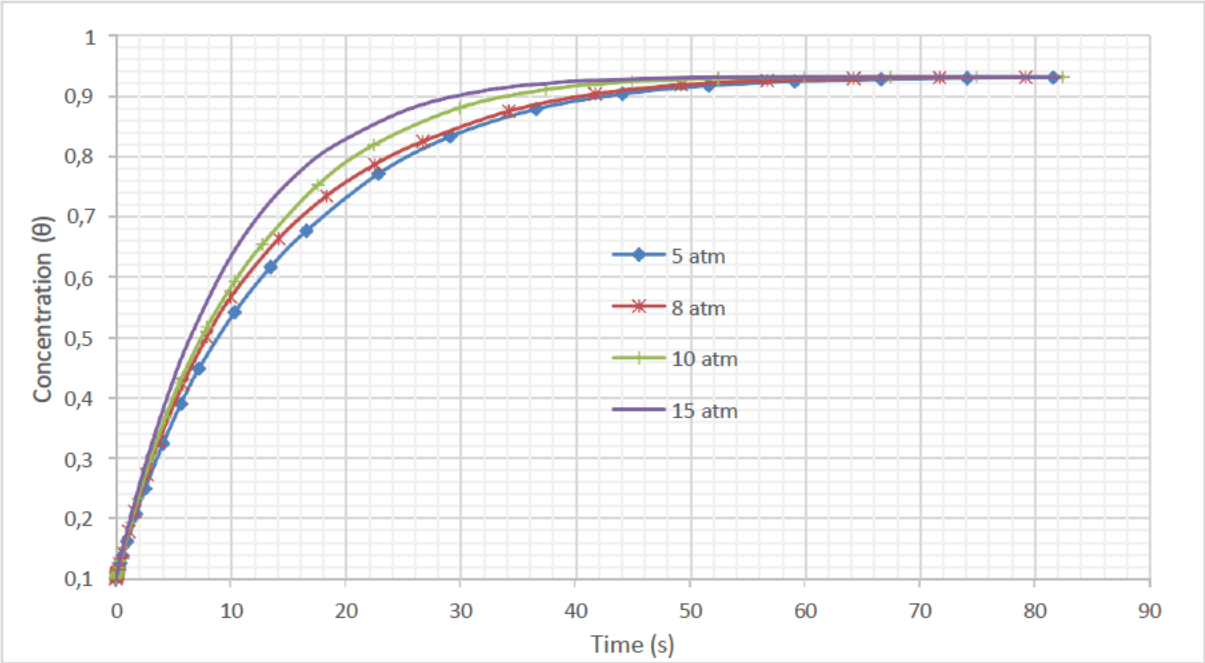

Figure 5.2.2: Impact of pressure on concentration

Figures 5.2.2 and 5.1.1 illustrate how pressure and temperature both affect concentration by raising both while maintaining a constant value for the other. As a result, concentration upsurges as a result of both temperature and pressure increases. The graph's curves mirror the curve in figure 4.1.2 at 303.15 K, however, they peak at different points in time due to various pressure supplies. Peaking out at 66.65, 64.26, 52.48, and 52.19 seconds from the lowest to the highest pressure respectively, to reach the concentration of 0.93. The supply pressure of 1'013'683.40 Pa (10 atm) may be a useful operating parameter when considering the peak out time. In the figure legend pressure is indicated as atmospheric (atm) pressure because in Pascal is a huge number, so the units will be used interchangeably.

Figure 5.2.4 depicts pressure-induced velocity; in this instance, hydrogen gas velocity increases as hydrogen gas supply pressure drops, whereas figure 4.1.4 depicts temperature-induced velocity increasing with temperature. In the scenario depicted in the preceding figure, the temperature was maintained at 303.15 K and the ETC was around 12 (W/m*K). The velocity shown in the figure is consistent with the assumption made to maintain the flow regime as laminar flow and Darcy's law of porous media since hydrogen gas has a low velocity that is under 0.65 m/s at all supplied gas pressures. The maximum velocity measured at 5 atmospheres was 0, 6126 (m/s), while the lowest was 0, 3496 (m/s) at 15 atmospheres. In general, it may be claimed that at the same operational parameters, pressure and temperature-induced velocity are the opposite of one another.

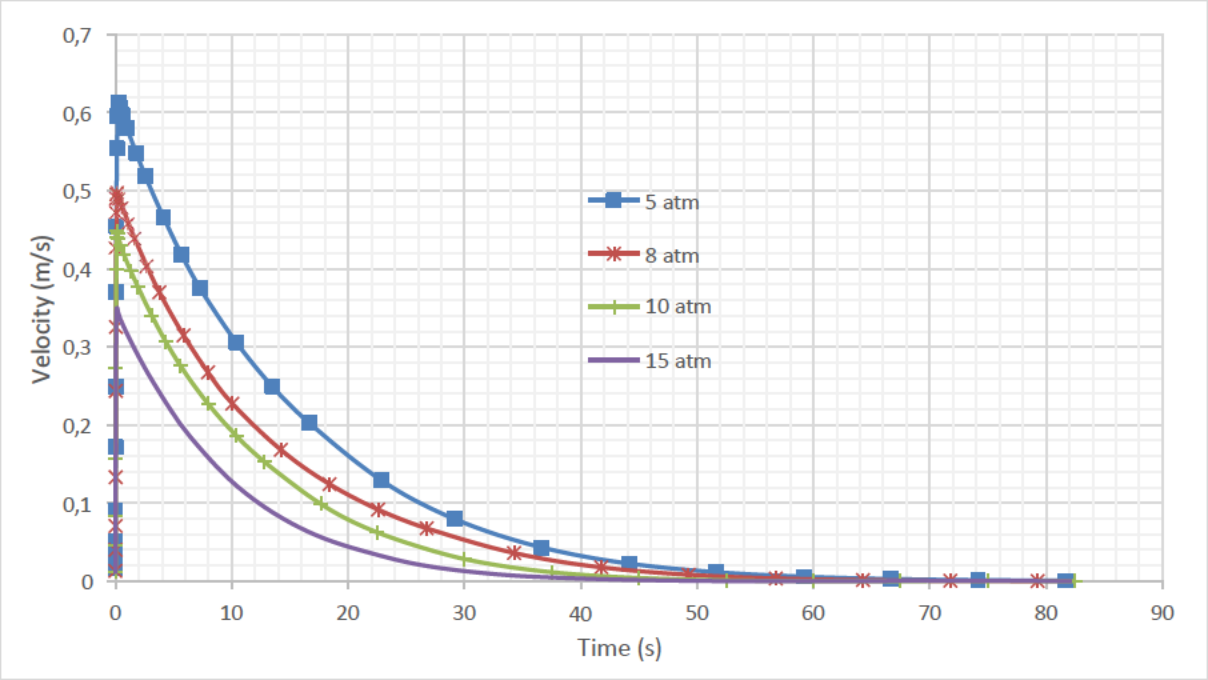

Figure 5.2.3: Pressure-induced velocity profile

5.3. Operational parameters

5.3.1. Temperature

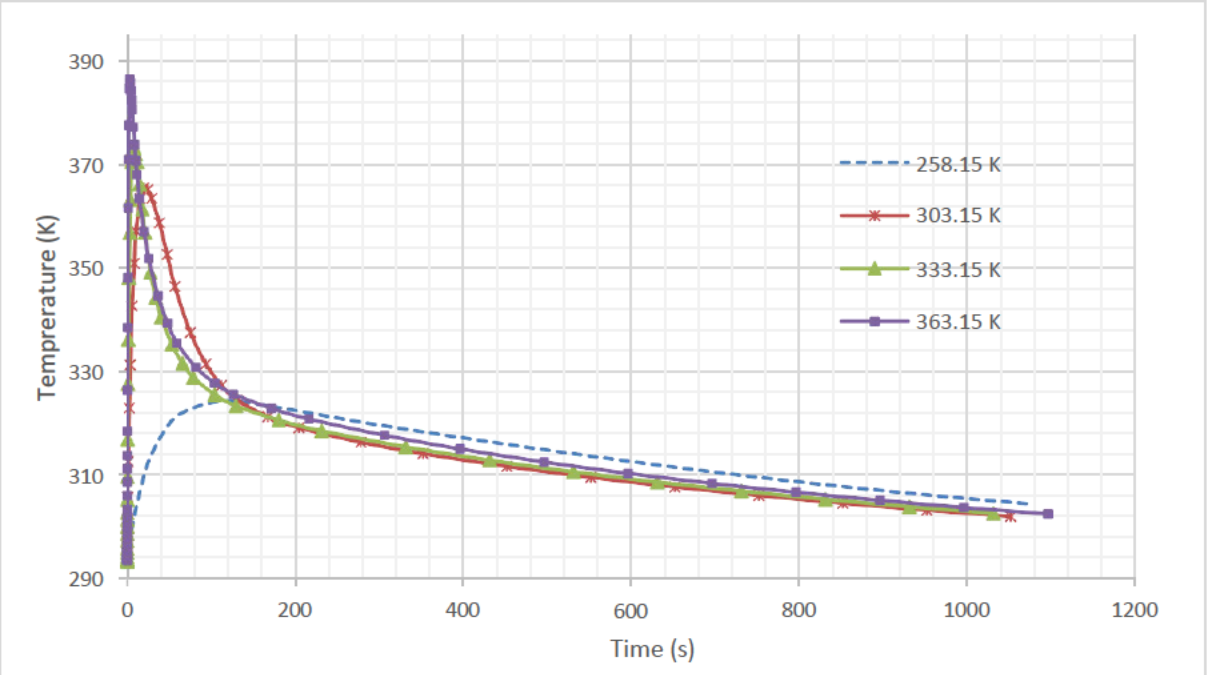

Figure 5.3.1.1: Temperature profile at different gas temperatures

The illustration of the MH temperature profile at various hydrogen gas feeding temperatures is shown in Figure 5.4.1. Absorption reactions are characterized by profile trajectories, which show a sharp rise in temperature from an initial value of about 293.15 K to various peaks. Chapter 2 of the literature described the phenomena's behavior. Convection with the surrounding fluid, which causes the temperature to drop, encourages hydrogen storage and absorption in the reactor. From lowest to highest, the peak temperatures are 324.14 K, 365.52 K, 373.13 K, and 386.54 K, respectively. The results indicate that the ideal gas temperature at 303.15 K, shown as a solid line with asterisks shows potential as an ideal temperature for operating as it is supported by scaling of hydrogen on the metal alloy as illustrated in figure 5.1.1. This is because, with except 15 K, the temperature difference between the beginning reactor temperature and the reaction's peak is rather modest. Following the patterns, it is evident that the gas inlet at 363.15 K is where it achieves the largest peak. High-temperature trends can also have an impact on other components used onboard (or mobile). Due to the low temperature, which causes the reaction to remain stagnant and lengthens the fueling time of hydrogen, which is the problem of hydrogen storage, hydrogen gas at an input temperature of 258.15 K profiling does not reflect the predicted temperature profile. Another finding showed that absorption is influenced by the temperature differential between the reactor and intake gas (hydrogen).

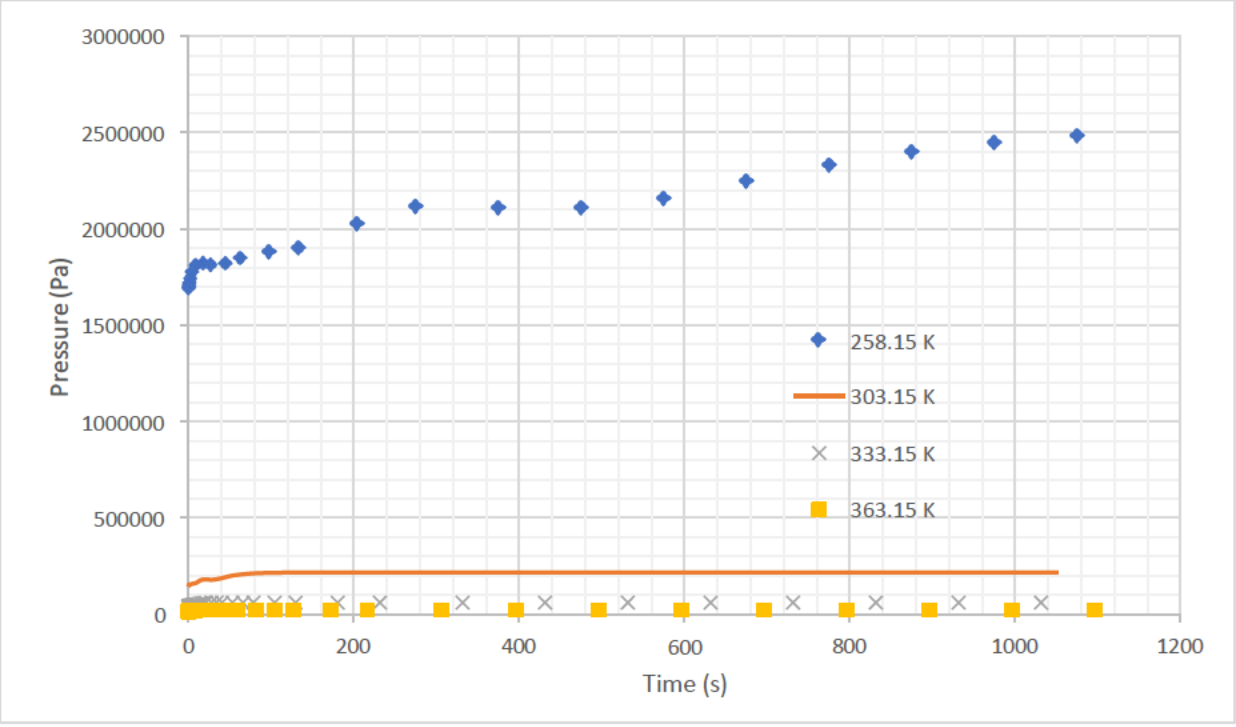

Figure 5.3.1.2: Equilibrium pressure rate

The equilibrium state was observed to be significantly influenced by temperature; wherein lower temperatures were found to result in elevated equilibrium pressures. This phenomenon increased the demand for input gas pressure at the same time, thereby posing operational hazards and undermining the safety protocols governing storage facilities. Moreover, the challenges

encountered under conditions of cool temperature were compounded by diminished concentration of hydrogen in the metal hydride. At exalted temperatures, the equilibrium pressure plummets as depicted by the area between the pressure at 258.15 K and 303.15 K in fig 5.4.2, also suggesting 303.15 K is suitable rather than other temperatures which yield low or high concentration and heat management issues as illustrated in figure 5.4.1. In the appendices, Figure 5.4.1 a, and b illustrate the pressure equilibrium profiling and the phenomenon that occurs for hydrogen absorption to take place in the metal hydride between gas and equilibrium pressure.

5.3.2. Pressure

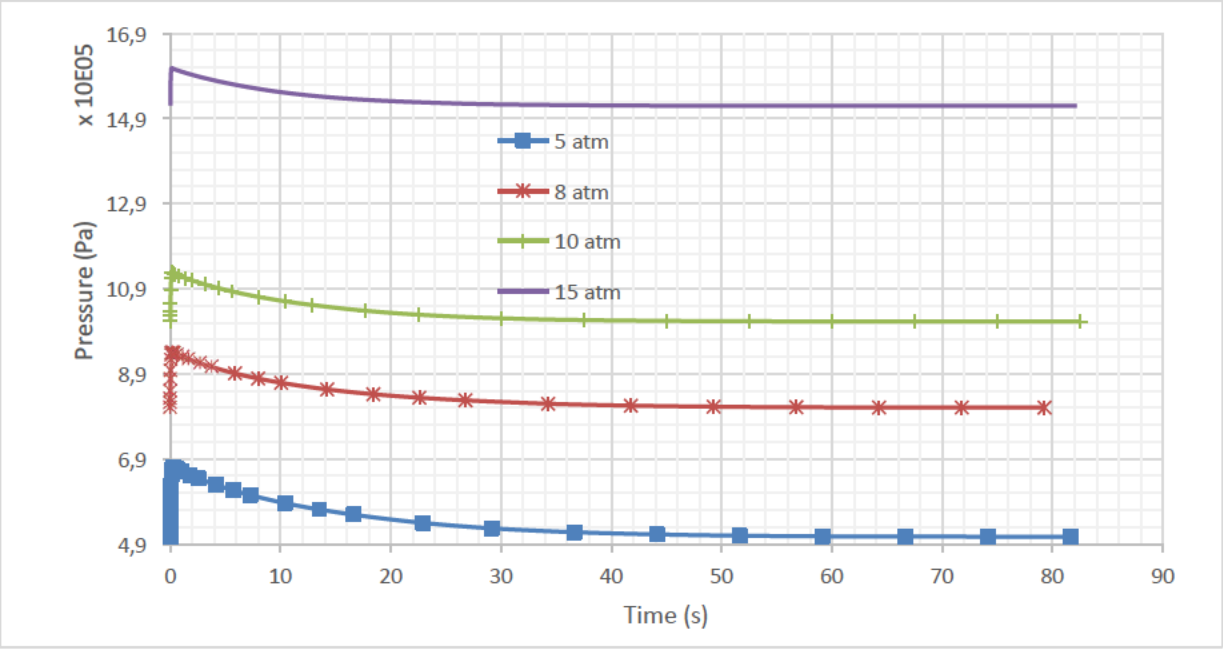

Figure 5.3.2.1: Supplied pressure

The hydrogen pressure delivered to the metal-hydride beds inside the reactor is shown in Figure 5.4.2.1 above. The curves or graphs on the figure all have the same general shape, beginning at the applied pressure and then rising sharply as a result of the compression between hydrogen gas and metal alloy during absorption after the applied pressure falls and stabilizes. And after being applied, the supply pressure becomes the working pressure (absorption pressure) during the sorption process. The graphs crest are as follows respectively to supplied pressure: 670'013, 4 Pa, 939'608 Pa, 1'128'413 Pa, and 1'608'624 Pa. The pressure starts exactly from the supplied to reach their crest with 506'971. 30 Pa (about 5 atm) is the lowest supplied and has the lowest crest and the graphs are separated with no intercepts, each having its asymptotes.

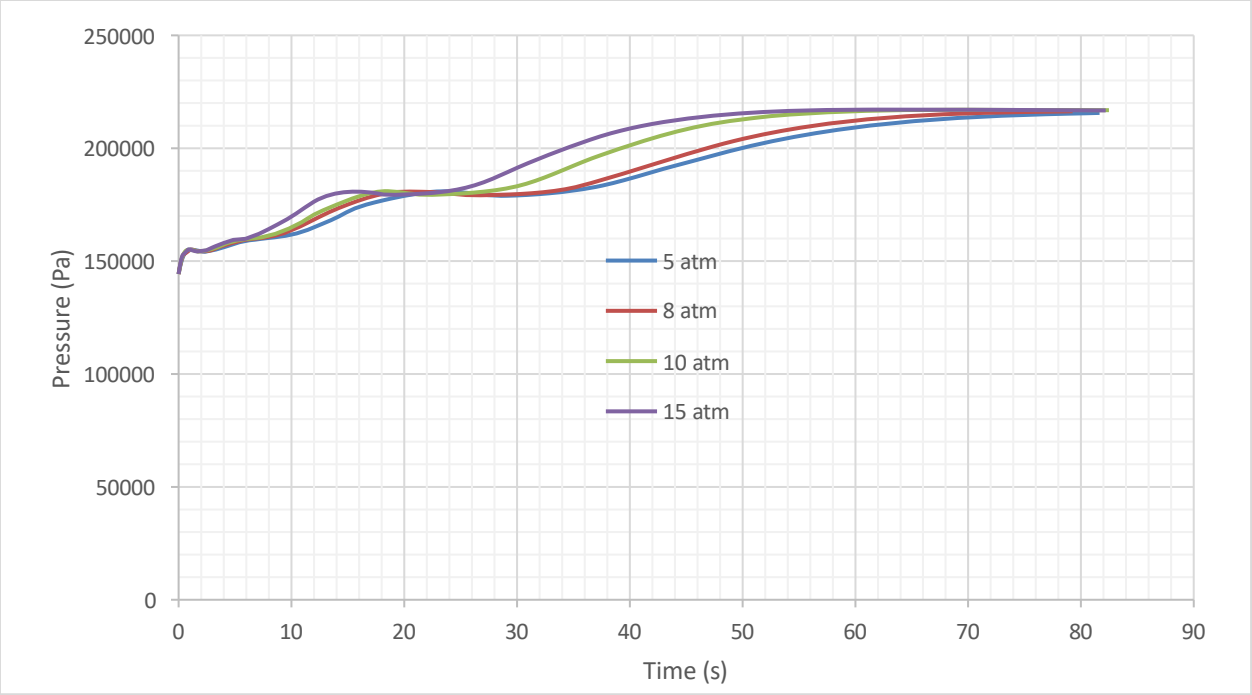

Figure 5.3.2.2: Pressure effect on equilibrium

The impact of hydrogen pressure on the equilibrium state is graphically depicted in Figure 5.3.2.2 above, elucidating pressure variation at a fixed temperature exhibit different outcomes in comparison to temperature variations under conditions of constant pressure refer to fig 5.3.1.1. And the area between each operating pressure has diminished. Considering Figures 5..2.1 and 5.3.2.2 in conjunction, it is evident that a substantial elevation in the supplied pressure results in a noteworthy augmentation of the operating pressure, as is evident within the range spanning from 5 to 15 atmospheric pressures. Based on the observed results, taking into account the concentration data portrayed in Figure 5.2.2 and considering the previously mentioned operational constraints, a pressure of 10 atmospheres can be deemed as the optimal choice for operating the storage system. Figure 5.3.2.2 illustrates the interrelation between hydrogen gas operating parameters and equilibrium pressure, providing new insights on the parameters required for the effective development of hydrogen-storage activities.

5.4. Desorption

5.4.1. Effect of temperature

In figure 5.4.1.1 describes the effect of heating fluid temperature on the concentration of hydrogen on the metal hydride. The desorption of hydrogen from metal hydride is sensitive to high temperature. At low temperature the desorption of hydrogen occurs smoothly, the concentration falls to low content in the metal alloy. As the temperature increases, the concentration of hydrogen until it reaches a constant value showing that the desorption process can no longer proceed.

At temperatures of 288.15 K, 293.15 K, and 303.15 K, the rate of decline in concentration accelerates significantly as the hydrogen desorption process approaches near depletion, thereby impeding the attainment of elevated concentration levels requisite for energy generation. As the temperature ascends, precisely at 318.15 Kelvin, the phenomenon of desorption experiences a pronounced hindrance. The efflux of hydrogen is observed to be below 0.025 units of concentration per unit temporal increment. Subsequently, the system begins to manifest attributes akin to the suppression of hydrogen uptake. The prompt uptake of hydrogen following its release signifies an excess of energy favouring the absorption process. At temperatures exceeding 318.15 K, the desorption process ceases to exhibit preferential behaviour, yielding dominance to the absorption process. Figure 5.4.1.1 depicts the thermodynamic response of the sorption process as a function of increasing temperature.

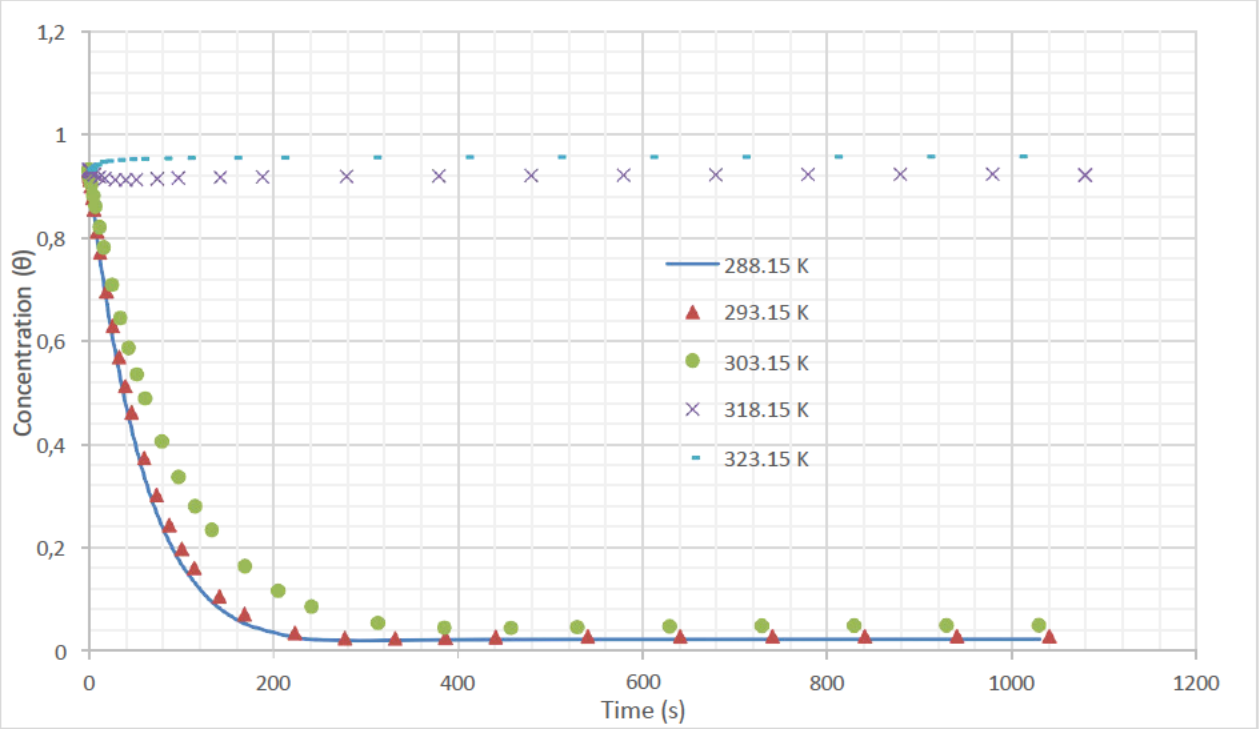

Figure 5.4.1.1: Effect of temperature on dehydrogenation

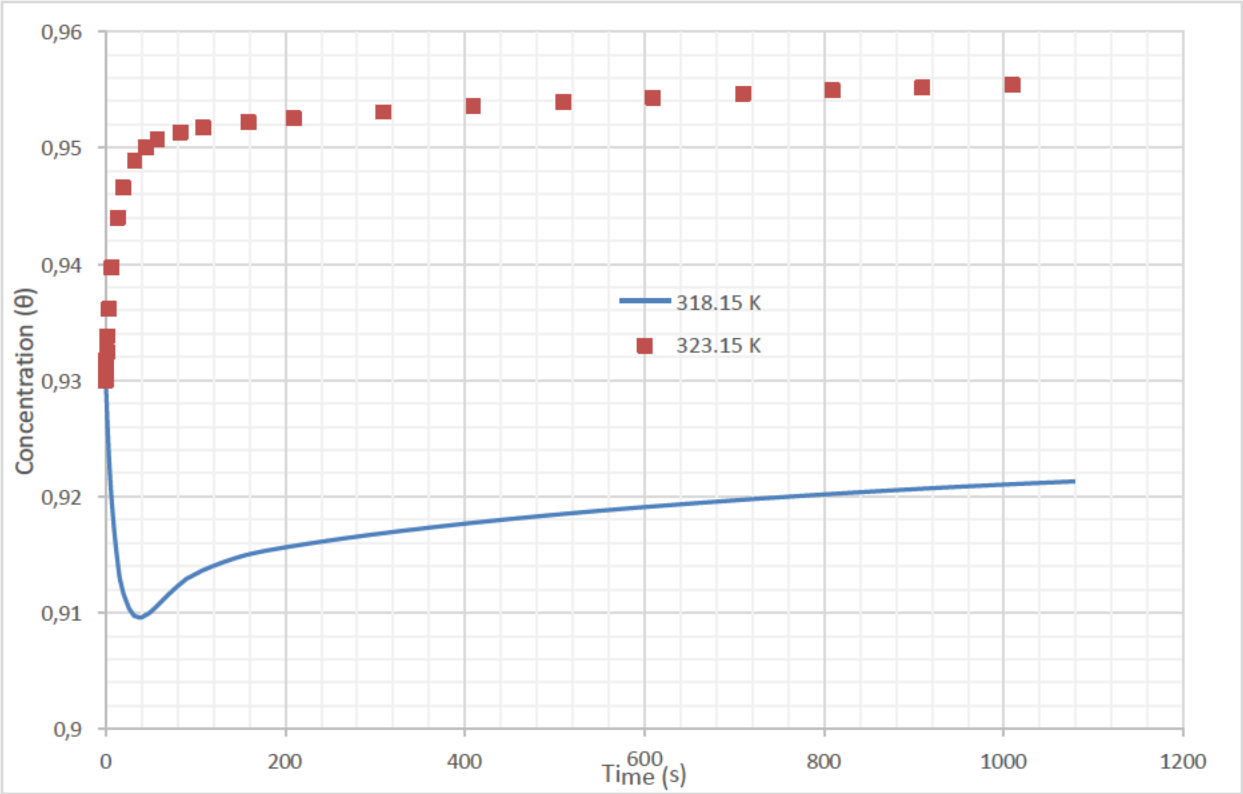

Figure 5.4.1.1.a: Effect of temperature on dehydrogenation

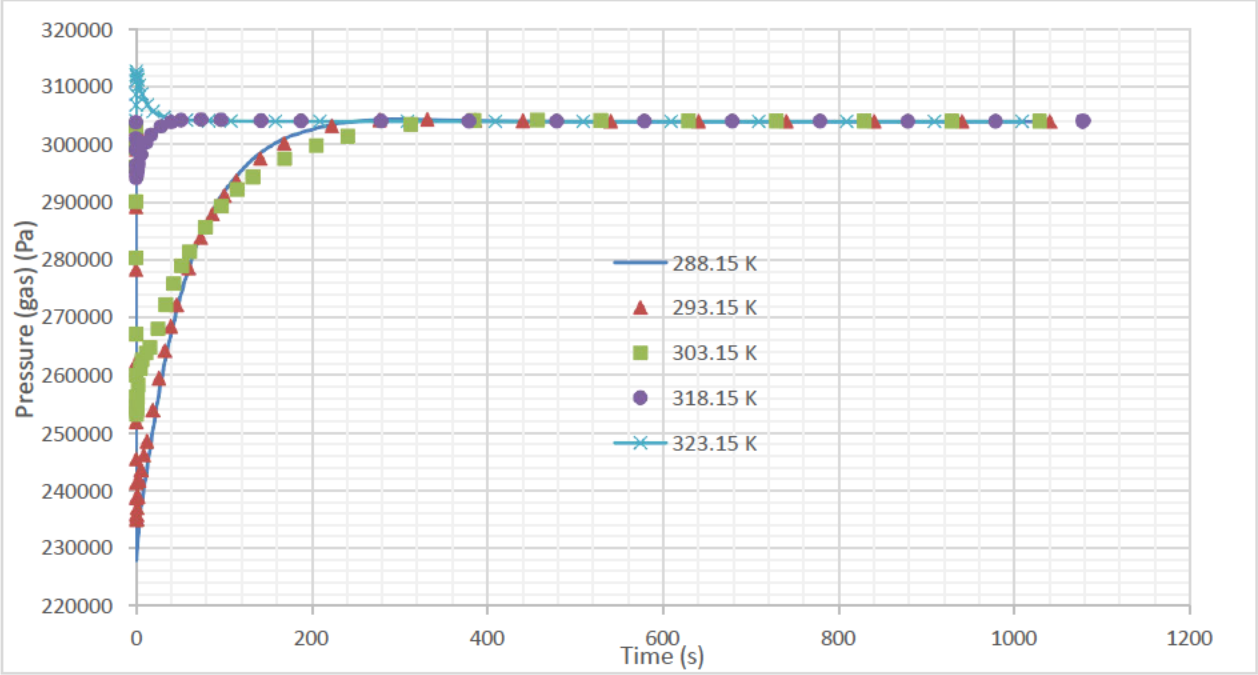

Figure 5.4.1.2: Effect of temperature on pressure

In the context of hydrogen desorption, it is stipulated that the gas pressure must remain below the equilibrium pressure for the process to proceed. Figure 5.4.1.2 illustrates the temporal

evolution of the working pressure of hydrogen within the containment vessel during the course of the process. At all heating temperatures, apart from 323.15 K, the pressure initially starts at 3 atm, subsequently exhibits a decline to a minimum, and then undergoes a recovery phase to reach its initial level. However, at 323.15 K, the pressure profile mirrors the absorption trend depicted in Figure 5.1.4. and 5.4.1.2a. The pressure profiles for desorption and absorption processes exhibit distinct characteristics. In absorption, there exists a direct proportionality between temperature and pressure, where an increase in temperature corresponds to a commensurate rise in pressure. However, in the case of desorption, such a direct relationship does not hold true. Instead, each temperature manifests its unique pressure trend until it converges back to the initial pressure level.

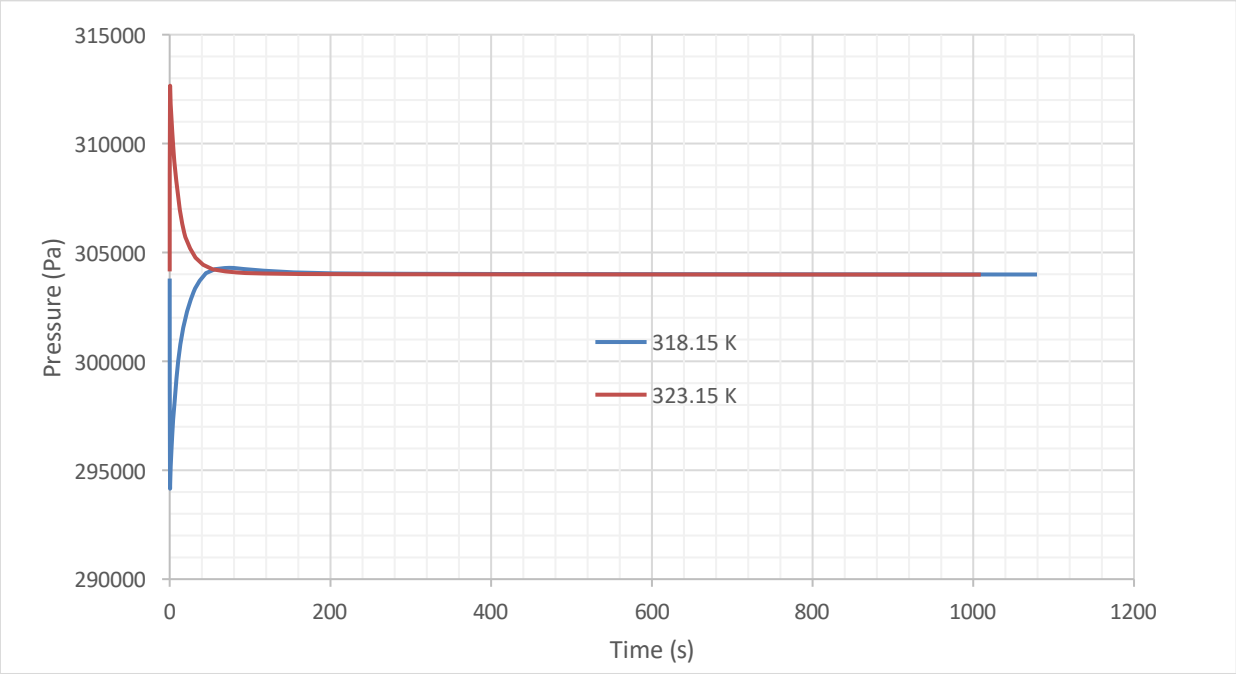

5.4.1.2.a: Effect of temperature on pressure

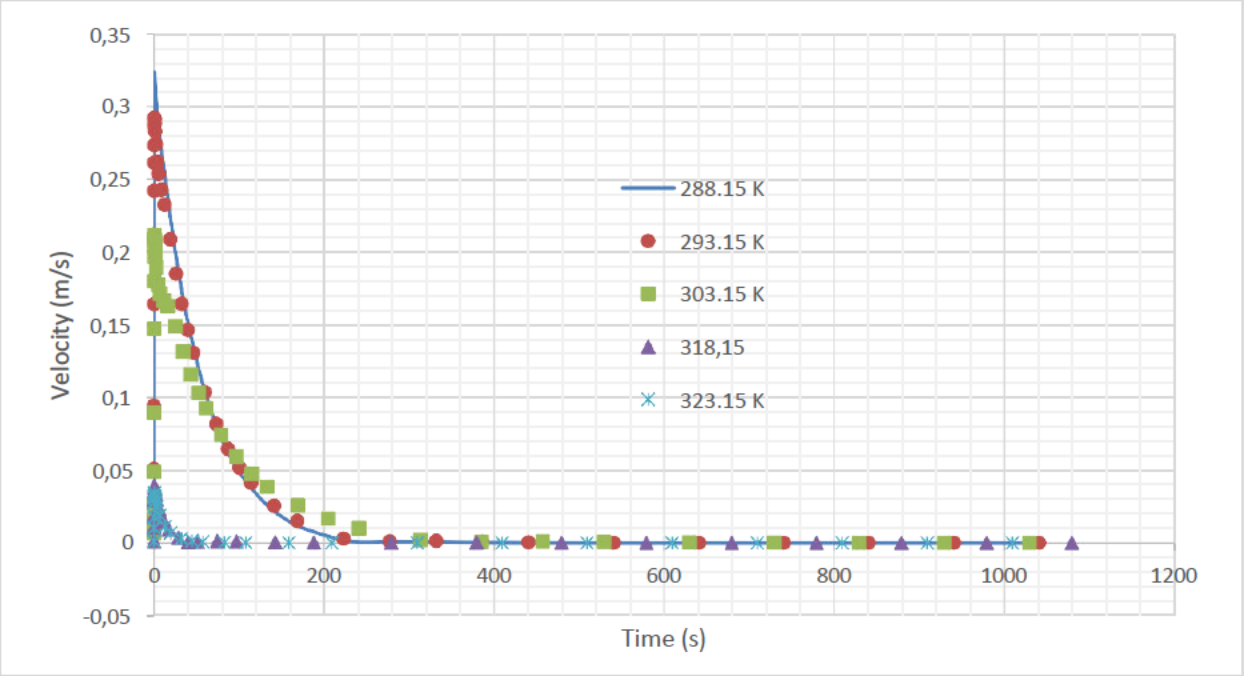

Figure 5.4.1.3: Effect of temperature velocity

The diagram presented herein illustrates the velocity gradient pertaining to hydrogen desorption, as denoted in Figure 5.4.1.4. At varying temperatures, the velocity commences at 0 meters per second, related to the initial stages of absorption, and subsequently ascends to maximum in concordance with the respective temperatures. In these instances, the velocity profile exhibits an inverse behaviour relative to that encountered during absorption. At lower temperatures, the velocity peaks attain greater magnitudes, while diminishing as temperatures elevate. Throughout the sorption process, the decline in velocity profiles exhibits a pronounced gradient at all corresponding temperatures, with the notable exception being at 303.15 K, where the descent occurs at a comparatively gradual rate in contrast to the operational temperature employed. In general, it can be asserted that both sorption processes follow a similar pattern; however, in the case of desorption, the velocity does not exhibit an augmentation as temperature escalates.

5.4.2. The effect of pressure

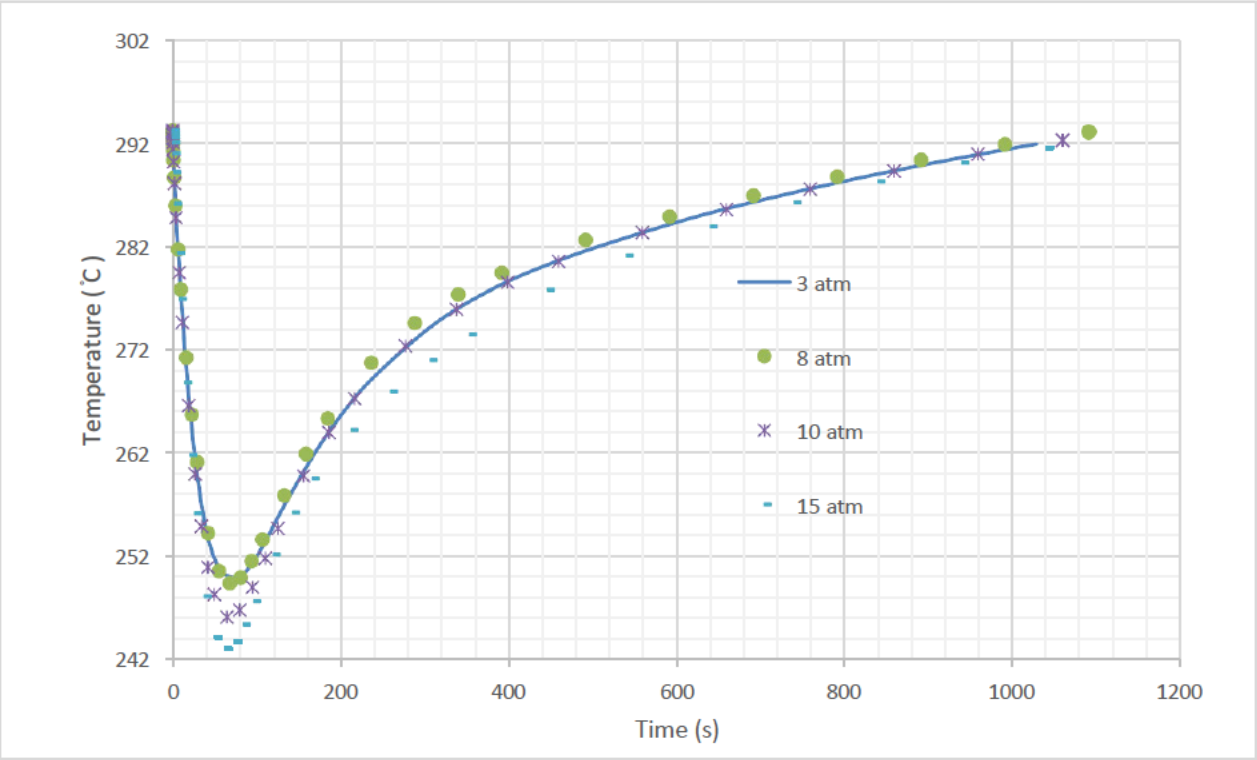

Figure 5.4.2.1: The effect of pressure on temperature

At constant temperature, the desorption process was subjected to different pressure conditions as illustrated in fig 5.4.2.1 above. The temperature takes a deep decline concerning pressure applied during the dehydriding. Pressure increase from 3 to 15 atmospheric pressure causes a decrease in temperature from 248.88 to 243.00 K, and the deeps occur at different times, 79.32- and 61.42 seconds. All that means by increasing pressure, you also increase the rate of desorption. The temperature trends are indistinguishable before reaching their peaks and after for pressures for 3 and 10 atmospheric pressures. Generally, it can be said that the trajectories at different pressure conditions are the same due to the fact that desorption is an endothermic reaction meaning it requires energy for the reaction to occur.

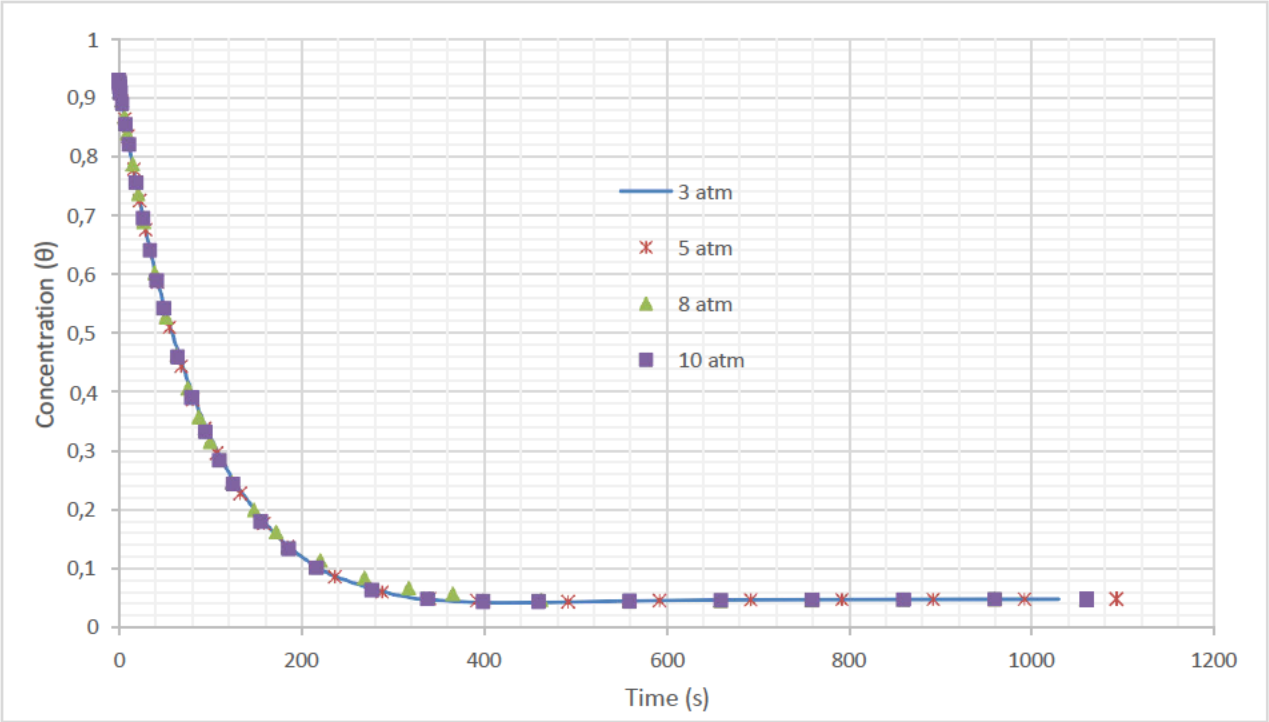

Figure 5.4.2.2: Pressure effect on concentration

Hydrogen release it is associated with energy absorption as it was depicted in figure 5.4.2.1, in this case the temperature was kept constant, and pressure was varied to observe the concentration. Figure 5.4.2.2 shows the concentration profiling from 3 to 10 atmospheric pressure, and the concentration does not vary with change in discharging pressure. With change in discharging pressure, concentration variation is expected to either be discharging at a faster or slow rate. If the observed discharge pressure exhibits no discernible alteration, it becomes imperative to exam the reactor dimensions, as they hold paramount significance in the sorption process, as documented by researchers in the domain of metal hydride studies. The results confirm literature that an AB_2 metal hydride desorb hydrogen at low pressure and ambient temperature. And high pressures are not suitable for operational safety reasons.

The pressure effect on velocity during dehydrogenation is inverse to the effect of temperature as demonstrated in fig. 5.4.4.3 and fig.5.4.1.3, below and from previous section. At a low temperature, hydrogen outflow was detected to be high as shown in the figure. The velocity flow decreases as temperature and pressure increases as profiled. In the case of dehydrogenation, pressure has a little to no effect in concentration on the type of reactor designed and the effect was seen when it comes to temperature and velocity.

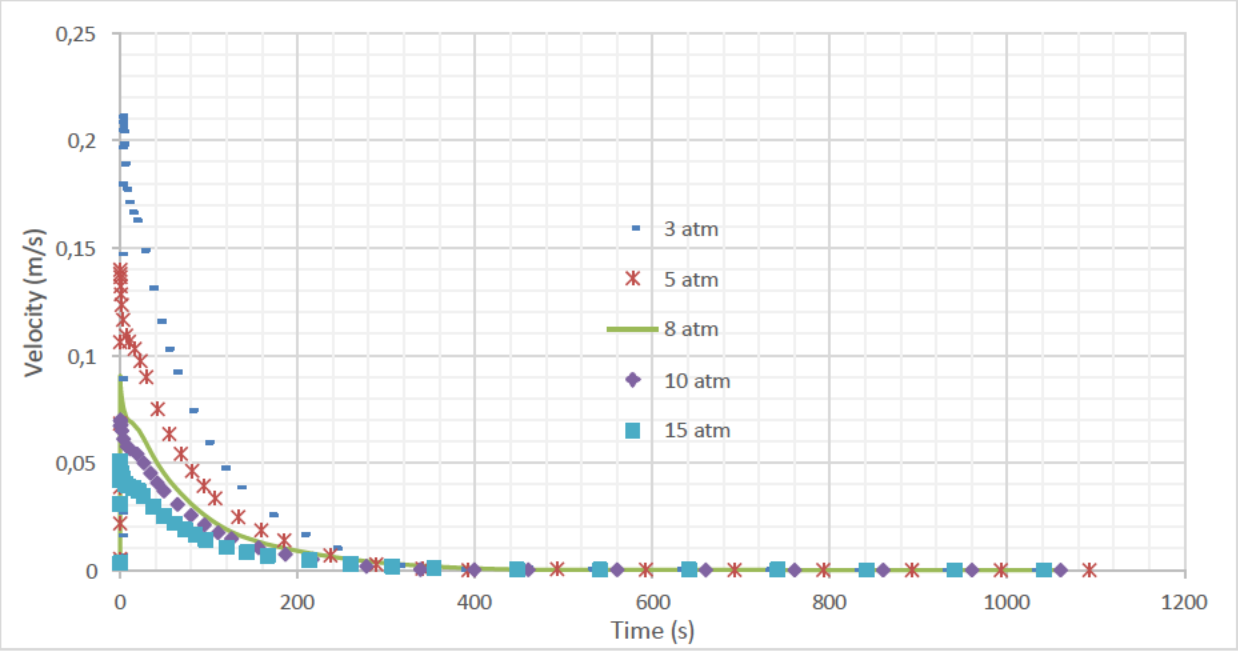

Figure 5.4.2.3: Pressure-velocity profile

5.5. Desorption operation parameters

5.5.1. Temperature

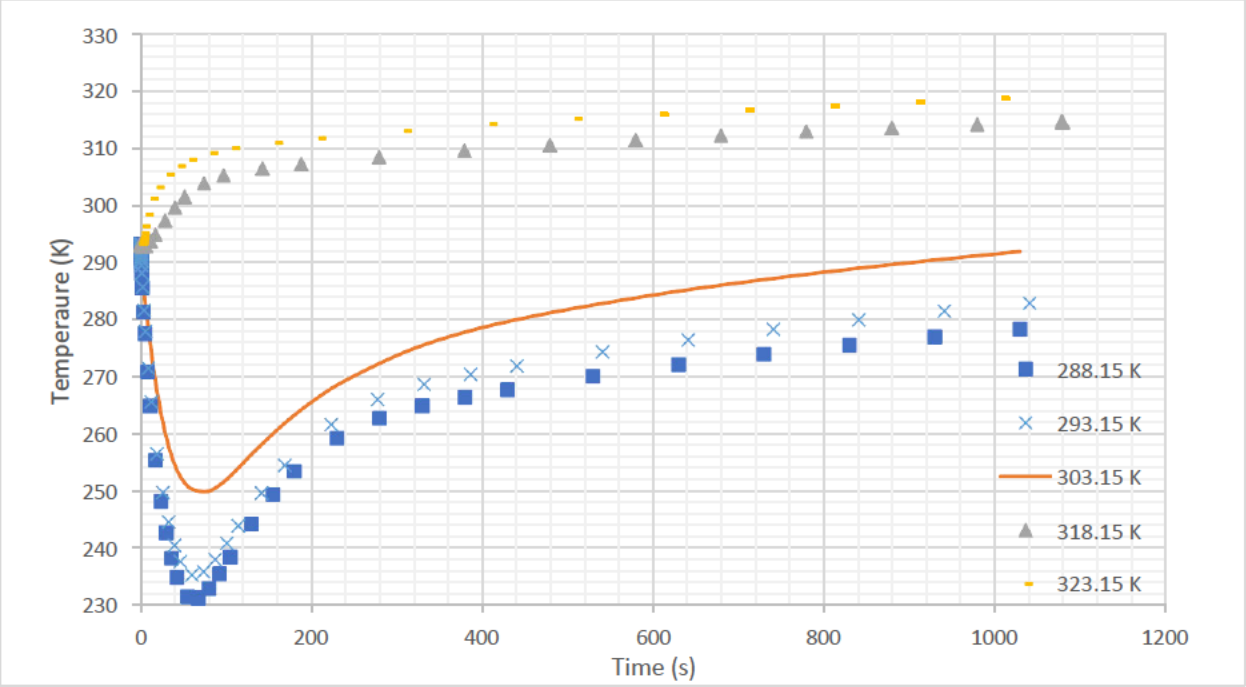

Figure 5.5.1.1: Heating temperature

Desorption is an energy demanding process to obtain hydrogen from metal hydride to provide to a fuel cell for power generation. Figure 5.5.1.1 displays heating temperature conditions, they all follow the same trajectory, starting from the metal hydride reactor temperature to their lowest points before increasing near the heating temperature. The sorption process and the metal hydride favour lower temperatures than high temperatures as illustrated by figure 5.4.1.1, and it is evident enough when looking at the figure above, the graphical representation at 323.15 K manifests the phenomenon through the shortest descent followed by an ascent, thereby highlighting the critical temperature for the observed transition. The observations substantiate the assertion that the optimal operational parameters for hydrogenation occur at 293.15 K, collaborating existing literature claims that the AB2 metal hydride employed in this project can indeed easily desorb hydrogen under ambient or near-ambient conditions.

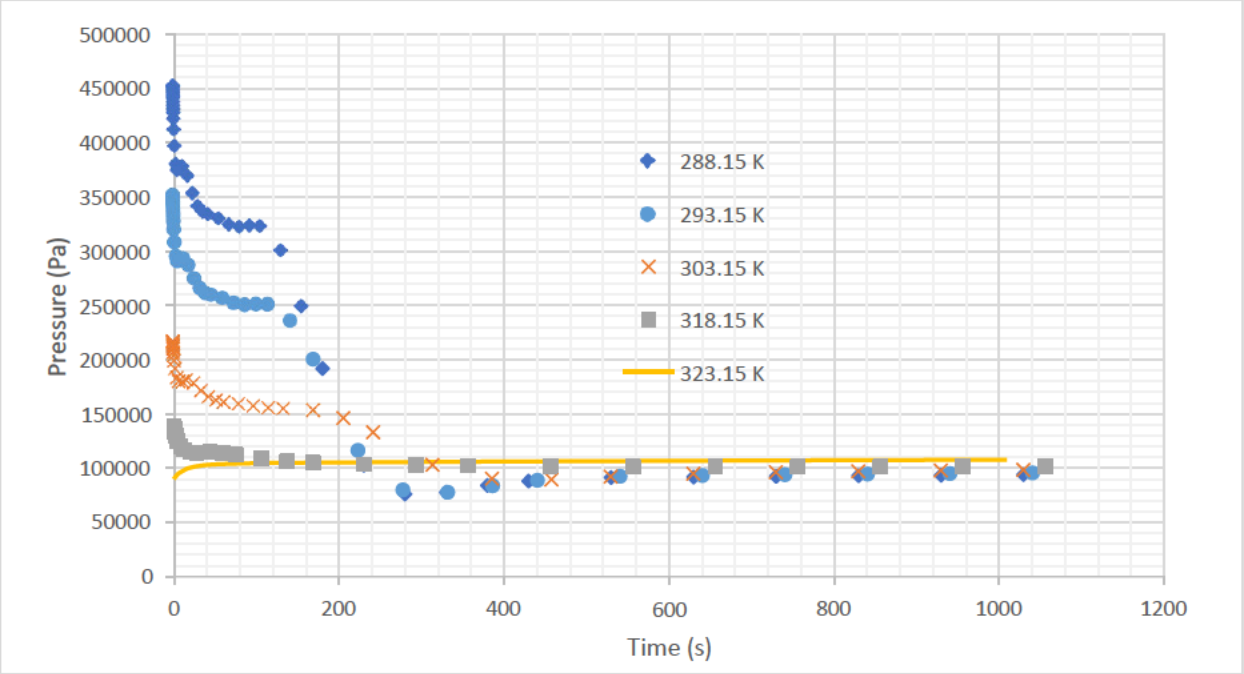

Figure 5.5.1.2: Desorption equilibrium pressure rate

Temperature has the same effect on both absorption and desorption processes, as it increases the equilibrium pressure rate decreases as shown in figure 5.5.1.2. However, it should be noted that deviations from this trend occur at temperatures of 323.15 K and above. At these elevated temperatures, the equilibrium rate notably exhibits absorption properties, initially commencing with an increase, as elucidated in Figure 5.5.1.3a in the appendices, which provides a graphical representation of the gas and equilibrium pressure rate dynamics. Figure 5.5.1.3 below offers a comprehensive depiction of desorption characteristics. Notably, it illustrates that the equilibrium pressure rate initiates at an elevated pressure level and subsequently diminishes as the gas pressure starts below the equilibrium pressure and subsequently undergoes an increase, ultimately stabilizing at a given point.

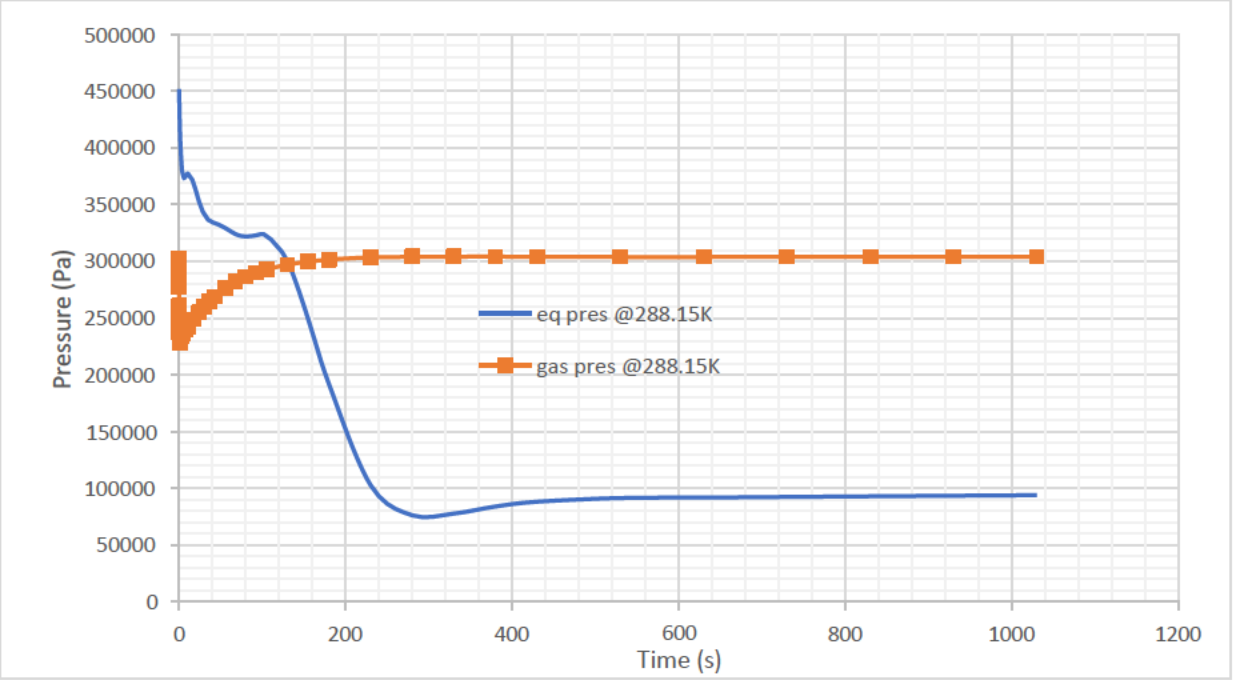

Figure 5.5.1.3: Equilibrium-gas pressure rate

5.5.2. Pressure

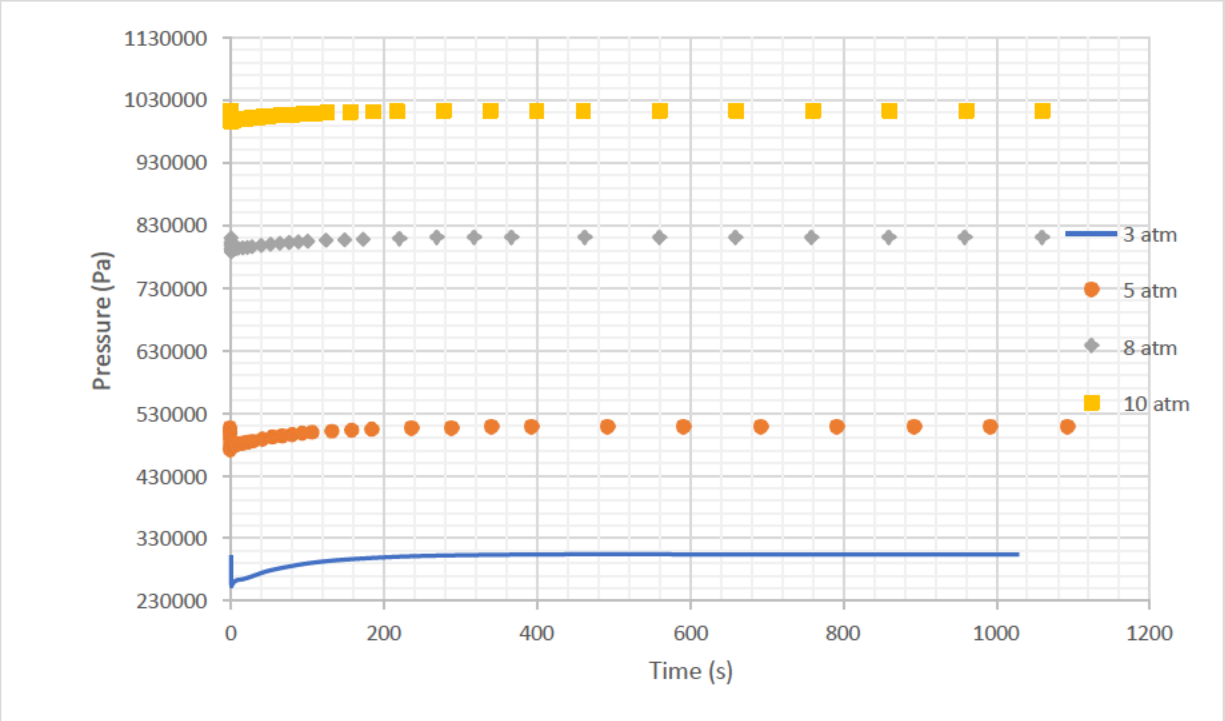

Figure 5.5.2.1: Reactor-hydrogen pressure

The operational capacity of the reactor is contingent upon the hydrogen pressure employed within the reactor. As the pressure magnitude escalates, it subsequently poses challenges to both

environmental and safety considerations within operational parameters. Refer to figure 5.5.2.1 to check the difference in magnitude between the pressure parameters. The figure has resembled absorption at different operating pressure parameters, fig 5.4.2.1. Consequently, in this instance, 3 atmospheric pressure was determined as the ideal operational pressure for the specific type of reactor constructed within the scope of the study. Figure 5.4.2.2 further supports this conclusion, as it reveals a lack of significant distinction in the hydrogen concentration flow emanating from the metal hydride reactor within the pressure range of 3 to 10 atmospheres. While figure 5.5.2.2 suggest that there was supposed to be distinguishability in concentration as the equilibrium pressure at operating pressure of 8 atm has visible deviation from 3, 5 and 10 atm. It is worth noting that equilibrium pressure typically exerts an influence on concentration; however, under these specific circumstances, the observed deviation from this trend could be attributed to the characteristics of the reactor itself. And in the appendices figure 5.5.2.3 represents the mechanism between reactor-hydrogen and equilibrium pressure.

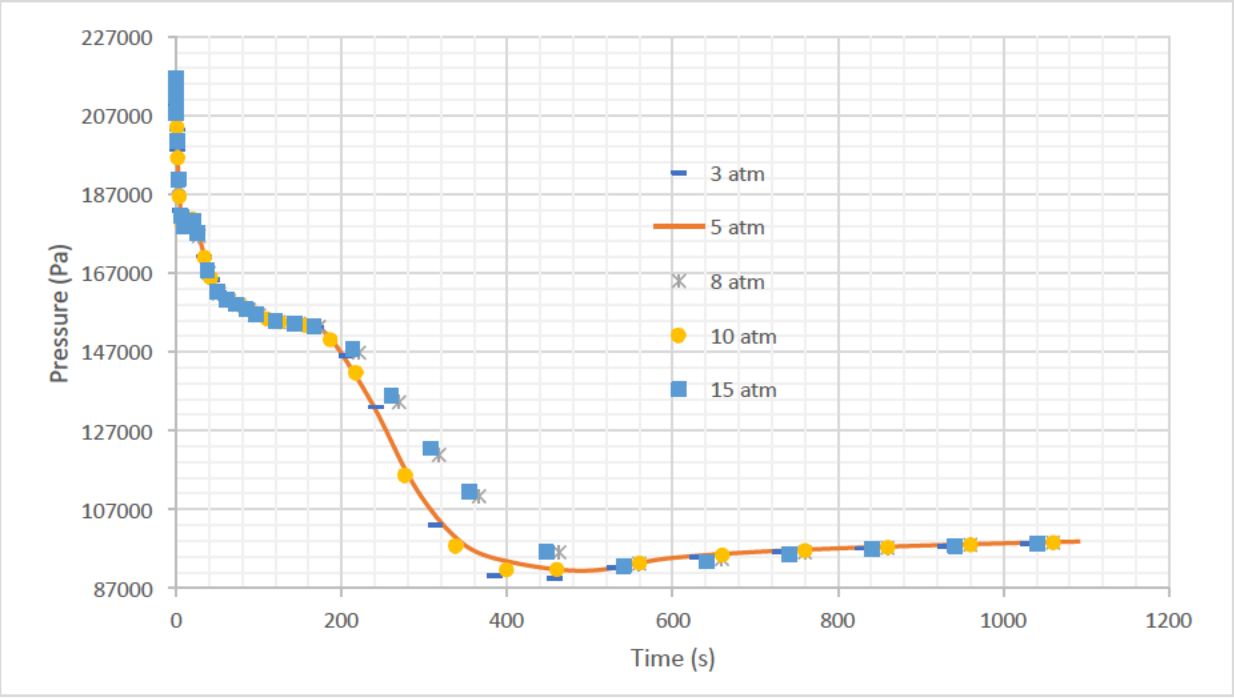

Figure 5.5.2.2: Equilibrium pressure rate at different operating pressure

5.6. Model development

5.6.1. PCT

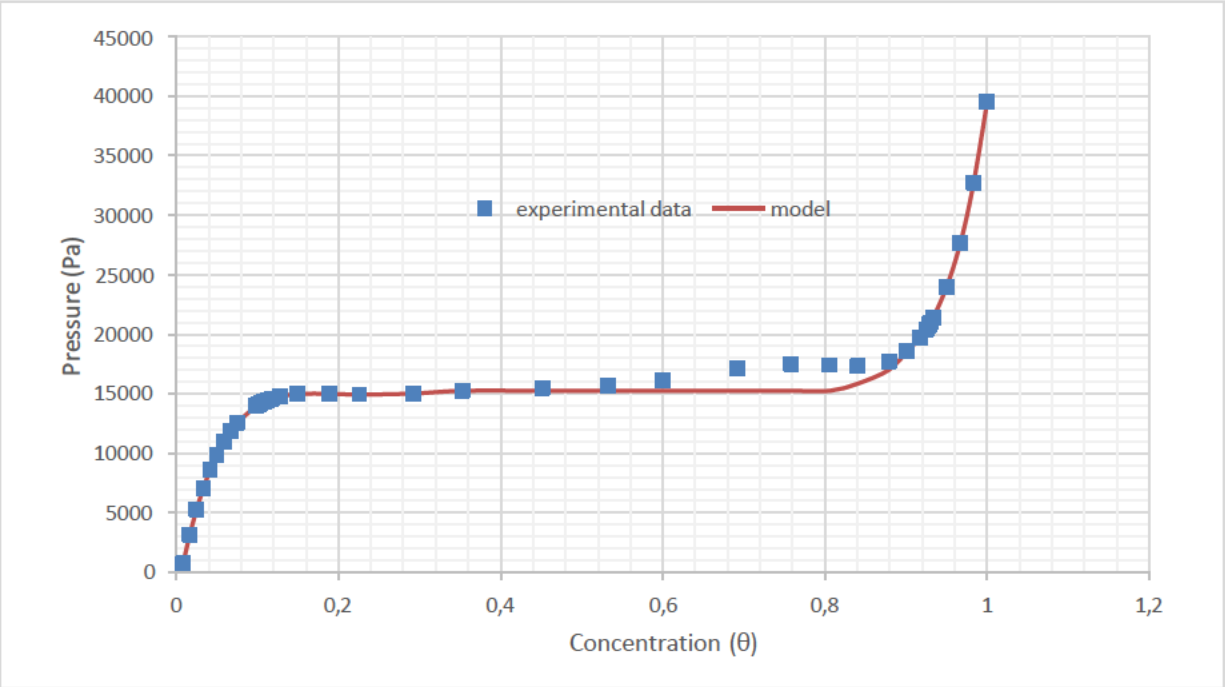

Figure 5.6.1: PCT model

The PCT model (Pressure-Concentration-Isotherm) serves as the foundation for modelling metal-hydride heat and mass transportation (Moropeng, Kolesnikov, et al. 2019). The experimental data are shown in Figure 5.4.1 together with the regression-predicted model. In this instance, a graphically experimental model was utilized to calculate the behaviour of heat and mass transfer inside the MH reactor, from sections 5.1 to 5.3 instead of a numerical technique. In order to visually represent PCT, the experimental data graph was created using pressure polynomials. To forecast a new model, the graph was altered by flattening (while maintaining the equilibrium pressure constant) the curves before and after absorption. The pressure polynomial of H/M and pressure graph can be predicted using a curve-fitting regression using MATLAB. Then the curve was used as a model in the simulation software to predict heat and mass transfer and operating parameters.

5.6.2. Temperature profiling

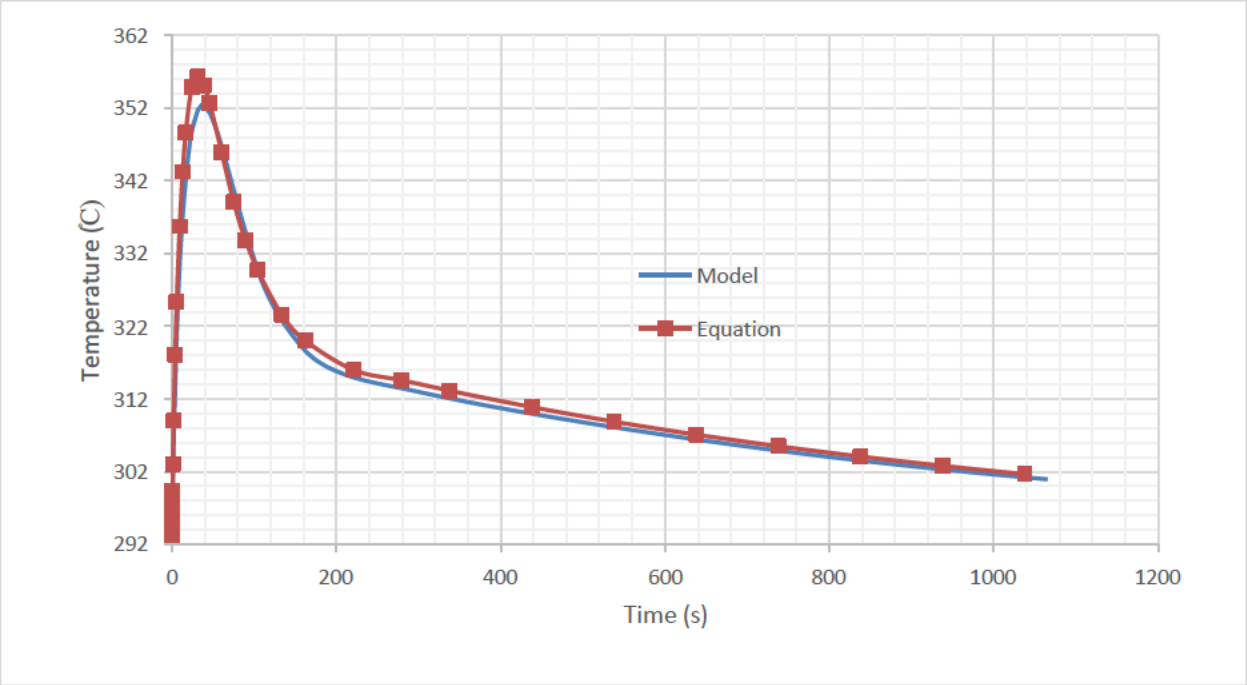

Figure 5.6.2.1: Absorption temperature profile

In the consecutive figures presented above and below, they illustrate temperature profiles corresponding to the processes of absorption and desorption. These profiles were acquired under the operational conditions of approximately 303.15 K and 10 atmospheric pressure. Based on the temperature profiling data, it is evident that flattening the plateau of the Pressure-Composition-Temperature (PCT) model exerts an influence on the reaction temperature within the reactor during both sorption processes. In the course of the absorption reaction, the temperature of the reaction within the model is observed to be lower than when utilizing pressure polynomial equations. The reduction in reaction temperature may be attributed to the lowering of the plateau within the Pressure-Composition-Temperature (PCT) model when maintaining it in an idealised state.

Conversely, in the desorption reaction, the temperature decreases below the level observed when the Pressure-Composition-Temperature (PCT) model was not idealized. At the commencement of the process, the temperature profiling exhibits a lack of clear distinction until the temperature reaches approximately 255 K. In contrast, during the absorption phase, the profile displays distinguishable characteristics from around 343 K, and after reaching the peak, it becomes indistinguishable between 356 K and 323 K.

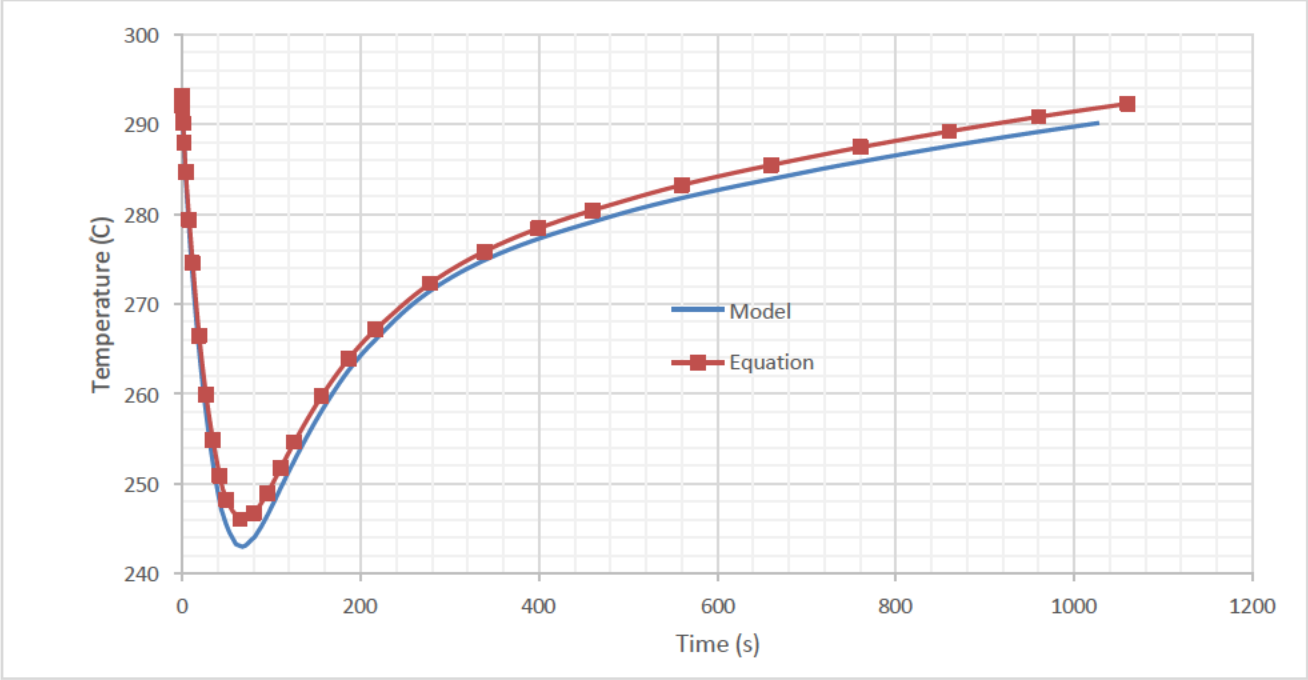

Figure 5.6.2.2: Desorption temperature profile

5.6.3. Concentration profiling

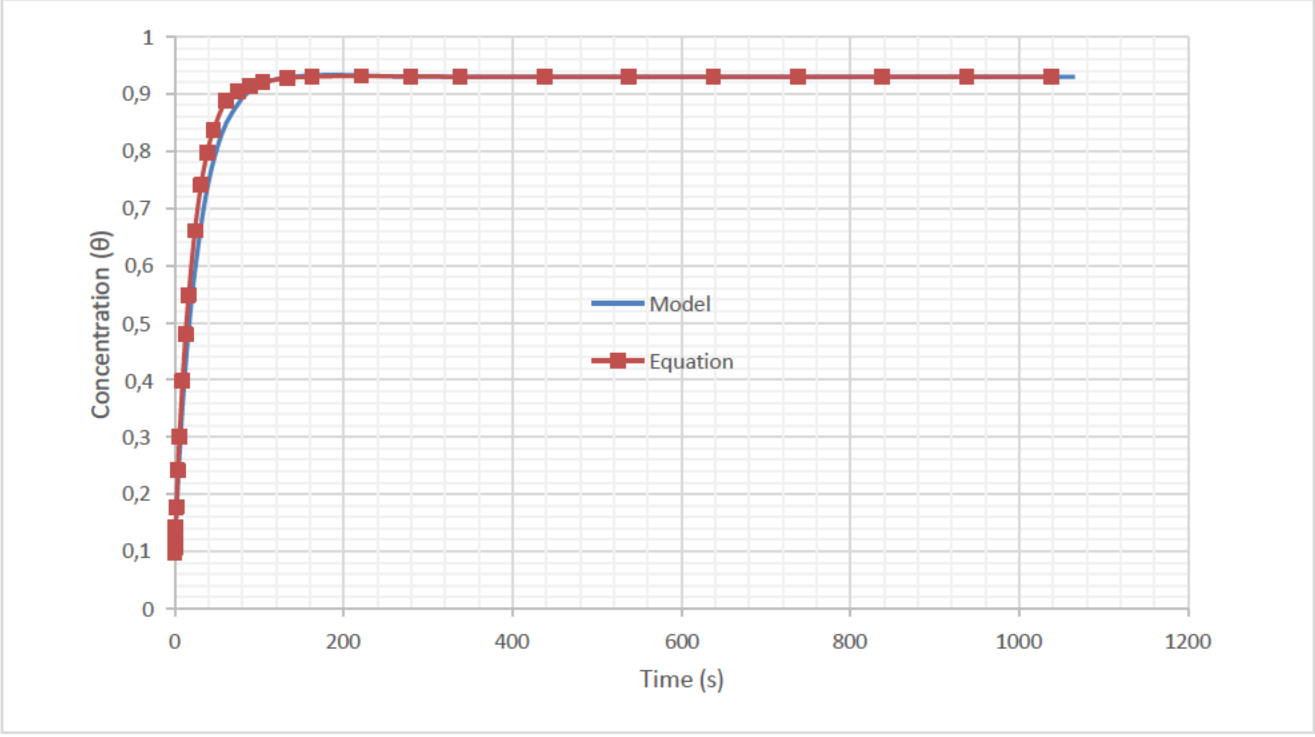

Figure 5.6.3.1: Absorption concentration profile

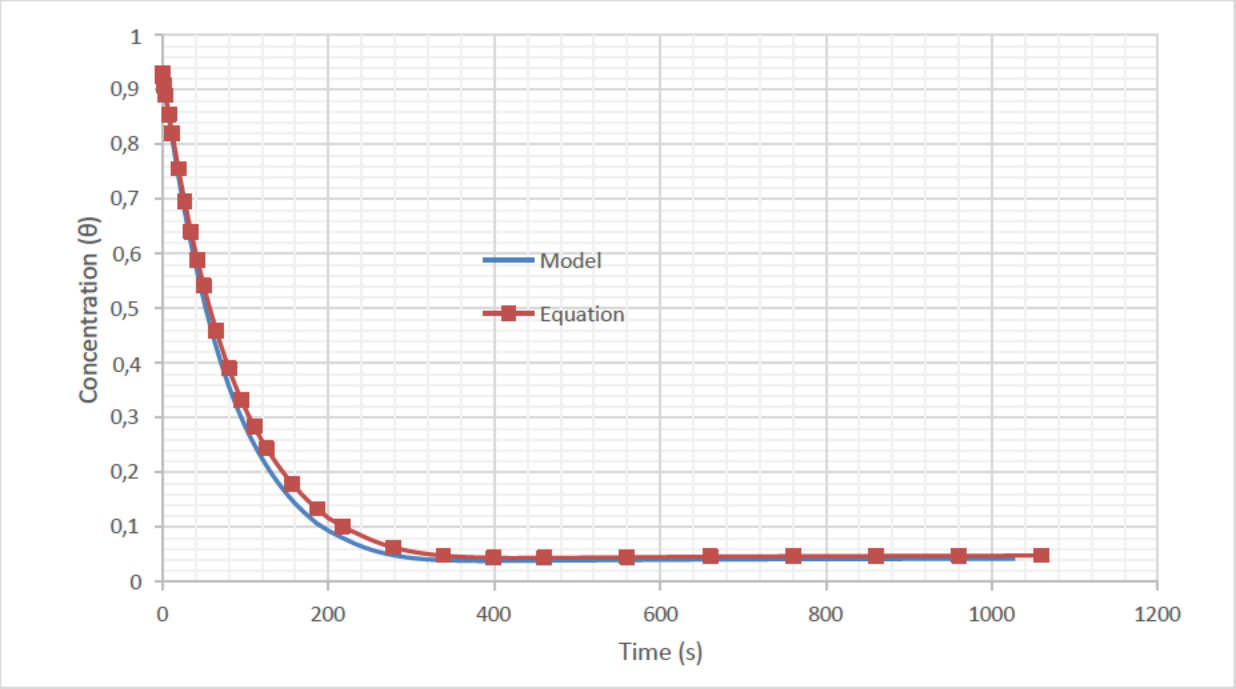

Figure 5.6.3.2: Desorption concentration profile

The figures presented in subsection 5.6.3 display analogous trends that are linked to the specific type of sorption processes they are undergoing for both the developed model and the PCT polynomial equation. During the absorption process, a minor regression is observed in the rate at which hydrogen is absorbed, with the rate decreasing by a fractional amount of time. The observed regression may be attributed to a decrease in the reaction temperature, as there is a correlation between temperature and the rate of hydrogen absorption. The noticeable deviation in distinguishability can be observed within the concentration range from approximately 0.53 to 0.91, whereas beyond this range, the distinctions become indiscernible.

In the desorption process, as depicted in Figure 5.6.3.2, the concentration remains indistinguishable from the initial heating of the reactor until it reaches a concentration of approximately 0.587, at which point it commences to decrease. In contrast to the absorption process, the rate of desorption within the model is releasing hydrogen at a more rapid pace. In this context, it can be inferred that the developed model exhibits a preference for desorption, as it enables efficient release of energy within the reactor during the process.

5.6.4. Pressure and Velocity Profiling

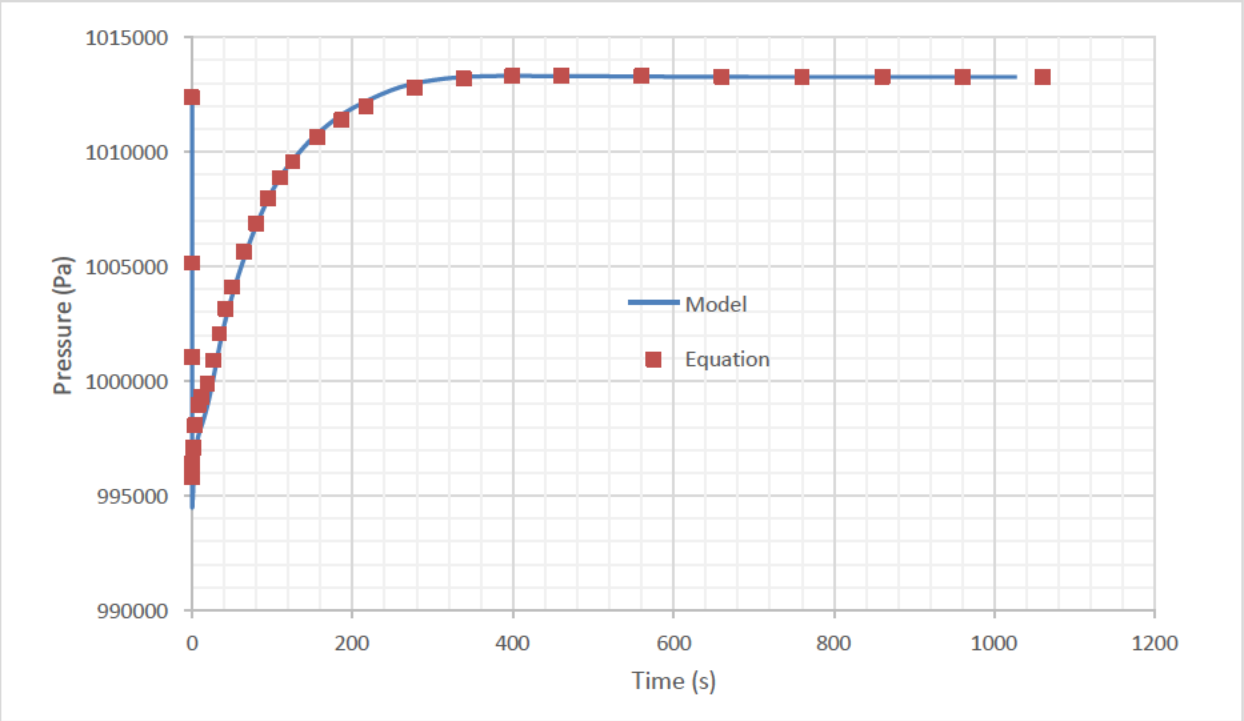

Figure 5.6.4.1: Desorption pressure profile

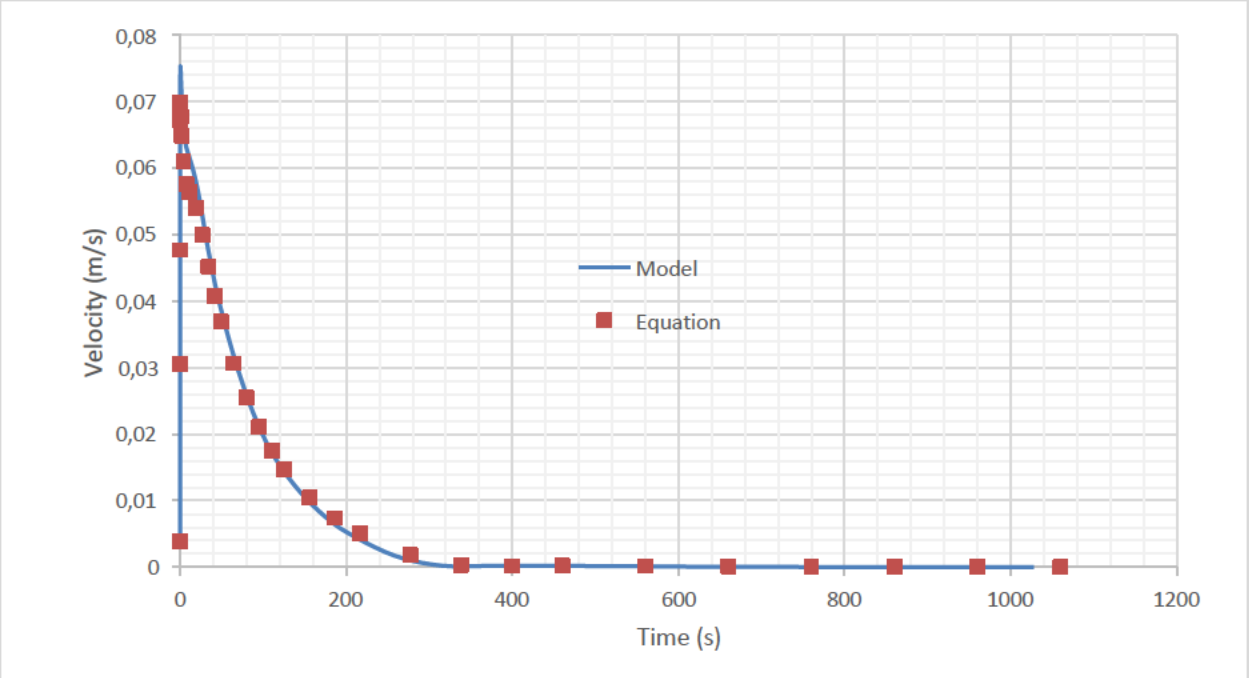

Figure 5.6.4.2: Desorption velocity profile

The profiling of pressure and velocity for desorption on the preceding page indicates minimal to negligible impact on the velocity and pressure within the hydrogen reactor tank, for both absorption and desorption. In this instance, it can be concluded that the model does not exert a discernible impact on the velocity and pressure. Additional information regarding the desorption rate can be found in the figures from Section 5.6.4, which depict pressure and velocity profiling. This was observed despite the changes in the reaction temperature and concentration. The absorption profiling can be examined in the appendices, and it is evident that they similarly indicate no significant distinctions.

5.7. Effective thermal conductivity influence

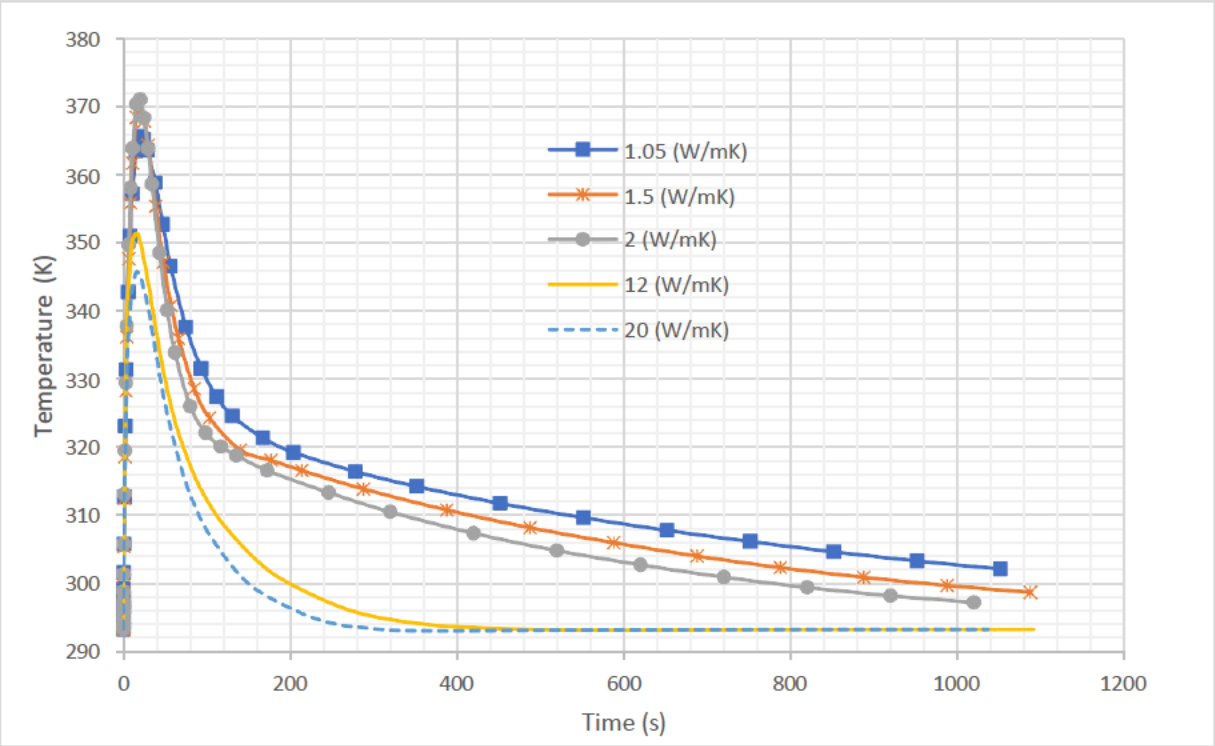

Figure 5.7.1: Temperature profile using various ETC.

The effective thermal conductivity of powered MH is insignificantly low for metal hydride alloys, ranging from 1 – 2 [W/m*K] as estimated by other scientists in the field. The ETC graphs are shown in figure 5.7.1, it can be said that it causes a chain of setbacks as it hinders the cooling of the reactor and means the reaction during absorption will take long and increase the charging (or hydrating) time of hydrogen. All the knockback accounts for creating an MH reactor not being suitable for onboard use. By observing the trends, the increase in ETC reduces the cooling time, temperature impulse, and attaining the desired cool temperature. All that is applicable for ETC above 2 [W/m*K] and from the assumption made by Suissa, E., et al (1984), the output trends are reversed from 1 - 2 [W/m*K] the temperature crest increases and to attain the desired cool temperature takes time as well. At higher ETC or as it increases from 2 [W/m*K], cooling is more

efficient and the crest point of temperature also lowers, as it can be seen from the graph of 12 and 20 [W/m*K] that the tank can be able to cool to cooling fluid temperature when absorption is taking place inside the tank. The results show that the ETC must be above the assumed values by Suissa, E., et al (1984) for effective heat management. It is well known from the literature that powdered MH alloy has low ETC, to overcome this characteristic the MH alloy must be improved to reach a value above its lowest values.

Temperature distribution inside the MH reactor tank is shown in figures 5.7.1 for effective thermal conductivities, 1.05 [W/m*K] and 12 [W/m*K]. The tank design as described in chapter 3, figure 3.8.1 and 3.8.2, is not the conventional type of a design where a tank is filled with the MH to form a bed to absorb hydrogen. In our case, the tank has several compartments made of similar material and holds MH alloy with a hollow tube-like stream in the middle of each

compartment from the inlet to the bottom of the tank. Instead of the thermal evolution during absorption (or hydrogen charging) starting from the center of the bed outwards, the heat starts inside the compartments to the outward, to the center (hollow stream), and between the compartments. At 0 seconds the reactor is at ambient conditions with MH beds inside the compartments at different ETC. after charging, exactly at 5 seconds each compartment had reached a different with the lower compartment reaching a high of 400 K and still increasing to reach a temperature above 600 k after 25 seconds, at ETC of 1.05 [W/m*K]. there other compartments with MH beds, the temperature increased gradually with time, to a stage that reached the average pinnacle temperature as presented on the temperature profile in figures 5.4.1.1 and 5.7.1 at 303.15 K. due to low ETC the heat evolution inside the tank takes time and cause a negative impact on cooling because it was time-consuming as well.

Charging hydrogen for 5 seconds in a reactor tank containing MH beds with 12 [W/m*K] in compartments reached above 400 K temperature till the charging time reached 15 seconds, in the first and last compartment beds. By comparing thermal evolution inside the reactor, there one in figure 5.7.1 is rapid with less average pinnacle temperature of 342 K consult with figure 5.7.1, temperature profiling. When looking at the cooling of the reactor, was more efficient, and rapid and reached the desired cool temperature at around 480 seconds. Referring to figure 5.7.1 shows the detailed temperature distribution and mechanism of cooling the reactor goes along. The cooling occurs from the external surface into the reactor, and it can be seen on the wall of the reactor where it is effective.

5.8. Validation of results

The validity of the results was established through comparison with the work of Lin X et al. (2019). It is important to acknowledge that the geometrical aspects of both projects were dissimilar, and their research scopes varied as well. Lin X was focused on densification of the metal hydride but at some stage they discovered similarities with normal density MH. Additionally, it is noteworthy that obtaining accurate thermodynamic and physical properties for AB2 metal hydrides can be challenging, hence literature-derived properties were employed to validate the obtained results. By using absorption results, a good agreement between the results was found even though at the developed PCT model has high temperature evolution inside the reactor.

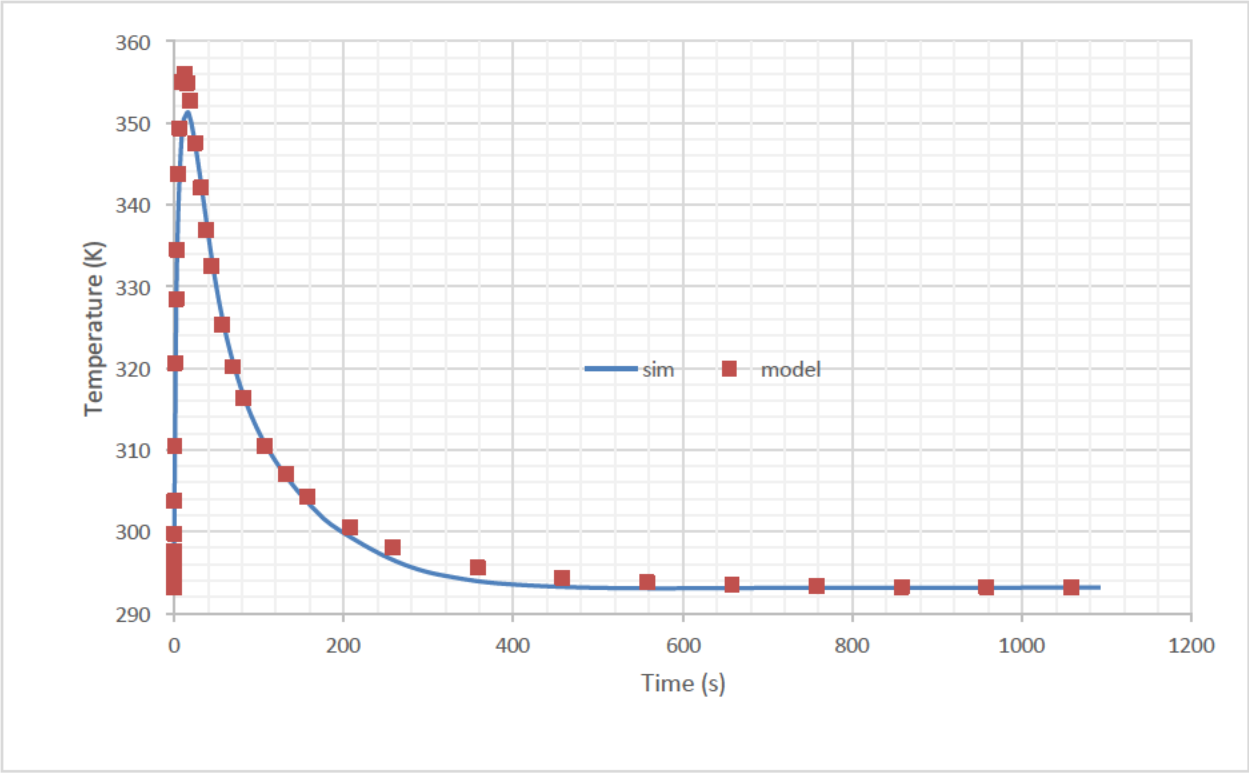

Figure 5.8.1: Simulation validation

Chapter 6

Conclusion and recommendations

In conclusion, this thesis addresses the pressing need for alternative energy sources due to concerns related to fossil fuels. Hydrogen, recognized as an energy carrier, presents challenges in storage for mobile use, with current methods being energy-intensive. The study advocates for metal hydrides as a favourable storage form, emphasizing their benefits in terms of operational conditions and energy efficiency. A comprehensive mathematical model is developed using COMSOL Multiphysics software, accounting for mass, momentum, energy conservation, and adsorption/desorption kinetics, facilitating extensive parametric studies.

The incoming hydrogen temperature significantly raises the reactor's operating temperature during hydriding, posing challenges for energy management. However, higher temperatures positively impact concentration by improving absorption rates, although they may result in slower cooling. The effects on pressure and velocity are characterized by a steep initial decline before reaching a constant phase. The optimal temperature of 303.15 K, close to ambient temperature, is identified for a balance between effective absorption and manageable energy costs, as depicted in section 5, sub-section 5.1. Analysis of desorption revealed that low temperatures are favourable than higher ones. At temperatures above 318.15 K, the decomposition of the metal hydride ceases to occur, and the reaction reverses, leading to hydrogen absorption. Which can cause energy deficiency.

According to the literature, the fundamental issue that metal hydrides face is the effective heat conductivity of the metal hydride since it is in powder form. The metal hydride must be adjusted to respond to heat since the findings in Chapter 5.2 demonstrate that raising the ETC of the MH heat management becomes a lot more effective than when it is at normal characteristics. It is the sole issue impeding the widespread use of metal hydride technology, although it is the greatest option for energy providers. ETC has almost to nothing impart concentration, pressure, and velocity.

Concentration and velocity were more impacted by supplied pressure than temperature inside the reactor chambers. As the provided pressure increases, so does the concentration of hydrogen inside the MH. The velocity of the gas increases with the pressure supply before it can also respond to a stable phase indicating that the reaction can no longer move forward as the is no surface for the reaction. Conversely, during desorption, there is an inverse relationship, where the concentration of hydrogen increases while the velocity decreases.

The metal hydride equilibrium curve (PCT) is a critical thermodynamic factor determining the occurrence of reactions. Experimental data was used to predict a flat plateau PCT curve, aligning with literature suggesting its assumption by the metal hydride (MH, AB2). This data-driven model, distinct from empirical formulas, was idealized to predict system behavior. Results show absorption leads to a temperature decrease, impacting hydrogen concentration rates. During desorption, effective energy

absorption enhances hydrogen concentration rates. Under the same operational conditions, the model and polynomial equations exhibit minimal distinctions in pressure and velocity profiles. This approach offers insights into metal hydride reactions, aiding system understanding and optimization.

Future studies could leverage the model to optimize metal hydride selection for specific applications, offering intriguing possibilities. Enhancing the model to mimic real-life cyclic adsorption and desorption phenomena is a promising direction. Moreover, incorporating the detailed internal structure and morphology of the metal hydride into the model could improve its alignment with experimental results. These advancements hold the potential to deepen our understanding and practical application of metal hydride systems.

Reference

Adelhelm, P. and P. E. de Jongh (2011). "The impact of carbon materials on the hydrogen storage properties of light metal hydrides." J. Mater. Chem. **21**(8): 2417-2427.

Amhamed, A. I., et al. (2022). "Ammonia Production Plants—A Review." Fuels **3**(3): 408-435.

Askri, F., et al. (2004). "Prediction of transient heat and mass transfer in a closed metal–hydrogen reactor." International Journal of Hydrogen Energy **29**(2): 195-208.

Baroutaji, A., et al. (2019). "Comprehensive investigation on hydrogen and fuel cell technology in the aviation and aerospace sectors." Renewable and Sustainable Energy Reviews **106**: 31-40.

Ben Nasrallah, S. and A. Jemni (1997). "Heat and mass transfer models metal-hydrogen reactor." International Journal of Hydrogen Energy **22**: 67-76.

Bouzgarrou, F., et al. (2016). "Numerical Investigation of Heat and Mass Transfer during the Desorption Process of a LaNi5-H2 Reactor." **138**.

Callister, W. D. and D. G. Rethwisch (2018). Materials science and engineering: an introduction, Wiley New York.

Charitos, A. and S. Makridis (2021). Hydrogen Technology, a Short Overview.

Cho, S. M., et al. (2021). "Lightweight hydrogen storage cylinder for fuel cell propulsion systems to be applied in drones." International Journal of Pressure Vessels and Piping **194**: 104428.

Cleveland, C. (2014). Chronologies, top ten lists, and world clouds. Handbook of Energy

Crabtree, G. W., et al. (2004). "The Hydrogen Economy." Physics today.

de Waele, A. T. A. M. (2017). "Basics of Joule–Thomson Liquefaction and JT Cooling." Journal of Low Temperature Physics **186**(5-6): 385-403.

Durbin, D. J. and C. Malardier-Jugroot (2013). "Review of hydrogen storage techniques for on board vehicle applications." International Journal of Hydrogen Energy **38**(34): 14595-14617.

Eberle, U., et al. (2012). "Fuel cell electric vehicles and hydrogen infrastructure: status 2012." Energy & Environmental Science **5**(10).

Gschneidner, K. A., et al. (2005). Handbook on the physics and chemistry of rare earths, Elsevier.

Hagström, M. T., et al. (2000). "High-pressure AB2 metal hydrides with low hysteresis." Journal of Materials Science **35**(1): 127-131.

Häussinger, P., et al. (2011). Hydrogen, 1. Properties and Occurence. Ullmann's Encyclopedia of Industrial Chemistry.

Heede, R. and N. Oreskes (2016). "Potential emissions of CO2 and methane from proved reserves of fossil fuels: An alternative analysis." Global Environmental Change **36**: 12-20.

Höök, M. and X. Tang (2013). "Depletion of fossil fuels and anthropogenic climate change—A review." Energy Policy **52**: 797-809.

Jemni, A. and S. Ben Nasrallah (1995). "Study of two-dimensional heat and mass transfer during absorption in a metal-hydrogen reactor." International Journal of Hydrogen Energy **20**: 43-52.

Jemni, A. and S. Ben Nasrallah (1995). "Study of two-dimensional heat and mass transfer during desorption in a metal-hydrogen reactor." International Journal of Hydrogen Energy **20**: 881-891.

Jemni, A., et al. (1999). "Experimental and Theoretical study of a metal-hydrogen reactor." International Journal of Hydrogen Energy **24**: 631-644.

Jianjun, L. and Z. Wenqing (2012). Improvement on Hydrogen Storage Properties of Complex Metal Hydride. Hydrogen Storage. L. Jianjun. Rijeka, IntechOpen**:** Ch. 2.

Koultoukis, E. D., et al. (2014). "High-temperature activated AB2 nanopowders for metal hydride hydrogen compression." International Journal of Energy Research **38**(4): 477-486.

Lacher, J. (1937). "A Theoretical Formula for the Solubility of Hydrogen in Palladium." The Royal Society **161**: 525-545.

Libowitz G.G. and N. J. Brookside (1976). Thermal energy storage systems employing metal hydrides. A. C. Corporation. Morris Township, N.J(US). **4,040,410**.

Lin, X., et al. (2019). "Numerical analysis on pulverization and self-densification for hydrogen storage performance of a metal hydride tank." Applied Thermal Engineering **161**.

Lototskyy, M., et al. (2012). "Thermally Driven Metal Hydride Hydrogen Compressor for Medium-Scale Applications." Energy Procedia **29**: 347–356.

Lototskyy, M. V. (2016). "New model of phase equilibria in metal – hydrogen systems: Features and software." International Journal of Hydrogen Energy **41**(4): 2739-2761.

MacDonald, B. D. (2006). Mathematical Modelling of a Metal Hydride Hydrogen Storage System. Mechanical Engineering, University of Victoria. **Master of Applied Sciences**.

MacDonald, B. D. and A. M. Rowe (2006). "A thermally coupled metal hydride hydrogen storage and fuel cell system." Journal of Power Sources **161**(1): 346-355.

Maceiras, R., et al. (2015). "Modellization of Metal Hydride Canister for Hydrogen Storage." European Journal of Sustainable Development **4**(2).

Madriklridis, S. S. (2016). Hydrogen storage and compression.

Mat, M. and Y. Kaplan (2001). "Numerical study of hydrogen absorption in an Lm – Ni5 hydride reactor." International Journal of Hydrogen Energy **26**: 957-963.

Mayer, U., et al. (1987). "Heat and mass transfer in metal hydride reaction beds: Experimental and theoretical results." J of the less –common Metals, **131**: 235-244.

Meng, X., et al. (2012). A comprehensive performance evaluation index for metal hydrides reactor,. World hydrogen energy conference.

Møller, K., et al. (2017). "Complex Metal Hydrides for Hydrogen, Thermal and Electrochemical Energy Storage." Energies **10**(10).

Moropeng, M., et al. (2019). "Modelling of thermodynamic Pressure – Composition – Temperature relationships in the systems of metallic hydride forming materials with gaseous hydrogen using C++ software." Chemical Product and Process Modeling.

Olaitan, A. and A. Kolesnikov (2011). MODELING OF HYDROGEN STORAGE DEVICE FOR FUEL CELL PLANT.USING COMSOL MULTIPHYSICS.

Panwar, N. L., et al. (2011). "Role of renewable energy sources in environmental protection: A review." Renewable and Sustainable Energy Reviews **15**(3): 1513-1524.

Popeneciu, G., et al. (2009). "Investigation on a three-stage hydrogen thermal compressor based on metal hydrides." Journal of Physics: Conference Series **182**: 012053.

Press, R. J., et al. (2008). Introduction to HydroGen Technology, Wiley & Sons, Incorporated, John.

Raghav, L., et al. (2021). "Utilization of Hydrogen Created From Waste Products." **9**(7).

Ramachandran, R. and R. K. Menon (1998). "AN OVERVIEW OF INDUSTRIAL USES OF HYDROGEN." ht. J. Hydrogen Enrvgy, **23**(7).

Reilly, J. J. and R. H. Wiswall (1974). "Formation and properties of iron titanium hydride." Inorganic Chemistry **13**(1): 218-222.

Rivard, E., et al. (2019). "Hydrogen Storage for Mobility: A Review." Materials (Basel) **12**(12).

Rodrigue, J.-P. (2020). The Geography of Transport Systems. Built Environment, Geography. London, Routledge**:** 27

Sadaghiani, M. S. and M. Mehrpooya (2017). "Introducing and energy analysis of a novel cryogenic hydrogen liquefaction process configuration." International Journal of Hydrogen Energy **42**(9): 6033-6050.

Sandrock, G. (1999). "A panoramic overview of hydrogen storage alloys from a gas reaction point of view." Journal of Alloys and Compounds **293-295**: 877-888.

Shaltiel, D. (1978). "Hydride properties of AB2 laves phase compounds." Journal of the Less Common Metals **62**: 407-416.

Stopić, S. and B. Friedrich (2020). "Recovery of cobalt from primary and secondary materials: An overiew." Vojnotehnicki glasnik **68**(2): 321-337.

Stwertka, A. (1996). A Guide to the Elements, Oxford University Press.

Suda, S., et al. (1981). "Thermal conductivity in metal hydride beds." International Journal of Hydrogen Energy **6**: 521-528.

Sun, D.-W. and S.-J. Deng (1988). "Study of the heat and mass transfer characteristics of metal hydride beds." Journal of the Less Common Metals **141**(1): 37-43.

Sun, D.-W. and S.-J. deng (1989). "Study of the heat and mass transfer characteristics of metal hydride beds: A two-dimensional model." J of the less –common Metals, **155**(2): 271-279.

Sun, D.-W. and S.-J. deng (1990). "Numerical solution of the two-dimensional non-steady heat and mass transfer problem in metal hydride beds." International Journal of Hydrogen Energy **15**(11): 807-816.

Sun, D.-W. and S.-J. deng (1990). "Theoretical descriptions and experimental measurements on the effective thermal conductivity in metal hydride powder beds." J of the less –common Metals, **160**(2): 387-395.

Sun, D.-W. and S.-J. Deng (1990). "A theoretical model predicting the effective thermal conductivity in powdered metal hydride beds." International Journal of Hydrogen Energy **15**(5): 331-336.

Taji, M., et al. (2018). "Real time optimization of steam reforming of methane in an industrial hydrogen plant." International Journal of Hydrogen Energy **43**(29): 13110-13121.

Thompson, P., et al. (1989). "The application of the Rietveld method to a highly strained material with microtwins: TiFeD1.9." Journal of Applied Crystallography **22**(3): 256-260.

Thompson, P., et al. (1979). "Neutron diffraction study of gamma iron titanium deuteride." Journal of Physics F: Metal Physics **9**.

Tserolas, V., et al. (2010). "Thermodynamical Modeling of P-C Isotherms for Metal Hydride Materials." Transactions of the Materials Research Society of Japan **35**(2): 221-226.

Tzimas, E., et al. (2003). Hydrogen storage: state-of-the-art and future perspective. Netherlands, European Cimmunities.

Visaria, M., et al. (2010). "Study of heat transfer and kinetics parameters influencing the design of heat exchangers for hydrogen storage in high-pressure metal hydrides." International Journal of Heat and Mass Transfer **53**(9-10): 2229-2239.

von Helmolt, R. and U. Eberle (2007). "Fuel cell vehicles: Status 2007." Journal of Power Sources **165**(2): 833-843.

von Helmolt, R. and U. Eberle (2014). Compressed and Liquid Hydrogen for Fuel Cell Vehicles. Encyclopedia of Applied Electrochemistry**:** 245-253.

Wang, C.-Y., et al. (2011). "HYDROGEN ABSORPTION/DESORPTION IN A METAL HYDRIDE REACTOR ACCOUNTING FOR VARIED EFFECTIVE THERMAL CONDUCTIVITY." Journal of Marine Science and Technology **19**(2): 168-175.

Xiao, B. and Q. Yuan (2009). "Nanoporous metal organic framework materials for hydrogen storage." Particuology **7**(2): 129-140.

Yartys, V. A., et al. (2019). "Magnesium based materials for hydrogen based energy storage: Past, present and future." International Journal of Hydrogen Energy **44**(15): 7809-7859.

Zhang, T. B., et al. (2012). "Hydrogen absorption properties of Zr(V1−xFex)2 intermetallic compounds." International Journal of Hydrogen Energy **37**(3): 2328-2335.

Zhao, Y.-J. and A. J. Freeman (2007). "Accurate heat of formation for fully hydrided LaNi5 via the all-electron full-potential linearized augmented plane wave approach." Journal of Applied Physics **102**(3).

Zuttel, A. (2004). "Hydrogen storage methods." Naturwissenschaften **91**(4): 157-172.

Züttel, A. (2003). "Materials for hydrogen storage." Materials Today **6**(9): 24-33.

Appendixes

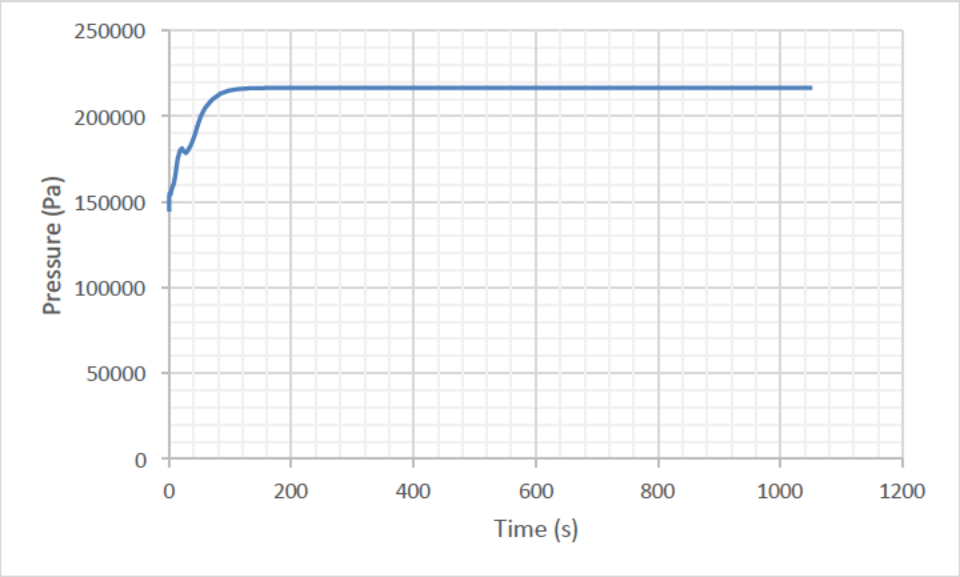

Figure 5.4.2 a: Equilibrium pressure rate

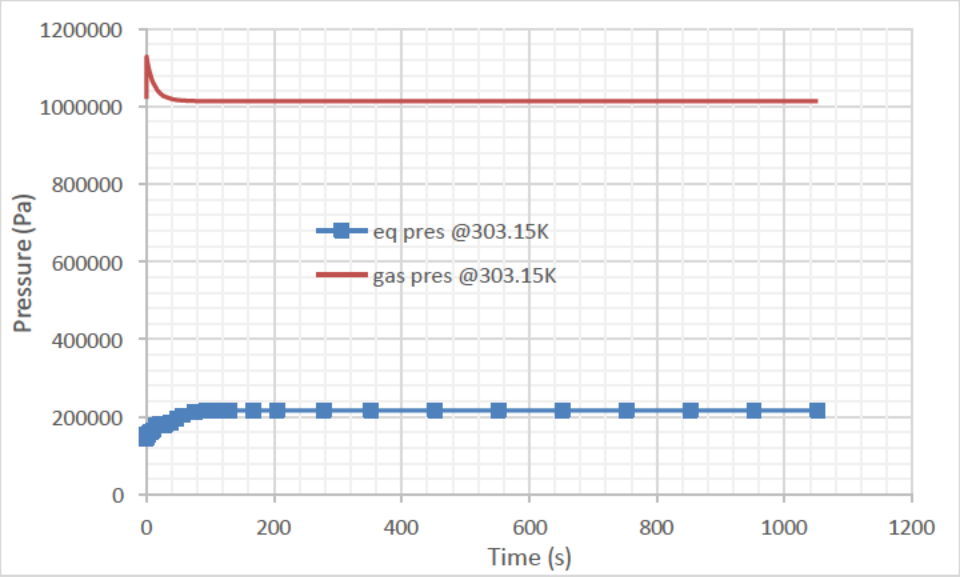

Figure 5.4.2 b: Rate of equilibrium and gas pressure

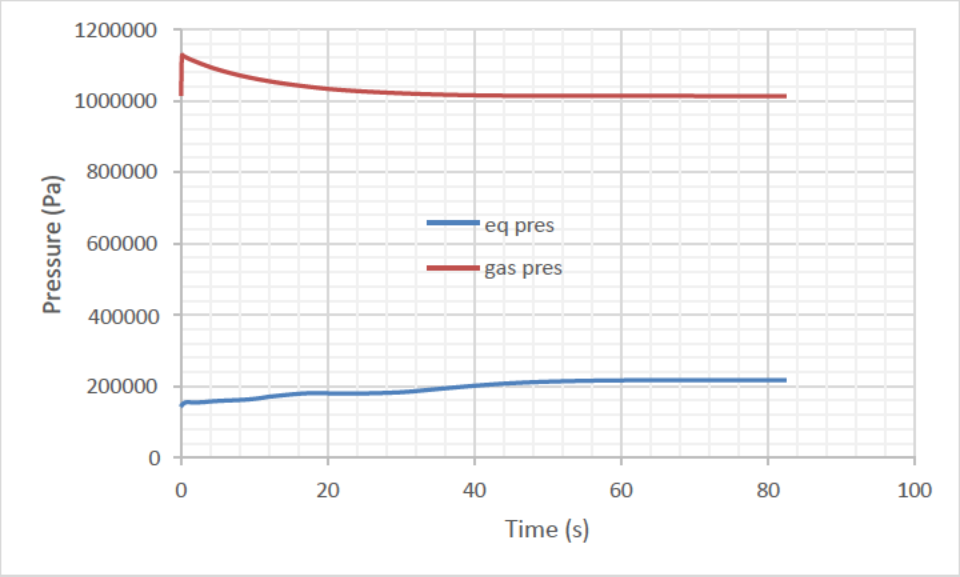

Figure 5.4.2.2 a: Hydrogen gas and equilibrium pressure rate

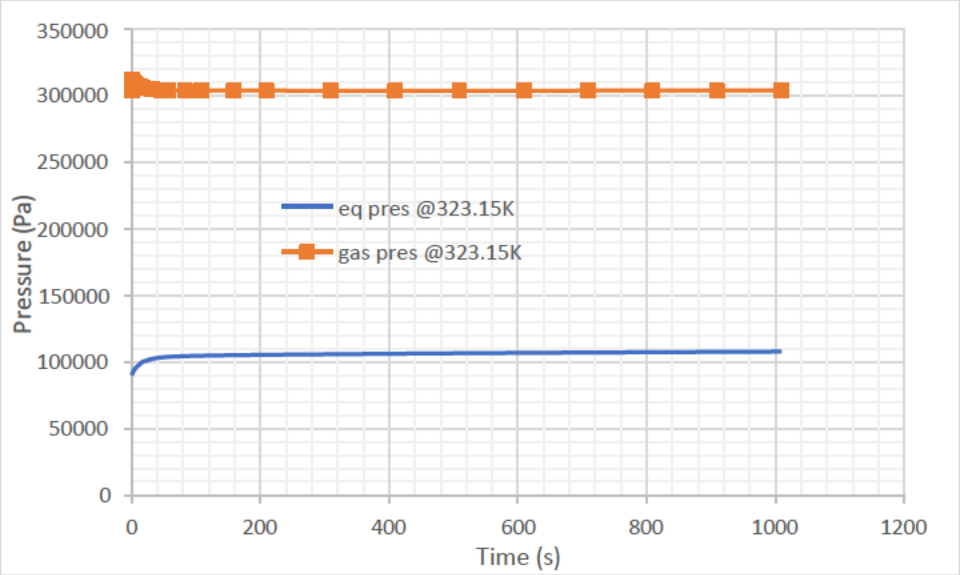

Figure 5.5.1.3a: Equilibrium-gas pressure rate

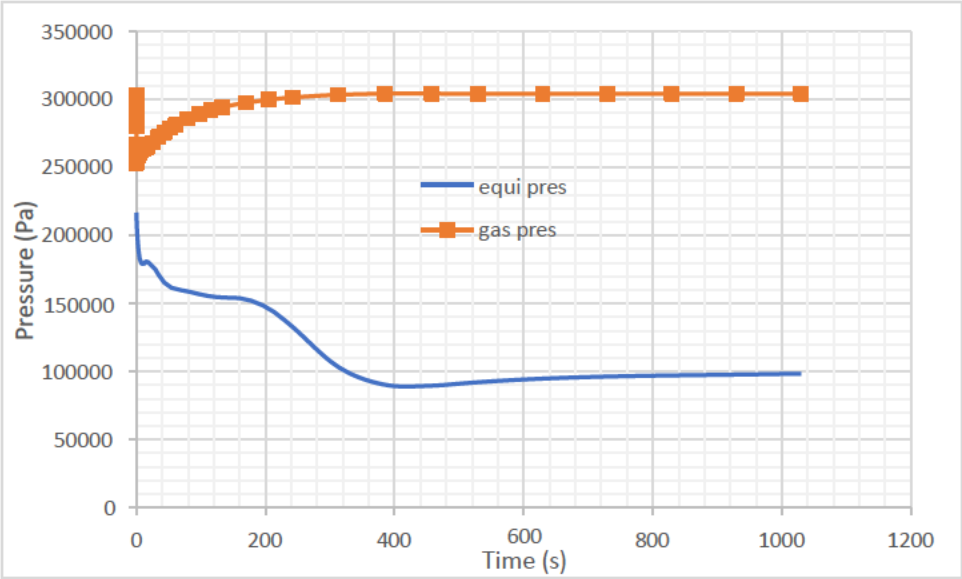

Figure 5.5.2.3: Equilibrium-gas pressure rate

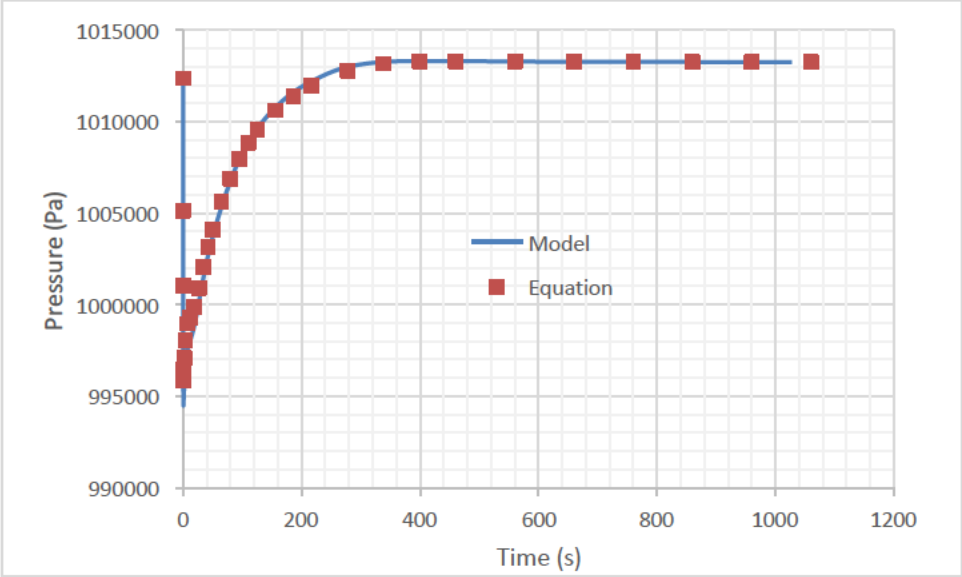

Figure 5.6.4.3: Absorption pressure profile

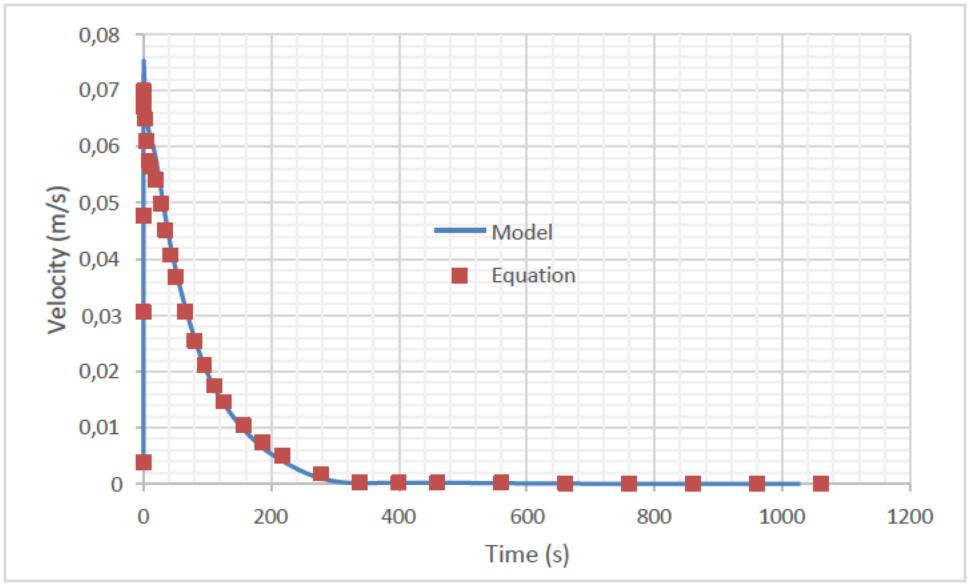

Figure 5.6.4.4: Desorption pressure profile

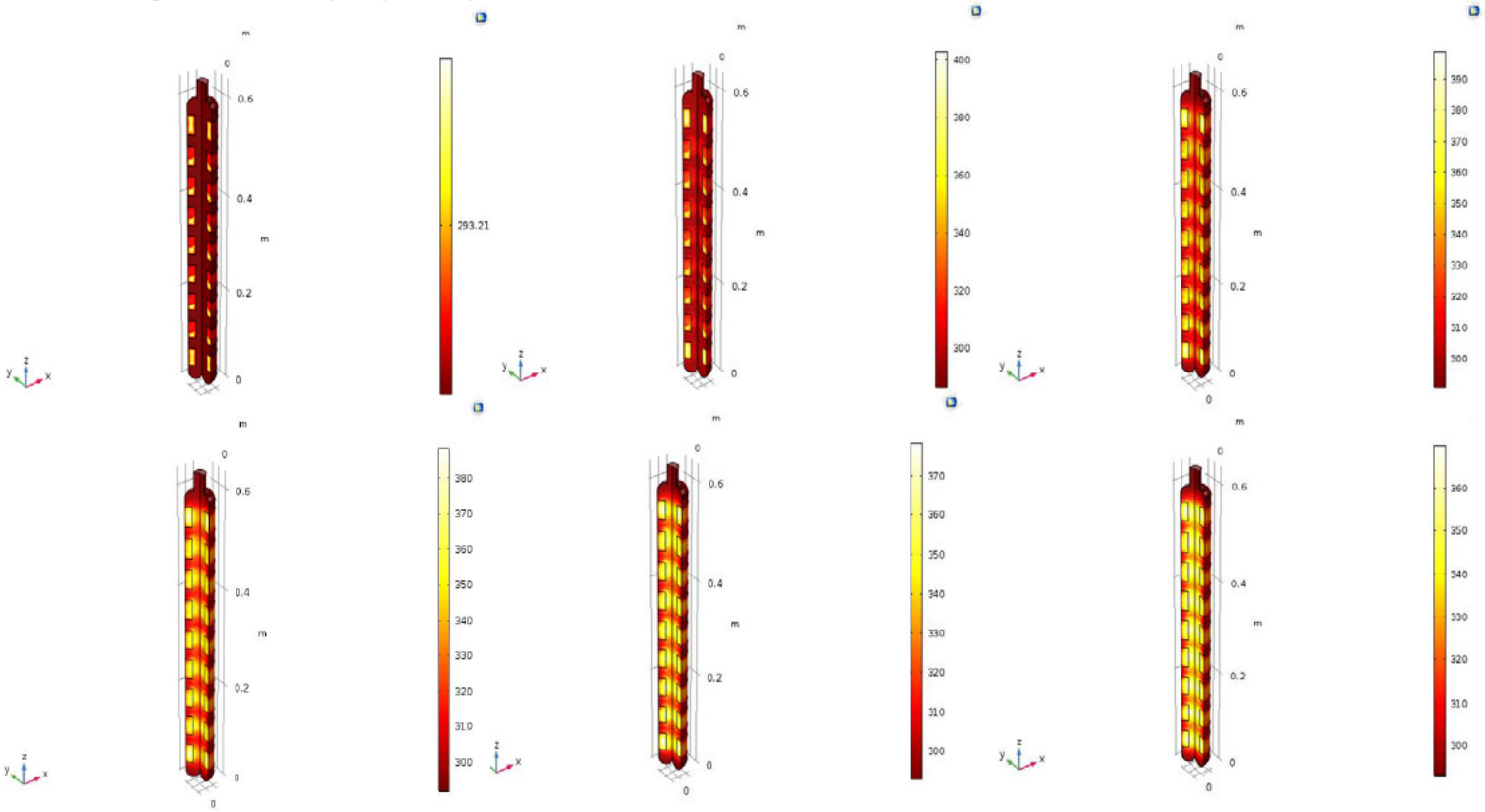

Figure 5.7.2: Heat distribution map